EXPERIMENTAL INVESTIGATION OF A LIFT AUGMENTED GROUND EFFECT PLATFORM

THESIS

Roberto T. Igue, Ensign, USNR
AFIT/GAE/ENY/05-S04

DEPARTMENT OF THE AIR FORCE
AIR UNIVERSITY

AIR FORCE INSTITUTE OF TECHNOLOGY

Wright-Patterson Air Force Base, Ohio

AFIT/GAE/ENY/05-S04

EXPERIMENTAL INVESTIGATION OF A LIFT AUGMENTED GROUND EFFECT PLATFORM

THESIS

Presented to the Faculty

Department of Aeronautics and Astronautics

Graduate School of Engineering and Management

Air Force Institute of Technology

Air University

Air Education and Training Command

In Partial Fulfillment of the Requirements for the

Degree of Master of Science in Aeronautical Engineering

Roberto T. Igue, BSE

Ensign, USNR

September 2005

AFIT/GAE/ENY/05-S04

EXPERIMENTAL INVESTIGATION OF A LIFT AUGMENTED GROUND EFFECT PLATFORM

Roberto T. Igue, BSE
Ensign, USNR

Approved:

//SIGNED//

_____ _____
Dr. Milton E. Franke (Chairman) date

//SIGNED//

_____ _____
Dr. Mark F. Reeder (Member) date

//SIGNED//

_____ _____
Lt Col Raymond C. Maple (Member) date

Abstract

This experimental study investigated the feasibility of applying the concept of a skirtless hovercraft into the production of an operational vehicle. A 0.255 m diameter prototype was designed, built and tested. An air bearing table was used as a testing platform, virtually eliminating the influence of friction and providing one degree of freedom for the experiments. Static tests were performed at various heights and craft configurations, providing a wide range of data for comparison. Lift, torque and efficiency were measured and calculated for each setting. Pressure and velocity information was also collected at specific points around the craft when operating at different heights above ground.

The results indicate a significant increase in total lift and efficiency when operating the model at close to the ground heights, in ground effect, compared to the lift produced by the propeller and motor alone. Even more significant changes were found when comparing the in ground effect results with the out of ground effect values of lift and efficiency. The study also investigated the use of Coanda nozzles on the peripheral region of the craft, and found them to be less efficient than straight nozzles with similar size and flow rates.

Comparisons between the experimental results and previous computational fluid dynamic analysis are also made and presented in this study.

To my family and friends.

Acknowledgements

I would like to thank my thesis advisor, Dr. Franke for his efforts and insightfulness in creating the opportunity and providing the resources necessary to complete this research. I would also like to express my sincere gratitude to Dr. Reeder for his invaluable help and advice in so many occasions. I am very thankful for the innumerous hours Mr. Andy Pitts, AFIT/ENY, dedicated to the set-up and calibration of all the testing equipment, and the many more he spent ensuring that I had the appropriate support, to successfully complete this project. I want to thank Mr. Randy Miller for aiding in the design and building the model in the ENY rapid prototyping machine.

Roberto T. Igue

Table of Contents

Page

Abstract iv

Acknowledgements vi

Table of Contents vii

List of Figures ix

List of Tables xiii

List of Symbols xiv

I. Introduction 1

II. Literature review 4

Section 1 – Hybricraft, Lift Augmented Ground Effect Platform 4
Section 2 – Kelleher's CFD Analysis 6
Section 3 - Ground Effect 8
Section 4 – Helicopters and Ground Effect 10
Section 5 - Coanda Effect 11
Section 4 – Goals of the Experimental Effort 16

IV. Experimental Setup 18

Section 1 - Designing and Building the Prototype 18
Section 1.1 – Motor and Propeller 19
Section 1.2 – Nozzles 20
Section 2 - Equipment 23
Section 2.1 Support Bar Drag 25
Section 3 – Data Collection 26

VI. Results & Analysis 27

Section 1 – Establishing Parameters for Comparison 27
Section 2 - First Group of Tests 29
Section 3 - Second Group of Tests 30
Section 3.1 - Torque Plots 30
3.2- Lift Plots 34
Section 3.3 - Efficiency 38
Section 3.4 - Constant Propeller Rotational Velocity, Varying Height 42
Section 3.5 – Propeller: Adverse Ground Effect 43
Section 4 – Coanda nozzles vs. Straight Nozzles 44
Section 5 – Flow and Pressure Distribution 50
Section 5.1- Pressure Distribution 1/8 Diameter Height 50
Section 5.2 - Pressure Distribution Out of Ground Effect (OGE) 56
Section 5.3 - Flow Attachment 60
Section 5.4 - Flow Velocities 61
Section 5.5 - Comparison to Kelleher's CFD Experiment 65

Page

V. Conclusions & Recommendations 70

Section 1 – Conclusions 70
Section 2 – Recommendations 72

Appendix A: Construction and Testing of an Internal Flow Separator 74

Appendix B: Full Data Set From the First Group of Tests 78

The following plots represent the data collected in the first group of tests. These plots show basic trends in performance for the different configurations at varying heights and propeller rotational velocities. The effect of vibrations can be noticed by the decrease in lift and efficiency for propeller speeds around 5850 rpm and to a smaller extent around the 3800 rpm range. The values at the remaining propeller rotational velocities were not affected. Plots of Torque vs propeller rotational velocity are presented in Figures 59 through 62. Figures 63 through 66 show values of lift versus propeller rotational velocity, and figures 67 throught 70 represent efficiency as calculated based on Equations [2], [3] and [4] 78

Appendix C: Equipment List & Specifications 87

Appendix D: Additional Figures: Equipment and Configuration 88

Bibliography 89

Vita 92

List of Figures

Figure Page

Figure 1: VZ-9AV, Avrocar Hovering During Tests in the 1950's (2) 2

Figure 2: Landing Craft Air Cushion (LCAC), US Navy's Hovercraft (5) 3

Figure 3: Coanda nozzle: exit gap with thickness t, and Coanda surface with radius R (7)5

Figure 4: Hybricraft illustration from Walter's *Hybricraft Primer* (7) 6

Figure 5: Kelleher's third design pressure distribution (4) 7

Figure 6: Cockerell's experiment (1955). The origin of the modern hovercraft (8) 8

Figure 7: Wings in ground effect: KM Kaspian Sea Monster (10) 9

Figure 8: Flow recirculation responsible for increase in power requirements when hovering in ground effect (11) 11

Figure 9: Coanda effect: entrainment of air into the jet and jet deflection towards the Coanda surface (12) 12

Figure 10: Balance between centrifugal force and 12

Figure 11: Experiment set-up used by Mason. Thrust vectoring is achieved by varying the mass flow rate in the secondary flow (12) 14

Figure 12: Thrust vectoring regions found by Mason: dead zone(A), control(B) and saturation zone(C) (12) 15

Figure 13: Half a cross sectional view of Kelleher's third model (4) 18

Figure 14: Cross sectional view of the model used in the experiment 21

Figure 15: A ring shaped attachment is placed around the Coanda nozzles to block the Coanda surface, forming the "straight nozzles" 22

Figure 16: Assembled prototype used in the experiment 23

Figure 17: Craft mounted on testing equipment 24

Figure 18: Effects of drag on the craft's support structure. The overall effect of drag is less than 2% of the total lift 25

Figure 19: Torque vs. propeller rotational velocity at 1/8 diameter height 31

Page

Figure 20: Torque vs. propeller rotational velocity at 1/4 diameter height 31

Figure 21: Torque vs. propeller rotational velocity at 1/2 diameter height 32

Figure 22: Torque vs. propeller rotational velocity out of ground effect 32

Figure 23: Lift vs. propeller rotational velocity at 1/8 diameter height..... 34

Figure 24: Lift vs. propeller rotational velocity at 1/4 diameter height..... 35

Figure 25: Lift vs. propeller rotational velocity at 1/2 diameter height..... 35

Figure 26: Lift vs. propeller rotational velocity out of ground effect..... 36

Figure 27: Percentage difference in lift between Coanda nozzles and straight nozzles configurations at 1/8 diameter height, and varying propeller rotational velocity..... 38

Figure 28: Efficiency vs. propeller rotational velocity at 1/8 diameter height 39

Figure 29: Efficiency vs. propeller rotational velocity at 1/4 diameter height 39

Figure 30: Efficiency vs. propeller rotational velocity at 1/2 diameter height 40

Figure 31: Efficiency vs. propeller rotational velocity out of ground effect 40

Figure 32: Lift coefficient vs. height - 6350 rpm range..... 42

Figure 33: Efficiency vs. height at 6350 rpm 43

Figure 34: Lift vs. propeller rotational velocity. Covered and partially covered nozzles at 1/8 diameter height 45

Figure 35: Lift vs. propeller rotational velocity. Covered and partially covered nozzles, out of ground effect..... 45

Figure 36: Lift vs. propeller rotational velocity. Covered and fully covered nozzles comparison with open nozzles configurations at 1/8 diameter height..... 47

Figure 37: Lift vs. propeller rotational velocity. Covered and fully covered nozzles comparison with open nozzles configurations, out of ground effect..... 47

Figure 38: Efficiency vs. propeller rotational velocity. Covered and fully covered nozzles comparison with open nozzles configurations at 1/8 diameter height..... 49

Figure 39 Covered and fully covered nozzles comparison with open nozzles configurations, out of ground effect..... 49

.....Page

Figure 40: Coanda nozzles pressure distribution at 1/8 diameter height 51

Figure 41: Straight nozzles pressure distribution at 1/8 diameter height..... 51

Figure 42: Close view of coanda nozzles pressure distribution at 1/8 diameter height.... 52

Figure 43: Close view of straight nozzles pressure distribution at 1/8 diameter height .. 53

Figure 44: Estimate of pressure distribution regions under the craft..... 55

Figure 45: Coanda nozzles pressure distribution out of ground effect 57

Figure 46: Straight nozzles pressure distribution out of ground effect..... 57

Figure 47: Tufts used to observe flow attachment to Coanda surface 60

Figure 48: Coanda nozzles configuration velocity distribution at 1/8 diameter height.... 62

Figure 49: Straight nozzles configuration velocity distribution at 1/8 diameter height ... 62

Figure 50: Coanda nozzles configuration velocity distribution, out of ground effect 63

Figure 51: Straight nozzles configuration velocity distribution, out of ground effect..... 64

Figure 52: Measured pressures for Coanda nozzles configuration at 1/4 diameter height66

Figure 53: CFD pressure analysis of Kelleher's model (4) 67

Figure 54: Coanda nozzles configuration velocity measurements at 1/4 diameter height 68

Figure 55: CFD velocity analysis of Kelleher's design at 1/4 diameter height 68

Figure 56: Flow separator inside the plenum chamber 75

Figure 57: Lift vs. propeller rotational velocity for craft with flow separator at 1/4 diameter height..... 76

Figure 58: Efficiency vs. propeller rotational velocity for craft with flow separator at 1/4 diameter height..... 76

Figure 59:Torque vs. propeller rotational velocity. 1st group of tests, 1/8 diameter height 78

Figure 60:Torque vs. propeller rotational velocity. 1st group of tests, 1/4 diameter height 79

Page

Figure 61: Torque vs. propeller rotational velocity. 1st group of tests, 1/2 diameter height 79

Figure 62:Torque vs. propeller rotational velocity. 1st group of tests, out of ground effect 80

Figure 63: Lift vs. propeller rotational velocity. 1st group of tests, 1/8 diameter height . 80

Figure 64:Lift vs. propeller rotational velocity. 1st group of tests, 1/4 diameter height .. 81

Figure 65:Lift vs. propeller rotational velocity. 1st group of tests, 1/2 diameter height .. 81

Figure 66:Lift vs. propeller rotational velocity. 1st group of tests, out of ground effect . 82

Figure 67:Efficiency vs. propeller rotational velocity. 1st group of tests, 1/8 diameter height..... 82

Figure 68:Efficiency vs. propeller rotational velocity. 1st group of tests, 1/4 diameter height..... 83

Figure 69:Efficiency vs. propeller rotational velocity. 1st group of tests, 1/2 diameter height..... 83

Figure 70: Efficiency vs. propeller rotational velocity. 1st group of tests, out of ground effect 84

Figure 71: Water manometer used for pressure measurements 88

Figure 72: Partially covered Coanda nozzles configuration 88

List of Tables

Table Page

Table 1: Difference in pressure between the two configurations at specific regions on the craft. Height: 1/8 diameter 54

Table 2: Estimated areas for each pressure region below the craft. Height: 1/8 diameter 55

Table 3: Difference in pressure between the two configurations 58

Table 4: Equipments list and specifications..... 87

List of Symbols

Symbol	Name
A_C	estimated central area
A_5	estimated area under 5cm pressure tap region
A_{10}	estimated area under 10cm pressure tap Region
A_{45}	estimated area under the 45 degrees pressure tap region, peripheral nozzles region
A_{15}	estimated area under the 15 degrees pressure tap region
C_L	coefficient of thrust
C_Q	coefficient of power
d_{craft}	diameter of the craft
η	dimensionless coordinate
L	lift force
M	mach number
μ_∞	viscosity
Ω	propeller's angular velocity
R	Coanda surface's radius of curvature
Re	Reynolds number
R_{rotor}	radius of main-rotor, or propeller
ρ_∞	air density
t_{gap}	thickness of nozzle's exiting gap
V_{exit_gap}	air speed at the peripheral nozzle's exit
$V_{downwash}$	downwash velocity

EXPERIMENTAL INVESTIGATION OF A LIFT AUGMENTED GROUND EFFECT PLATFORM

I. Introduction

During the 1950's, the Canadian company, Avro Canada, developed the concept of a circular-shaped aircraft. The Avrocar (Figure 1), as it became known to the world, had capabilities unmatched by any vehicle at the time. It was capable of vertical take off and land and could quickly transition from low altitude hovering to high altitude supersonic flights (1).

This ambitious design caught the attention of the United States military, and was adopted as a joint US Army and US Air Force project, designated as VZ-9AV (1). The US Air Force saw the potential of developing it into a new fighter-bomber aircraft. The US Army's version would be used in reconnaissance missions, with ability to hover below the radar and over terrains inaccessible to conventional vehicles, and then launch itself into the sky at supersonic speeds once the mission was completed. Soon, however, tests performed on the initial prototypes determined the craft to be unstable when hovering at heights over a meter, causing the project to be abandoned (1).

Figure 1: VZ-9AV, Avrocar Hovering During Tests in the 1950's (2)

In 1998, William Walter, a former sales engineering manager for Avro Canada during the Avrocar project (3), received a patent for his own vehicle, a *Lift Augmented Ground Effect Platform* (4). Among other devices, the patent describes the use of concentric nozzles to create an air cushion under the vehicle. These nozzles divide the air cushion into different sections. At the center of the arrangement, an inner air curtain surrounds a supercharged air cushion. This central region is surrounded by an outer supercharged air cushion, held in place by a second air curtain formed by the peripheral Coanda nozzles(4). Although Walter's design is not intended for supersonic flights as its predecessor, the Avrocar, a working vehicle with its capabilities would find many military and civilian applications in today's world.

Vehicles designed to benefit from ground effect could fulfill many missions currently assigned to helicopters, offering a larger payload capacity with smaller power requirements. The capability to also operate out of ground effect (OGE) would give a new craft advantages over existing ground effect vehicles such as hovercrafts. Conventional hovercrafts are often unable to operate over rough seas and overcome larger ground obstacles. This becomes an even more significant challenge when dealing

with military equipment such as the LCAC (Landing Craft, Air Cushion) currently employed by the US Navy and seen in Figure 2 (5).

Figure 2: Landing Craft Air Cushion (LCAC), US Navy's Hovercraft (5)

II. Literature review

Section 1 – Hybricraft, Lift Augmented Ground Effect Platform

In 2004, Kelleher investigated the feasibility of William Walter's design becoming an operational vehicle. Using computational fluid dynamics (CFD) in his studies, Kelleher provided deeper insight into the concept of a skirtless hovercraft (4).

Kelleher analyzed three different crafts during his studies, all designed based upon Walter's 1998 patent (6) and on additional information provided by Walter in his *Hybricraft Primer* (7).

The main concept introduced by Walter in his patent is the use of concentric nozzles placed on the lower surface of the craft to create an air cushion and support the vehicle. These nozzles are arranged in a specific manner to divide the air cushion into two semi-independent regions. A central supercharged air cushion is kept in place by an air curtain. This curtain is, in turn surrounded by a peripheral air cushion and a second air curtain created by Coanda nozzles. In his invention, Walter makes use of the Coanda effect to create the central and the peripheral air curtains designed to maintain the high-pressure areas under the craft. The nozzles placed on the peripheral regions of the vehicle must fulfill the same role as the rubber skirts found on conventional hovercrafts, maintaining a layer of air between the craft and the ground, minimizing the effects of friction on the craft. These nozzles consist of an outlet gap from which high-pressure air exits, and an inward curved surface that immediately follows this outlet. When hovering out of ground effect (OGE), these nozzles, according to Walter, operate as Coanda

nozzles. The air will attach to the nozzle's surface and follow its curvature towards the lower portion and the central axis of the craft.

Walter specifies in his patent a critical thickness to radius ratio (t/R). This value refers to the ratio between the thickness of the Coanda nozzle's outlet gap to the radius of curvature on the surface that follows it, Figure 3. The nozzles operate under the Coanda effect (further discussed later in this study) and this ratio is responsible for the proper operation of the nozzles (6).

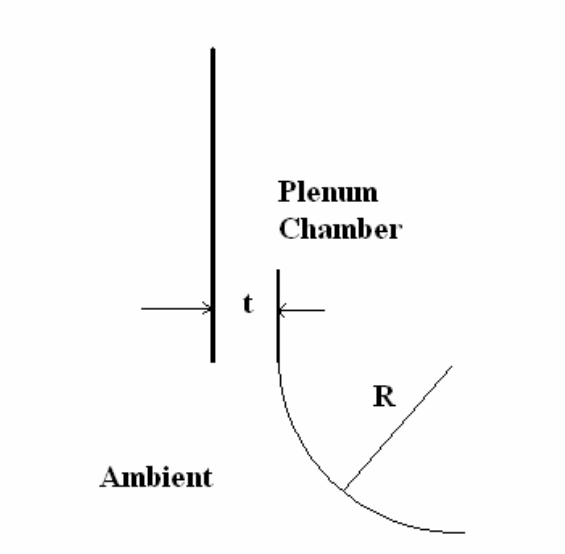

Figure 3: Coanda nozzle: exit gap with thickness t, and Coanda surface with radius R (7)

Another important feature described in by Walter (7) is the dome shaped outer surface, introduced as a Coanda wing (7), and which creates what would appear as the 'body' of the craft. Downwash from the propeller is accelerated on this surface as it follows a path towards the peripheral region of the vehicle, producing a lower pressure region on the Wing's surface and therefore contributing to the generation of lift. This feature can be seen in an illustration of the Hybricraft in Figure 4.

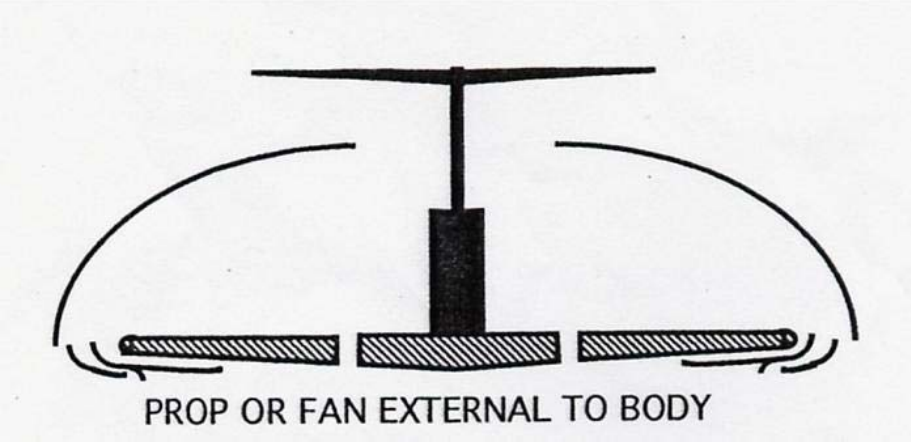

Figure 4: Hybricraft illustration from Walter's *Hybricraft Primer* (7)

Section 2 – Kelleher's CFD Analysis

Kelleher analyzed three different craft models using computational fluid dynamics (CFD). All three were designed based on Walter's ideas, either presented in his 1998 patent (6) or the "Hybricraft Primer" (7). The first model was the most similar to the patented design, but it was not successful in producing lift as desired. The second model contained elements from both papers, differing from the first mainly by the presence of a Coanda wing (introduced by Walter in the "Hybricraft Primer" (7)) and a plenum chamber. The third model tested by Kelleher was a close adaptation of Walter's design in the "Hybricraft Primer" (7). This last model produced the most lift of all three crafts. The use of CFD allowed Kelleher to test the craft at downwash speeds of 100 m/s (downwash from the propeller located on top of the craft, with velocities pointing in the downward direction). By integrating the pressures acting on the surfaces of his CFD model, Kelleher found that his 4 ft diameter model was able to produce lift in the order of 5388.8 N when tested at a height of 1 ft from the ground (4). The chart presented in

Figure 5 illustrates the pressure distribution found by Kelleher in his analysis of his third model.

.

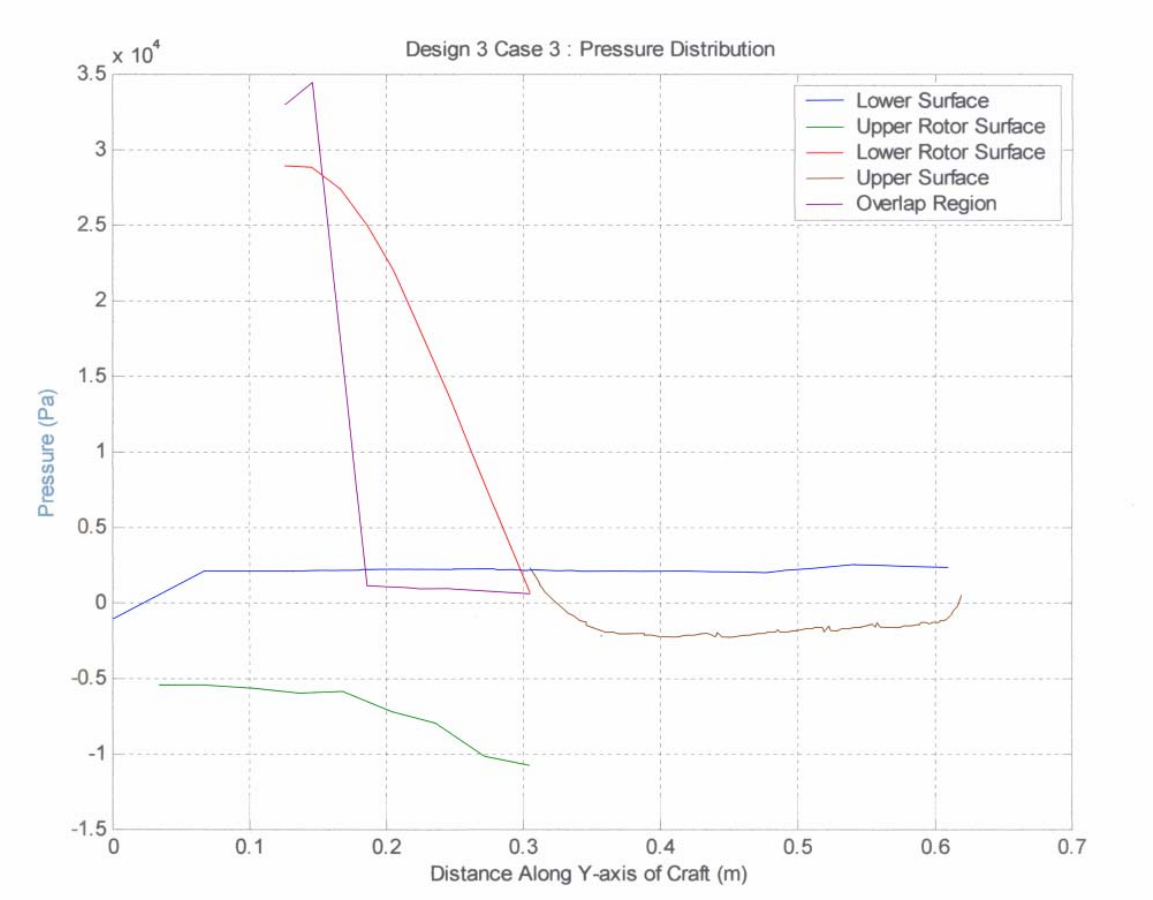

Figure 5: Kelleher's third design pressure distribution (4)

Kelleher's pressure distribution indicates high pressures under the rotor (or propeller), which also leads to a higher pressure on the overlap region of the craft (region on the Coanda wing directly under the rotor and its downwash). A small but somewhat constant positive pressure was found under the craft, also aiding in the production of lift.

This is an indication that his model was indeed benefiting from interactions with the ground, therefore operating in ground effect (IGE).

Section 3 - Ground Effect

Sir Christopher Cockerell invented the modern version of the Hovercraft. He envisioned a vehicle capable of traveling over water, floating on a layer of air, and therefore minimizing the effects of friction. His theory was first tested in 1955 by using a cat food can placed inside a coffee can, an air blower and a pair of kitchen scales (8), Figure 6. In his experiment, Cockerell was able to create a layer of air between the cans and the ground plane mounted on top of his scales, increasing the force produced with his air blower (8).

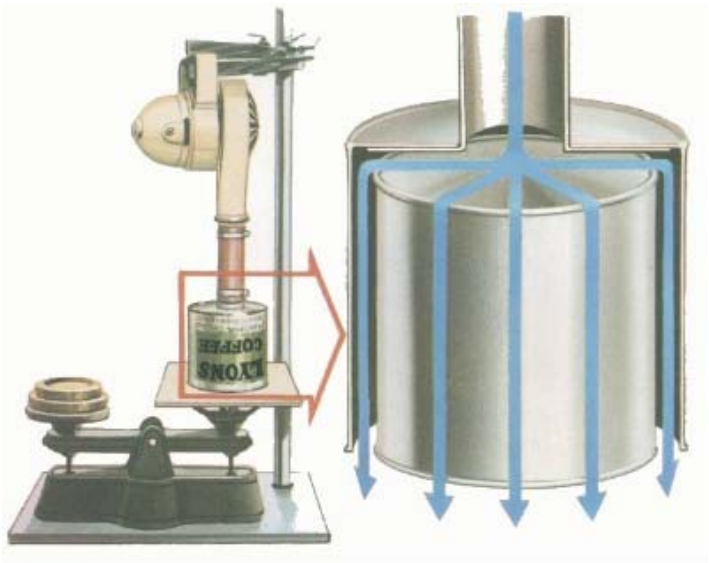

Figure 6: Cockerell's experiment (1955). The origin of the modern hovercraft (8)

Sir Cockerell's theory led to the many variants of the vehicle found nowadays, from high-speed ferries to military applications such as the LCACs currently used by the United States Navy for amphibious operations.

The ground effect is a phenomenon also experienced by other vehicles. Conventional airplanes benefit from it when flying close to the ground (less than one wingspan in altitude), experiencing an increase in lift with a constant amount of power requirement from the engines (9). Other aircrafts have been specifically developed in the past to make use of ground effect. WIGs, or Wings in ground effect are boats designed to fly close to the water and therefore benefit from the ground effect (10). An example of a WIG is the Russian KM Caspian Sea Monster (10) developed during the cold war and designed to fly close to the water surface, transporting large payloads at very high speed (Figure 7).

Figure 7: Wings in ground effect: KM Kaspian Sea Monster (10)

The concept of the Avrocar in the 1950's also used ground effect when hovering close to the ground. Design flaws, however, led to stability problems, which Walter

claims to have corrected in his invention with the use of Coanda nozzles on the peripheral region of the craft.

Section 4 – Helicopters and Ground Effect

Helicopters also experience ground effects when hovering at low altitudes. During take-off and landing, main-rotor down wash creates an air cushion below the helicopter. This allows the helicopter to hover at those altitudes with significantly smaller power requirements than if operating only a few meters higher. Cerbe (11) performed an experimental research and found that the effects of an air cushion under the helicopter are significant up to heights around 4 times the rotor radius. The benefits are more noticed below the critical height of 1.7 times the rotor radius, and adverse effects can be felt at heights closer to the 4 rotor radius range. When landing, these adverse effects can manifest in the form of acceleration in the vertical direction (at heights in the 4 rotor radius range) followed by deceleration once the helicopter reaches lower heights and the air cushion effect become more prominent. This seems to be explained by the process of recirculation of flow from the downwash, as illustrated in Figure 8. At these heights (4 times the rotor radius), helicopters operating IGE may require more power to hover than if operating OGE.

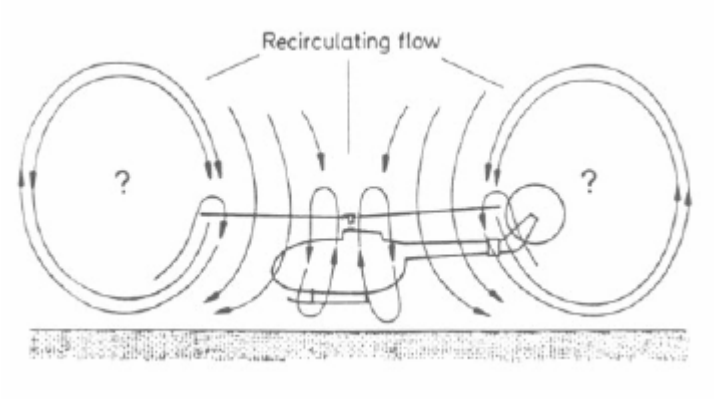

Figure 8: Flow recirculation responsible for increase in power requirements when hovering in ground effect (11)

Cerbe (11) also concludes that small increases in horizontal speeds cause large reductions in lift. This caused by the helicopter's inability to maintain the air cushion below the main rotor once it starts moving in any direction other than vertical (11).

Section 5 - Coanda Effect

The Coanda effect was first observed by Thomas Young in the 1800 but wasn't fully understood (27). Henri Coanda rediscovered this phenomenon in the early 1930's while designing and testing what could have become the first jet-powered airplane, had it not been ironically destroyed by this very same effect that later made him famous. This viscous effect can be described as the entrainment of ambient fluid into a jet, and occurs when the jet fluid has equal or higher viscosity than the fluid present in the discharge region. If a solid body is tangentially placed near the path of this jet, the fluid between the two may become entrained into the jet at a rate faster than it can be replaced, causing a change in the existing conditions. A lower pressure region is then formed between the body and the jet, causing the latter to deflect until it attaches to the surface. The same

process will occur at subsequent points along the solid surface, causing the jet to follow the body's contour.

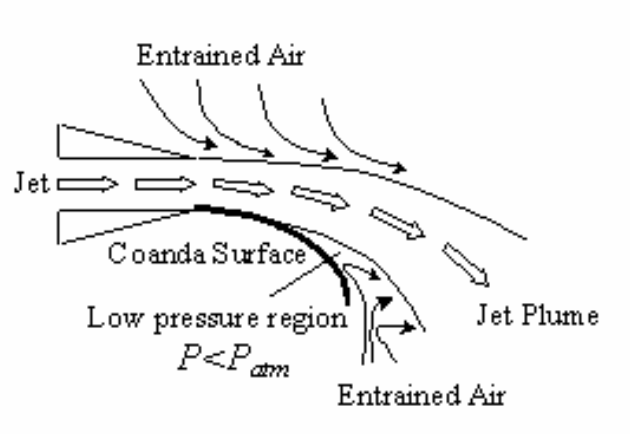

Figure 9: Coanda effect: entrainment of air into the jet and jet deflection towards the Coanda surface (12)

The attachment of the jet to the Coanda surface results in a pressure gradient normal to the original jet direction (12). This pressure gradient is illustrated in Figure 10.

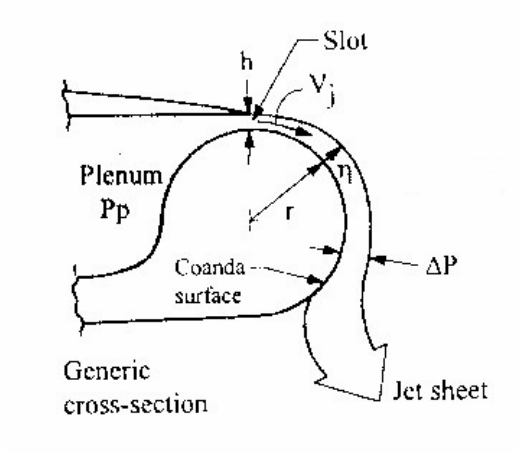

Figure 10: Balance between centrifugal force and pressures acting on a Coanda surface (13)

There must exist a balance between the pressure acting on the Coanda surface and the centrifugal forces on the system. For the illustration above, Imber (13) defines this balance as described in Equation [1] below.

$$\frac{dP}{d\eta} = \frac{\rho V_j^{\,2}}{r+\eta} \qquad [1]$$

The overall desired effect of thrust vectoring is to produce a force normal to the original jet's direction. This is accomplished not only by redirecting the jet around a Coanda surface, but also by the entrainment of free stream air (or air not originally present in the jet) into the jet, causing it to also be turned in the same direction as the vectored thrust.

Although there is no "Coanda equation" (14), the jet's angular deflection and point of separation from the curved surface are known to be dependent upon four major factors:

1. Total pressure of jet and the ambient pressure
2. The size of the gap from which the jet originates
3. The radius of curvature of the surface to which the jet is attaching (Coanda Surface)
4. The geometry of the surface

The last factor was observed by von Glahn (15), when performing jet deflection experiments with the use of Coanda surfaces placed at the exit of a jet. His conclusions show that Coanda nozzles composed of multiple flat plates could achieve a higher

deflected to undeflected thrust ratio than a Coanda nozzle composed of a single curved plate, on the order of 0.88 and 0.81 respectively (15).

The Coanda effect has been studied in configurations similar to the one found on the peripheral nozzles in this craft. The use of the nozzles here, however, appears to be unique to this design. Franke et al.(16) and Imber (13) investigated the effects of circulation control by blowing air through a slot and over a blunt trailing edge (Coanda surface). Both researchers verified the benefits of using Coanda surfaces to control the flow separation point of low aspect ratio wings (16) and circular platform wings (13).

Mason (12) performed experiments with varying gap height and radius of curvatures when studying the application of Coanda surfaces for thrust vectoring. The research tested two-dimensional models with a primary exit nozzle located between two secondary nozzles and two Coanda surfaces, Figure 11.

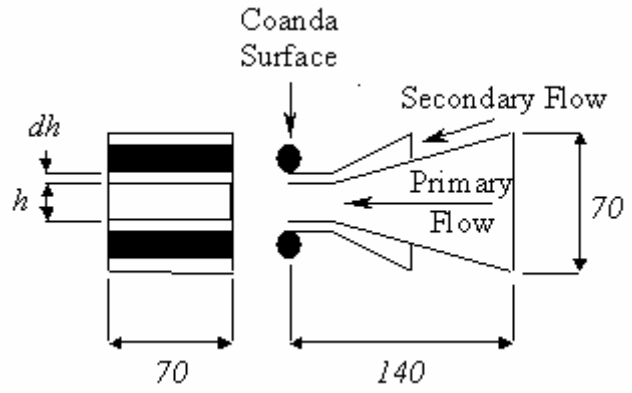

Figure 11: Experiment set-up used by Mason. Thrust vectoring is achieved by varying the mass flow rate in the secondary flow (12)

In his study, Mason (12) analyzed variations in the Coanda surface diameter to primary exit nozzle (h) ratio while keeping the dh/h value constant (Figure 11). He also varied the dh/h while maintaining the Coanda surface diameter to h ratio constant in a second set of tests. Mason identified relationships between these two ratios and the

primary and secondary flows ratios that determine the deflection angle of the thrust vector. Figure 12 shows the basic trends found by Mason (12).

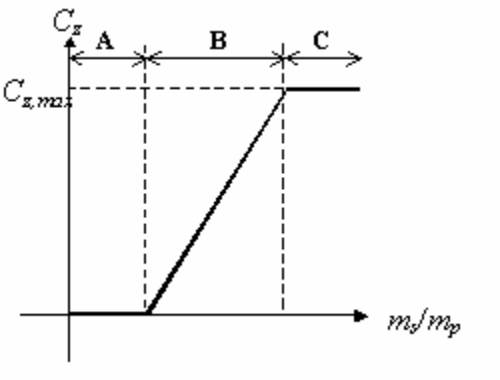

Figure 12: Thrust vectoring regions found by Mason: dead zone(A), control(B) and saturation zone(C) (12)

Cz is defined as a ratio between the total deflected thrust to the component of thrust in the desired direction (perpendicular to the original undeflected thrust direction). The experiment found trends among all the variations and determined the existence of three modes of operation. At low secondary to primary mass flow ratios there is a dead zone (A in Figure 12), where low secondary mass flow rates are unable to produce any effect on the primary flow. A saturation region is also found (C), where maximum deflection angle is achieved for all secondary to primary flow mass ratios (for thickness to radius above a certain minimum). Vector thrust control was achieved in the control region (B), where changes in the mass flow ratios produce changes in the force components along the desired direction (12).

Walter's design (7) makes use of Coanda nozzles that operate in a very similar manner as the devices used for circulation control and thrust vectoring. The goals of these nozzles, however, is to direct the flow towards the central axis of the vehicle, creating high pressure air curtains that surround the high pressure regions below the craft.

The peripheral Coanda nozzles are designed to operate under the Coanda effect during flights out of ground effect (6), but not when operating in ground effect (the air cushion creates an adverse pressure gradient, preventing the jet from attaching to the Coanda surface).

Section 4 – Goals of the Experimental Effort

Kelleher concluded that his third model produced positive results and should be studied further. His analysis also determined that while the Coanda wing contributed to the production of lift, the Coanda nozzles did not perform as expected. In order to better understand the aerodynamic behavior or a skirtless hovercraft, this research sets the following goals:

- design and build a prototype model based on Kelleher's third tested model;
- perform initial experimental analysis to investigate the feasibility of applying the concept of a skirtless hovercraft in the production of a full scale prototype;
- study this prototype's static hovering capabilities at various heights, in ground effect (IGE) as well as out of ground effect (OGE);
- develop an experimental method and set up to test and compare the performance of propeller-powered vehicles;
- understand the operation of the craft's nozzles, more specifically the peripheral Coanda nozzles;

- gain further insight into the capabilities, strengths and weaknesses of this concept;
- compare the results of this research to those described by Kelleher.

IV. Experimental Setup

Section 1 - Designing and Building the Prototype

The model used in this experiment was built based upon Kelleher's computational fluid dynamics analysis. It most closely follows the shape and specifications of the third design studied by Kelleher, which performed the best out of the three configurations analyzed with CFD. Kelleher's third design is presented in Figure 13.

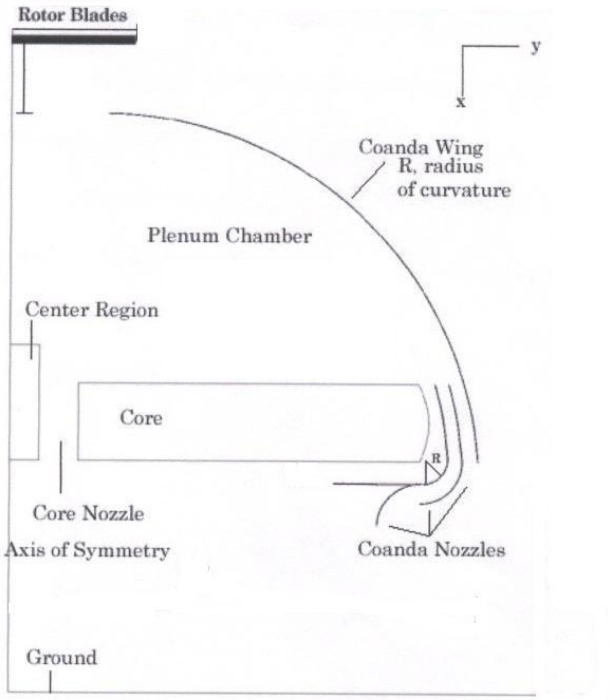

Figure 13: Half a cross sectional view of Kelleher's third model (4)

Kelleher's analysis reveals that the Coanda wing (seen in Figure 13) could aid in the production of lift. The downwash from the propeller speeds up as it flows along the

Coanda wing's outer surface, resulting in a reduction in pressure. For this experiment, a clear plastic dome was used as the Coanda wing. When attached to the lower portion of the craft, where the nozzles are located, the interior space of the Coanda Wing form the plenum chamber. The plenum chamber's inlet has an area of 0.21 m^2 and is located directly below, 1/4 diameter from the propeller, following the dimensions used by Kelleher. The plenum's inlet is positioned at the center of the propeller's downwash, allowing roughly 66% of the total air flow (downwash from the propeller) to enter the plenum chamber. The air mass in this region feeds the nozzles directly beneath it, allowing the formation of the desired air cushion.

Section 1.1 – Motor and Propeller

Kelleher's four-foot diameter (1.016 m) model was scaled down to allow the construction and testing of the 0.225 m prototype used in this study. Due to the flexibility provided for a CFD analysis, certain conditions used by Kelleher are not easily recreated in a laboratory testing setup. Sacrifices in the reproduction of the same aerodynamic qualities as Kelleher's design had to be made. Kelleher's CFD simulations involved uniform air speeds of 100 m/s coming out of his propeller (downwash), which could not be reproduced for this study.

The inability to reproduce the same CFD parameters is compensated by the realistic need to study a working craft capable of operating in many different conditions, and high and low air speeds. This experiment utilized an ElectriFly T-600R Reverse Motor, commonly used in airplane models. A standard airplane model propeller (manufactured by APC Propellers) was attached to this motor. With 8 inches in diameter

and a 4 inches pitch (ideally, the propeller advances 4 inches after one rotation), the propeller provided airspeeds of about 10.6 m/s at 6350 rpm, the upper end rotational velocity for this experiment. Following the same ratio of propeller height to the craft's diameter used by Kelleher, the motor was located at 1/4 diameter from the top of the Coanda Wing, and aligned with the craft's centerline.

Section 1.2 – Nozzles

Kelleher's results raised questions about the performance of a different part of the craft, more specifically the effectiveness of the nozzles located under and in the peripheral area of the craft. His positive results regarding the Coanda Wing allowed the efforts in the present experiment to be concentrated around the investigation of other parts of the craft. Particular interest was found in learning about the benefits provided by the nozzles in the lower portion of the craft, their effectiveness in maintaining a high pressure region below the vehicle when hovering in ground effect (IGE) as well as their operation when out of ground effect (OGE).

The nozzles in the craft used in this experiment had thickness to radius ratio close to that used by Kelleher in his CFD model (4). The thickness to ratio refers to the thickness (or height) of the exit gap from where the higher-pressured air leaves the plenum chamber, and the radius of curvature of the surface which immediately follows it, called the Coanda surface.

The thickness-to-radius relationship is important as one of the factors determining at what point the flow separates from the same Coanda surface. Mason's (12) studies regarding the use of the Coanda effect in thrust vectoring indicate that in order to achieve

maximum deflection angles, small gap sizes and larger radius of curvatures are desired. Mason's findings were incorporated into this experiment during the creation of a flow separator (or divider) placed inside the plenum chamber in order to direct the internal flow towards specific parts of the craft. The justification as well as the results are found in Appendix A.

The remaining nozzles were placed at 0.0923 m, 0.0743 m and 0.0300 m from the center of the craft. Figure 14 shows a cross sectional view of the prototype built for this experiment.

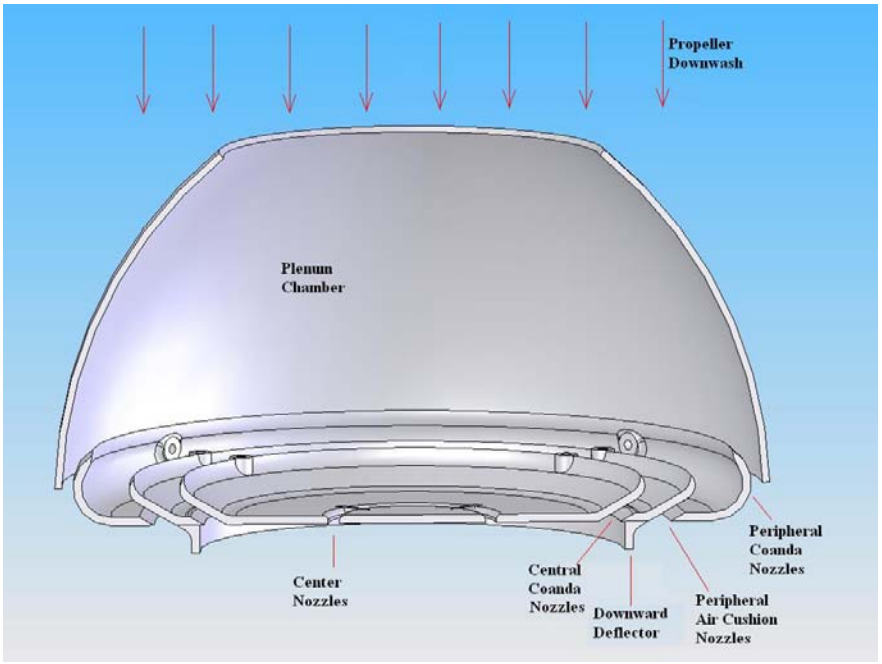

Figure 14: Cross sectional view of the model used in the experiment

A downward flow deflector, placed between the second and the third nozzles to direct air into the peripheral air cushion, was built separately and can be removed or added to the configuration. An outer attachment was also built and can be placed around the peripheral Coanda nozzles, canceling the curvature effect of the same and

providing a straight downward path for the flow coming out of the outer peripheral gap. This attachment creates the "straight Nozzles," and is used for performance comparisons during the tests, Figure 15.

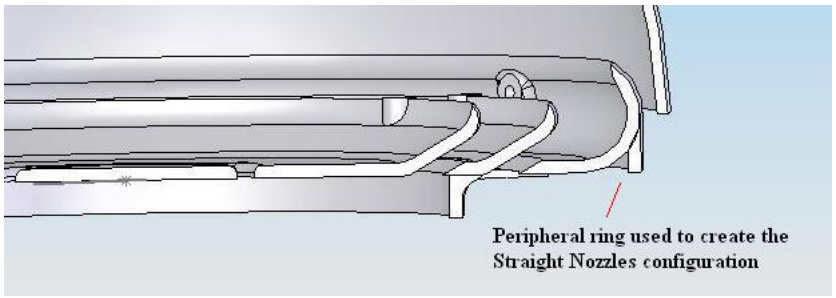

Figure 15: A ring shaped attachment is placed around the Coanda nozzles to block the Coanda surface, forming the "straight nozzles"

The AFIT rapid prototype machine was used to construct the nozzles. Figure 16 shows the nozzles built in the rapid prototype machine and the clear dome used as the Coanda wing. The picture also shows the aluminum bar that passes through the craft and is used to mount it on the testing apparatus (Figure 16).

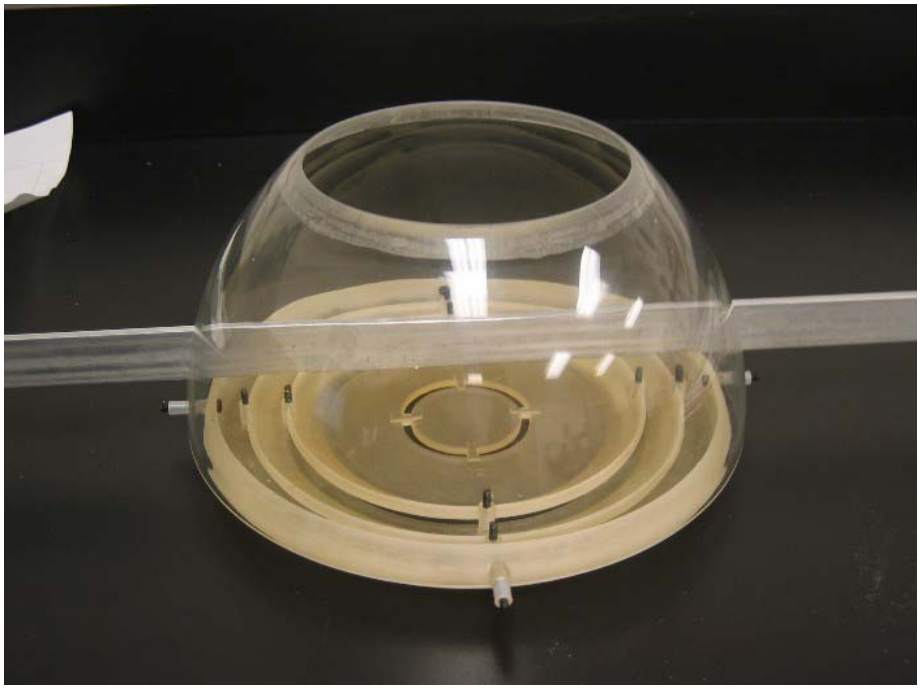

Figure 16: Assembled prototype used in the experiment

Section 2 - Equipment

A variable power supply allowed the collection of data at different propeller velocities. The motor was directly connected to a torque cell, and both were horizontally mounted to a vertical support bar attached to a base plate. The base plate was in turn mounted on an air-bearing table, lowering the effects of friction to negligible levels. The fully mounted testing set up, including the craft, can be seen in Figure 17.

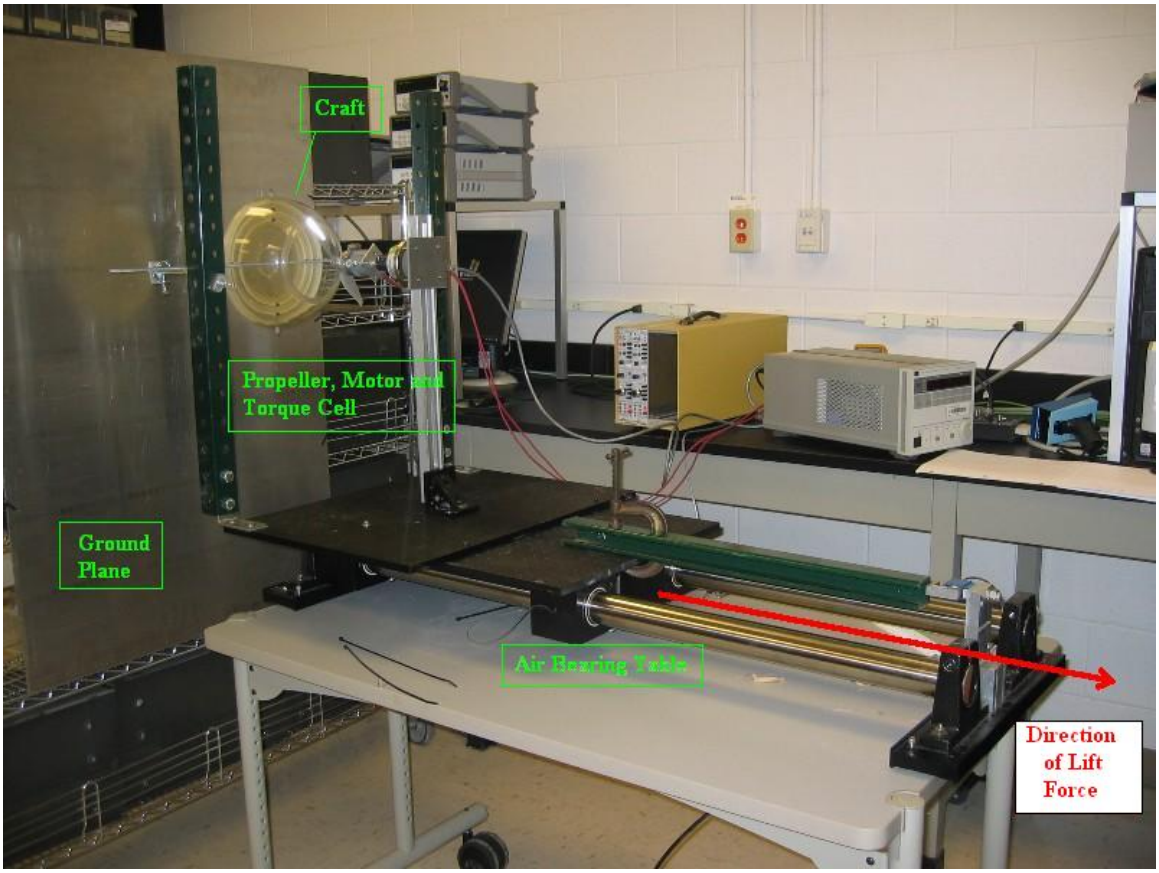

Figure 17: Craft mounted on testing equipment

In order to measure the influence of the ground effect on the platform, an adjustable ground plane was built using a vertically-mounted flat aluminum plate. The area affected by the craft's downwash was centered at the middle of the plate, ensuring that enough ground surface was available on all sides (more than one craft-diameter from the peripheral nozzles) and the correct ground-craft interactions were accounted for. The ground plane could be moved in relation to the craft, simulating operations at various heights and consequently benefiting from ground effect to varying degrees.

Section 2.1 Support Bar Drag

The craft was attached to the base plate by two vertical support posts and a 1/4 in by 1 in aluminum bar passing through the Coanda wing. Tests were performed to analyze the influence of this structure in the experimental results. With the propeller operating at velocities in the 6450 rpm range, 10 values of lift were collected without a perfectly clear path for the propeller's downwash. Without changing the propeller velocity, 10 more data points were collected with the aluminum bar installed on the path of the downwash flow, and therefore creating a drag force in the opposite direction to the lift produced by the propeller (the bar was place in the same position it would occupy when holding the craft in place during the remaining tests). Each of the two groups of data was averaged and the difference between these averages was calculated. The averaged drag force generated by the support bar (in the direction opposite to the lift force) lead to an average reduction in lift of less than 2%. Figure 17 below is a plot of the 20 values of lift measured during these tests.

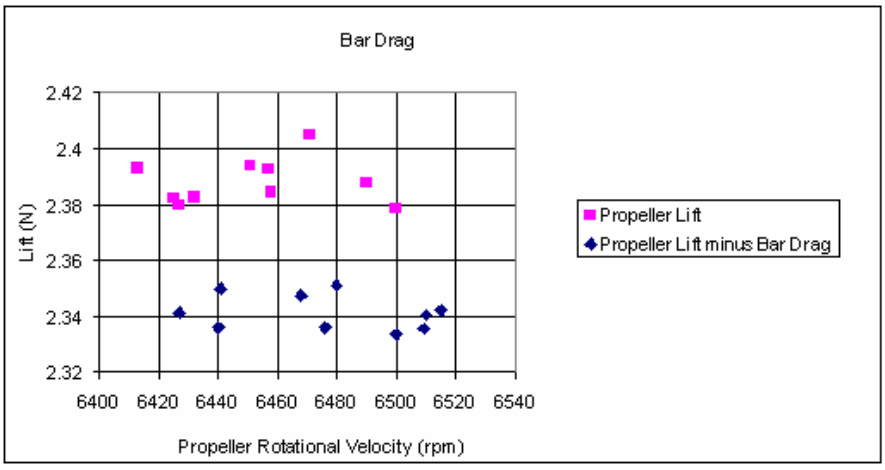

Figure 18: Effects of drag on the craft's support structure. The overall effect of drag is less than 2% of the total lift

The actual reduction in lift due to drag is likely smaller than the calculated value of 2%. This is a very conservative estimate of drag because a significant part of the bar is found inside the plenum chamber. The air speeds in the axial direction passing around the bar are expected to be a lot lower than the undisturbed downwash speeds to which the bar was subjected during the tests. Given the scope of the analysis performed in this experiment, the influence of the support structure's drag can be considered negligible.

Section 3 – Data Collection

The model craft and the propeller were oriented horizontally, directing the lift and drag forces along the one degree of freedom axis provided by the air-bearing table. A load cell was then placed at the end of the air-bearing table, allowing the measurement of the horizontal forces applied to the base plate, along the air bearing table's axial direction. The load cell and the torque cell attached to the motor were connected to a computer and the data were collected using National Instrument's Labview. Torque and load (lift) data were simultaneously collected for 1000 points at 100 Hz. The 1000 data points were averaged to provide the desired information about torque and force (lift). The propeller rotational velocity was measured using a photo tachometer. The relationships between torque, lift and propeller rotational velocity were calculated and plotted using Microsoft Excel.

VI. Results & Analysis

Section 1 – Establishing Parameters for Comparison

In order to allow comparison between the different configurations of the craft at the various heights above the ground plane, a few parameters had to be established. Singleton (17) and Noonan (18) performed studies on the performance of different helicopter rotor blades and used the parameters defined in Equations [2], [3] and [4] as a way to compare their performances. In the present experiment, these same parameters were used to compare the performance of the different craft configurations.

$$C_L = \frac{L}{\rho \pi R_{rotor}{}^2 (\Omega R_{rotor})^2} \qquad [2]$$

where:

L lift produced, N

R_{rotor} radius of the rotor or propeller, m

ρ density of the gas, kg/m^3

Ω angular velocity of the propeller, *radians/sec*

and a rotor torque coefficient C_Q, Equation [3] below:

$$C_Q = \frac{Q_R}{\rho \pi R_{rotor}{}^3 (\Omega R_{rotor})^2} \qquad [3]$$

where:

Q_R torque generated by the rotor at the shaft, $N.m$

. As presented in the equation above, the power required is a function of measured propeller angular velocity and torque.

The efficiency of the craft under different configurations and heights above ground was calculated based on a figure of merit. Figure of merits represent a ratio between the ideal power required to hover and the actual power required to hover (28). In Equation [4], the ideal power required to hover is established as a function of lift coefficient (Equation [2]). The actual power requirement is represented by the torque coefficient (Equation [3]).

$$FM = \frac{\sqrt{C_L^{\,3}/2}}{C_Q}$$

$$FM = 0.707\frac{C_L^{\,3/2}}{C_Q} \qquad [4]$$

Where :

C_L thrust coefficient defined in Equation [2]

$\sqrt{C_L^{\,3}/2}$ ideal power required to hover

C_Q torque coefficient defined in Equation [3], actual power required to hover

Noonan (18) used the figure of merit presented in Equation [4] to calculate the efficiency of helicopter main rotors, but in this experiment it is used to evaluate the overall efficiency of the craft being tested.

The ambient pressure and temperature were monitored and remained relatively constant throughout the various tests. The density of air was recalculated and a value of 1.2 kg/m^3 was used for the calculations in this experiment.

Section 2 - First Group of Tests

The first group of tests was important in establishing the trends in performance for the different configurations and conditions. In this section, part of the data collected at heights above the ground plane equal to 1/8 diameter and in free flight, or out of ground effect (OGE), for different configurations of the craft is presented in 6 separate graphs. These results include values of torque versus propeller rotational velocity (Figures 19 and 20), lift versus propeller rotational velocity (Figures 21 and 22) and finally efficiency (based on the Figure of Merit calculated from Equation [4]) versus propeller rotational velocity (Figures 23 and 24). The results were affected by vibrations at certain specific rotational velocities, more specifically 5850 rpm and a narrow band around it, and also to a lesser extent at 3800 rpm. These rotational speeds translate into propeller tip speed of about 62 m/s and 33.5 m/s, Mach numbers of 0.18 and 0.1 respectively. The vibrations were possibly caused by the natural frequency of the propeller and motor setup. No abnormal vibrations were noticed at other propeller velocities and the remaining data points remained unaffected. The propeller vibrations resulted in a decrease in total lift measured by the load cell. A likely explanation for the reduction in lift is the decrease in the propeller blade's performance and the loss of energy in the form of vibration.

Plots of lift, torque and efficiency versus propeller rotational speed for the data collected during the first group of tests are presented in Appendix B. The benefits of ground effect were clearly observed through the larger values of lift from the straight and

Coanda nozzles configurations operating at lower heights, compared to the lift produced by the same nozzles at distances farther from the ground plane.

The first set of data also indicated that the straight nozzles configuration performed more efficiently than the Coanda nozzles configuration (data plots in Appendix B). Based on these findings, three main configurations were selected for the second group of tests:

1. The propeller (only) configuration
2. Coanda nozzles configuration with downward flow deflector
3. Straight nozzles configuration with downward flow deflector

Section 3 - Second Group of Tests

In the second group of tests, the three selected configurations were tested in a manner similar to the first test group. The data sets in the second group were composed of fewer points than the first set of data (4 less data points per run), but special attention was taken at the measurements around 5850 rpm to ensure that the effects of vibration (in the form of a reduction in lift) had been corrected or minimized.

Section 3.1 - Torque Plots

The second group of data was analyzed and plotted. Figures 19 through 22 are plots of the torque versus propeller rotational velocity.

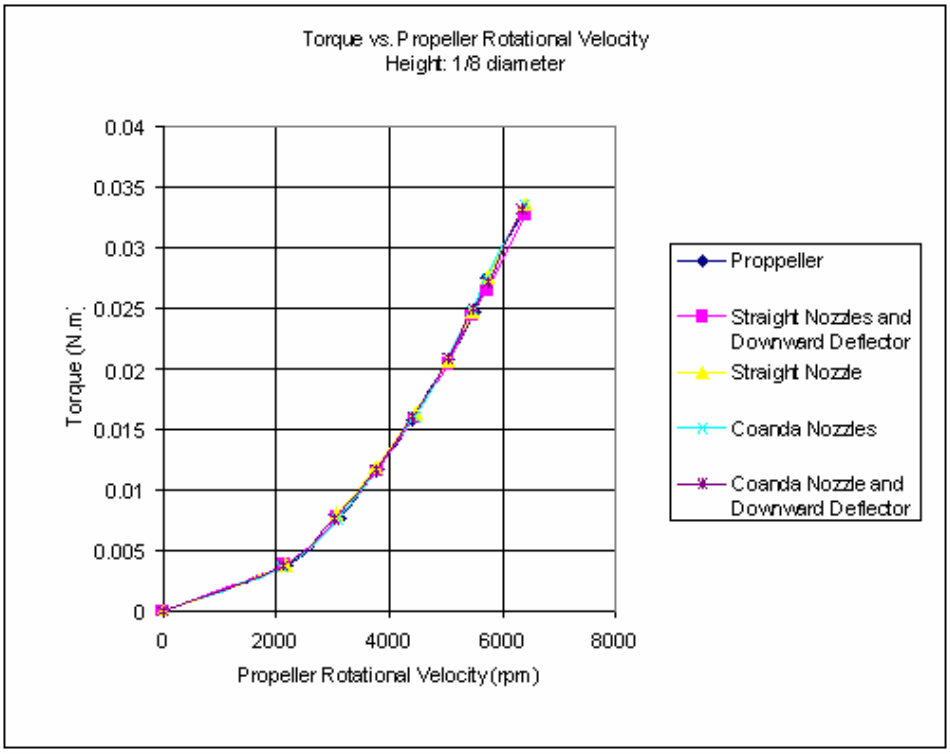

Figure 19: Torque vs. propeller rotational velocity at 1/8 diameter height

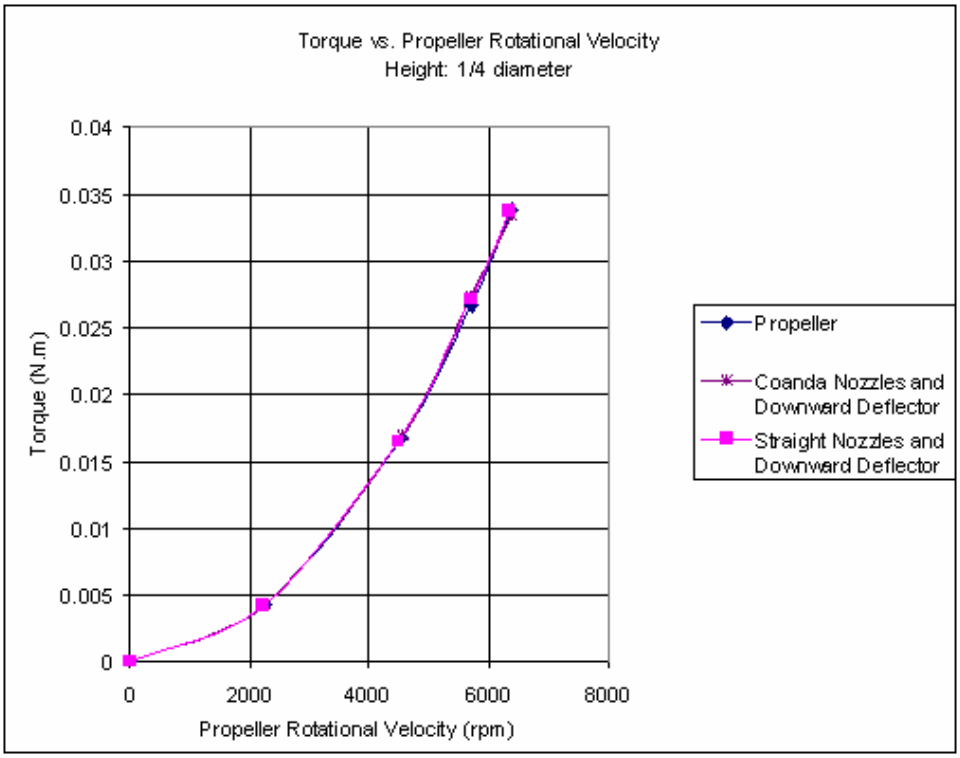

Figure 20: Torque vs. propeller rotational velocity at 1/4 diameter height

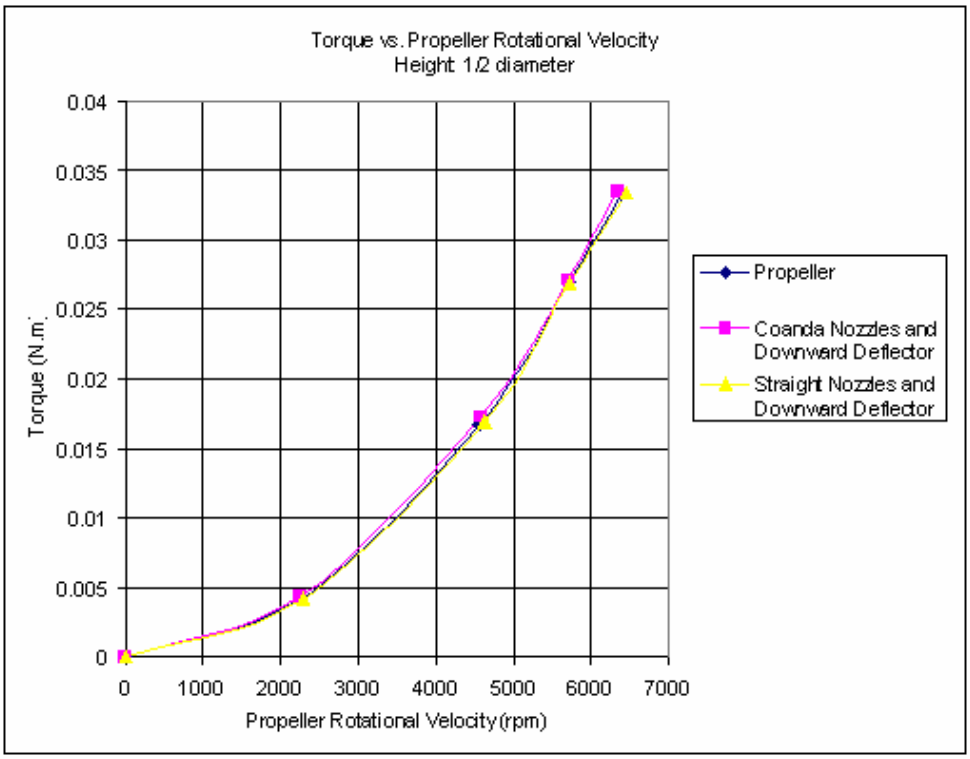

Figure 21: Torque vs. propeller rotational velocity at 1/2 diameter height

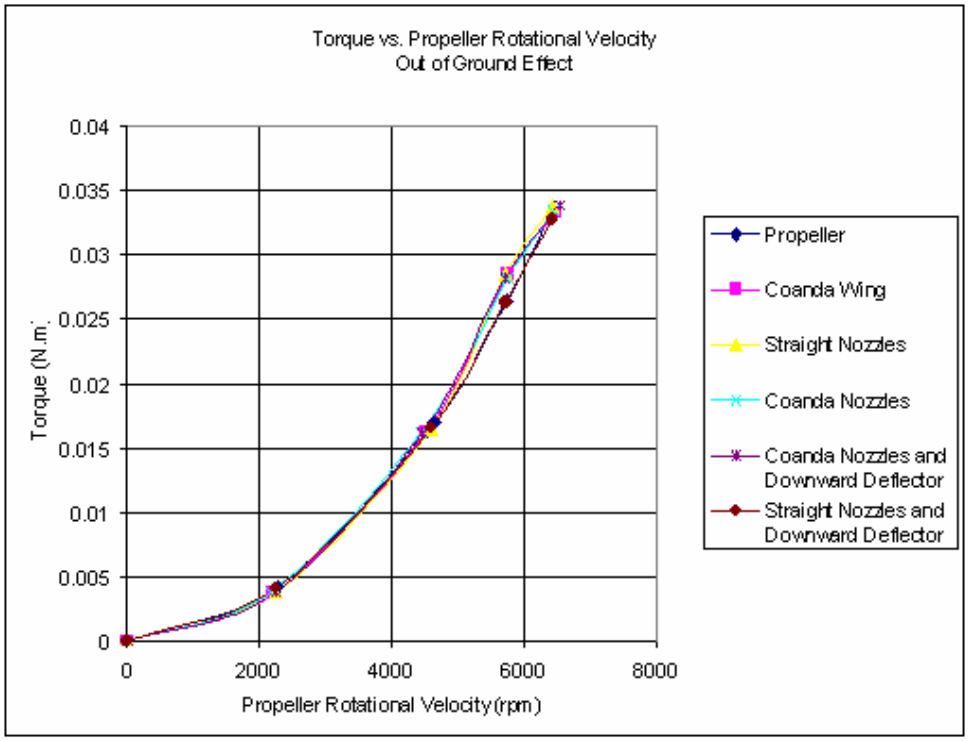

Figure 22: Torque vs. propeller rotational velocity out of ground effect

The results from the torque measurements, presented in Figures 19 through 22, agree with observations made regarding torque in the first group of tests, confirming torque to be a function of rotational velocity in the range of 0 rpm to 6400 rpm (the range used in this experiment). Also observed in the first data group, were the effects of the different configurations and distances on torque and rotational velocity relations, which seemed negligible in the tested conditions. All three configurations and craft heights demonstrated the same basic values and trends for all data points. It is important to notice, that although the effects of vibration were greatly reduced in the 5850 rpm range, they were still present and became more noticeable when operating at larger distances from the ground.

In addition, the tests performed at heights 1/8 diameter and OGE included configurations with the Coanda nozzles and the Straight nozzles without the downward deflector nozzles. These tests were made to confirm and compare the performance of the craft with and without the deflector. However, the comparisons and analysis made here (using the data collected in the second group of tests) refer to the configurations that include the downward deflector, although they are often simply referred to as "Coanda nozzles configuration" and straight nozzles configuration."

The tests performed OGE also include the Coanda Wing configuration (no nozzles present on the lower portion of the craft) as a means to validate the previous observations and provide an extra parameter for comparisons.

3.2- Lift Plots

Greater insight into the performance of the different configurations is gained by studying the values of lift versus propeller rotational speed. The information collected at all four tested heights is presented in Figures 23 thru 26.

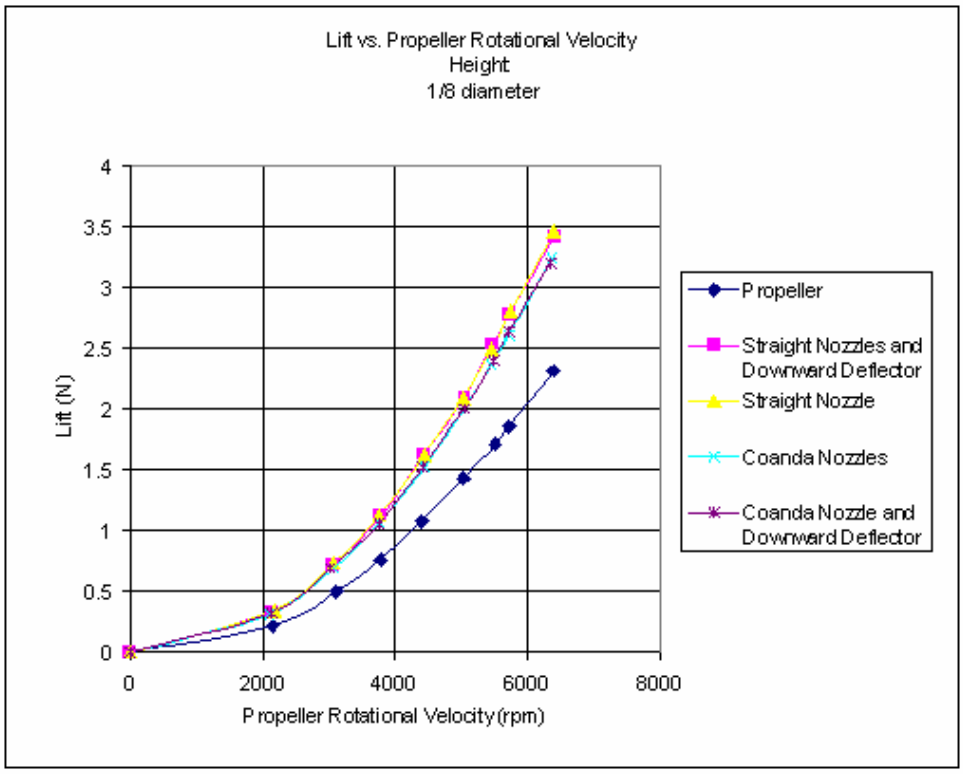

Figure 23: Lift vs. propeller rotational velocity at 1/8 diameter height

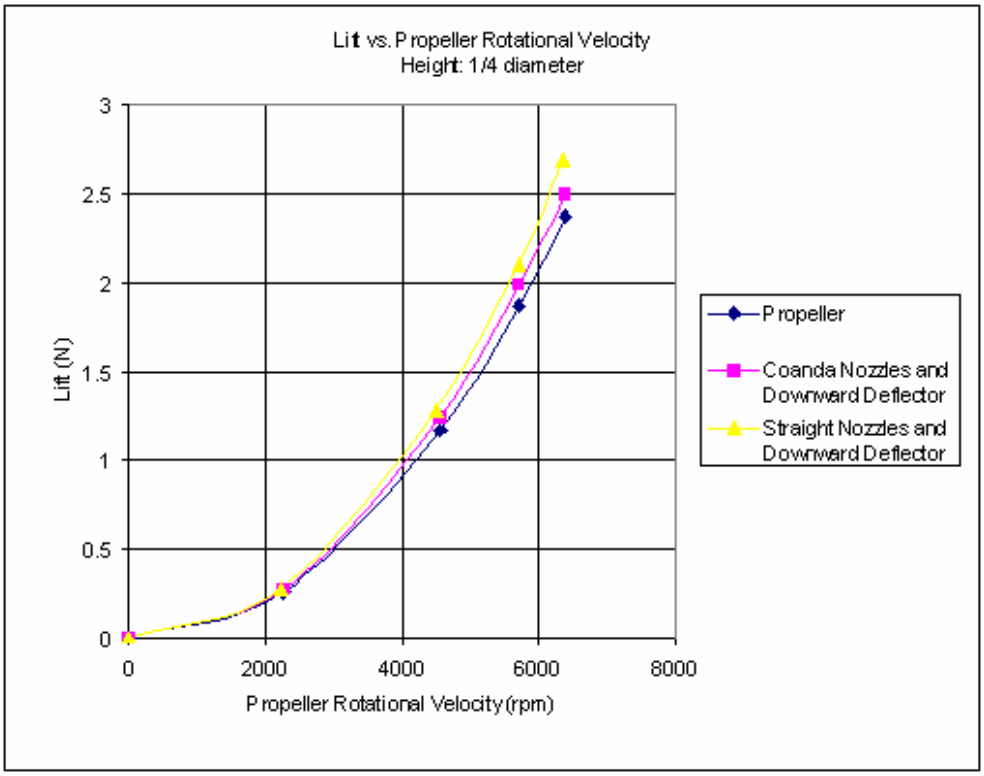

Figure 24: Lift vs. propeller rotational velocity at 1/4 diameter height

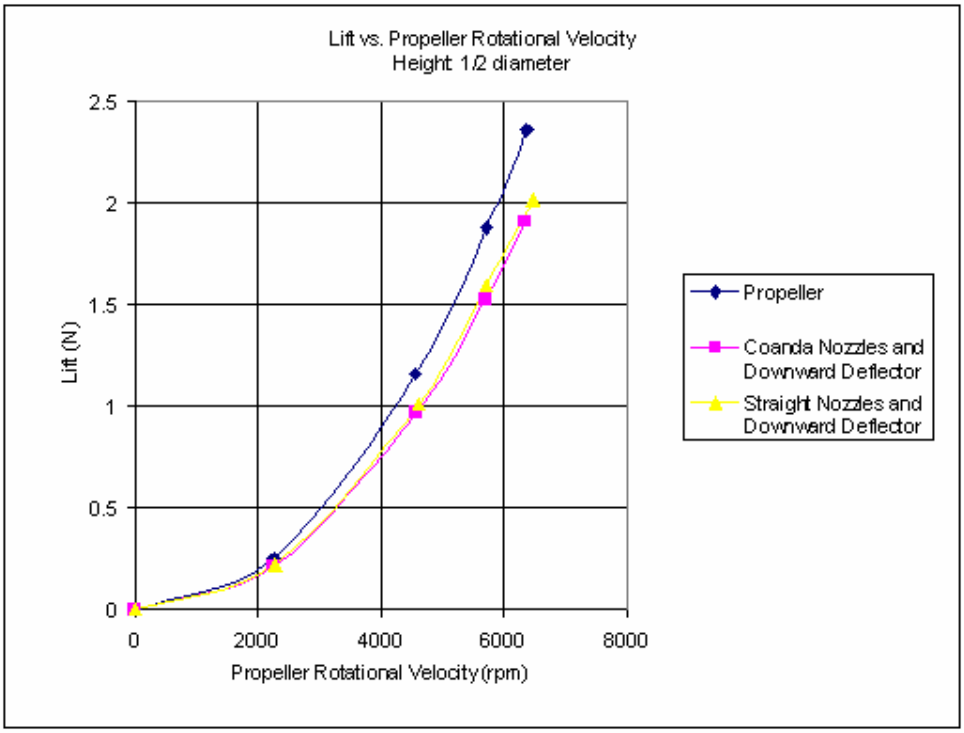

Figure 25: Lift vs. propeller rotational velocity at 1/2 diameter height

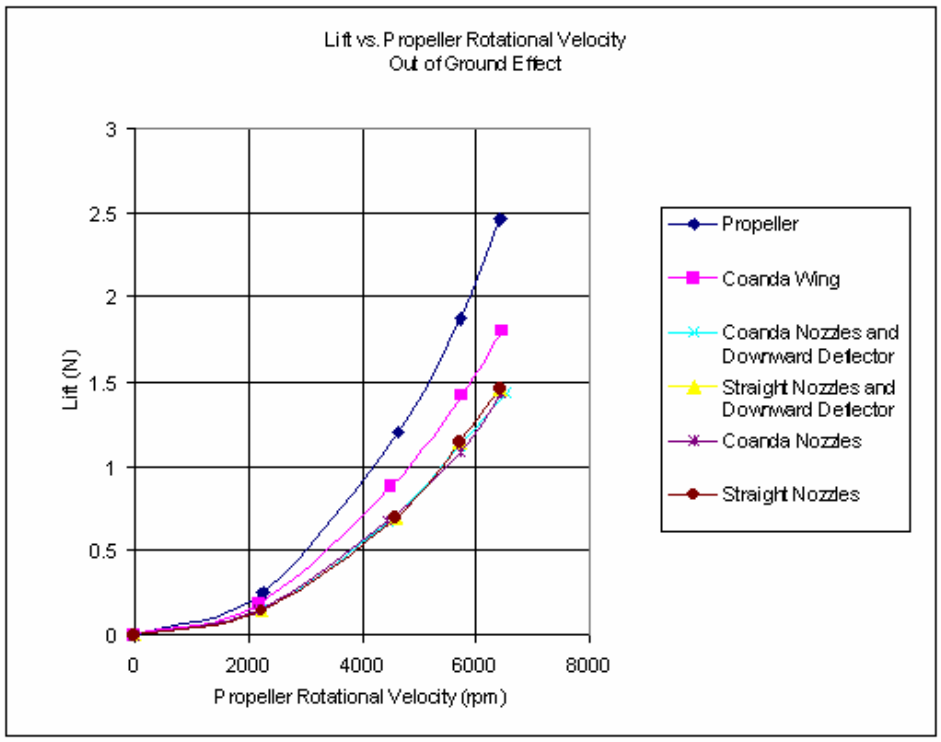

Figure 26: Lift vs. propeller rotational velocity out of ground effect

As it can be seen in Figures 23 through 26, the data collected at propeller velocities in the 5850 rpm range show a significant reduction in the influence of vibrations when compared to those found in the first group of tests. The reduction in vibration was achieved by performing adjustments to the testing setup and ensuring that its components were properly secured in place. Once again, lift was found to be inversely affected by height above the ground plane for the two configurations where nozzles were present (straight nozzles and Coanda nozzles), confirming the existence of a beneficial interaction between the craft and the ground plane regarding the production of lift. These benefits are significant, especially at the lower tested heights of 1/8 diameter, where the Coanda nozzles and the straight nozzles configurations improved the overall lift by 37% and 48% respectively, in relation to the lift generated by the simple propeller

configuration (at speeds around 6350 rpm. At a height between 1/4 and 1/2 diameter, however, the propeller begins to produce more lift than the other two configurations, a clear reflection of the diminishing interactions with the ground plane.

The benefits from the nozzles are clearly suppressed by the increase in cross sectional area and subsequent increase in the total drag for the craft. This can be confirmed by comparing the lift when tests were performed OGE for the Coanda and straight nozzles configurations to the results obtained for the Coanda wing configuration (in which the nozzles are simply removed - only the clear plastic dome seen in Figure 16 was left in the path of the propeller's downwash, allowing a more clear path for the flow)

Agreeing with observations made in the previous group of tests, the straight nozzles configuration generated more lift than the Coanda nozzles configuration at similar propeller velocities. This was true for all 4 heights. Although the overall larger value of lift can be noticed in the plots, a specific relation for the difference in lift between the two configurations could not be established due to small imperfections in the tests and the overall complexity of all the mechanisms involved in the production of lift. Figure 27, however, illustrates the constantly larger (although not constant in magnitude) values of lift obtained with the straight nozzles configuration over the Coanda nozzles configuration. The plot was made with data collected at a height of 1/8 diameter and varying propeller speeds.

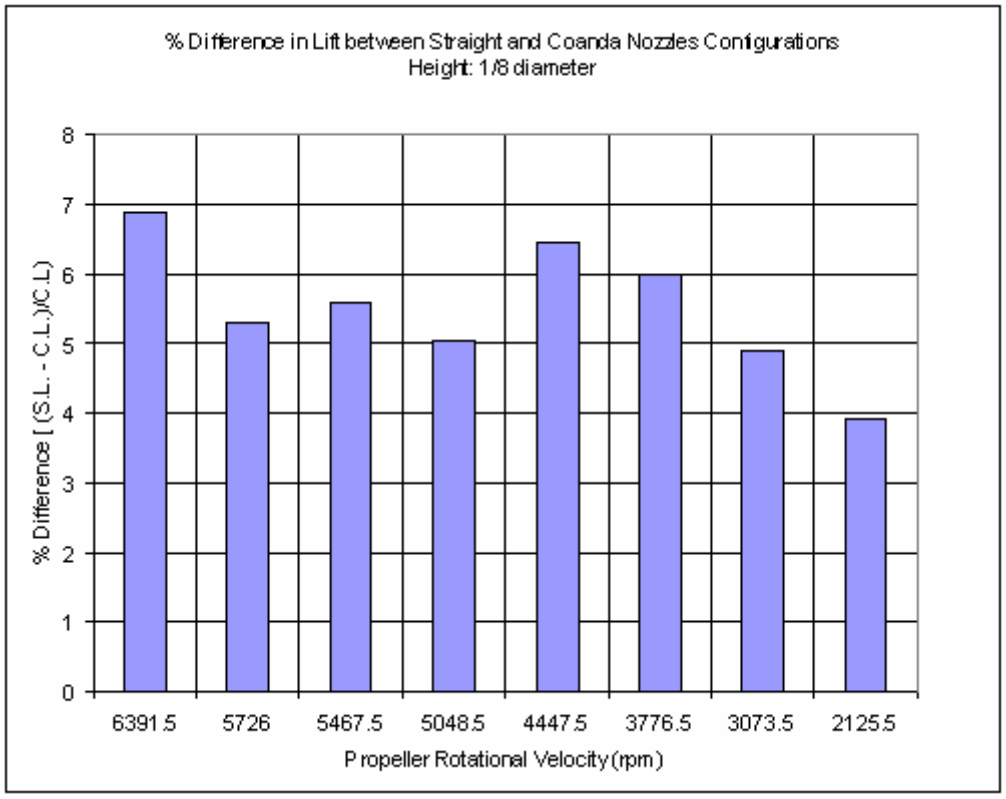

Figure 27: Percentage difference in lift between Coanda nozzles and straight nozzles configurations at 1/8 diameter height, and varying propeller rotational velocity

Section 3.3 - Efficiency

A better comparison between the tested configurations can be made by calculating and analyzing the efficiencies of each variant. A more efficient configuration is capable of providing more lift for a given amount of power compared to other less efficient configurations of the same vehicle. Following the same formula to calculate a figure of merit, presented in Equation [4], the efficiencies at all four heights were calculated and are presented in Figures 28 through 31. From the previous observations of torque and lift, the trends presented in these figures come as no surprise.

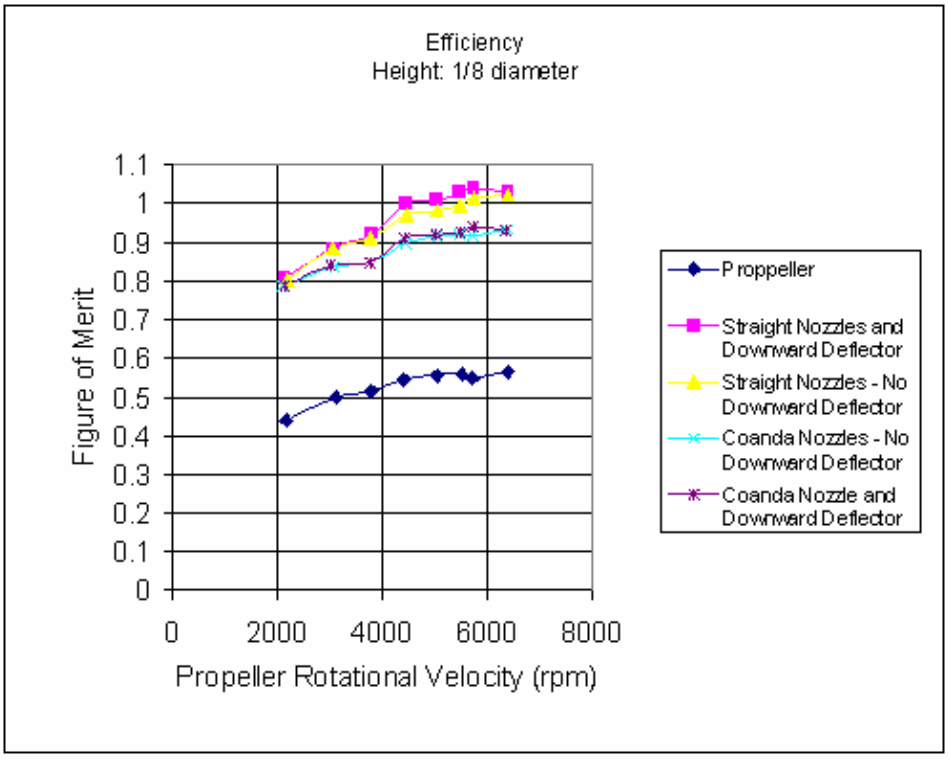

Figure 28: Efficiency vs. propeller rotational velocity at 1/8 diameter height

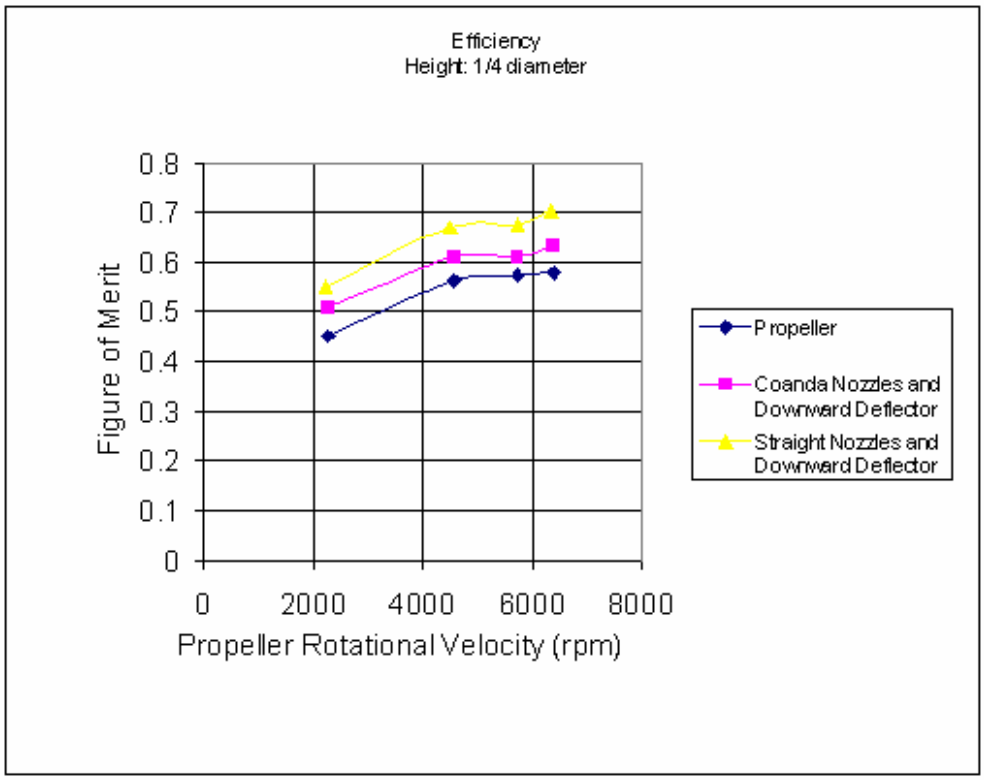

Figure 29: Efficiency vs. propeller rotational velocity at 1/4 diameter height

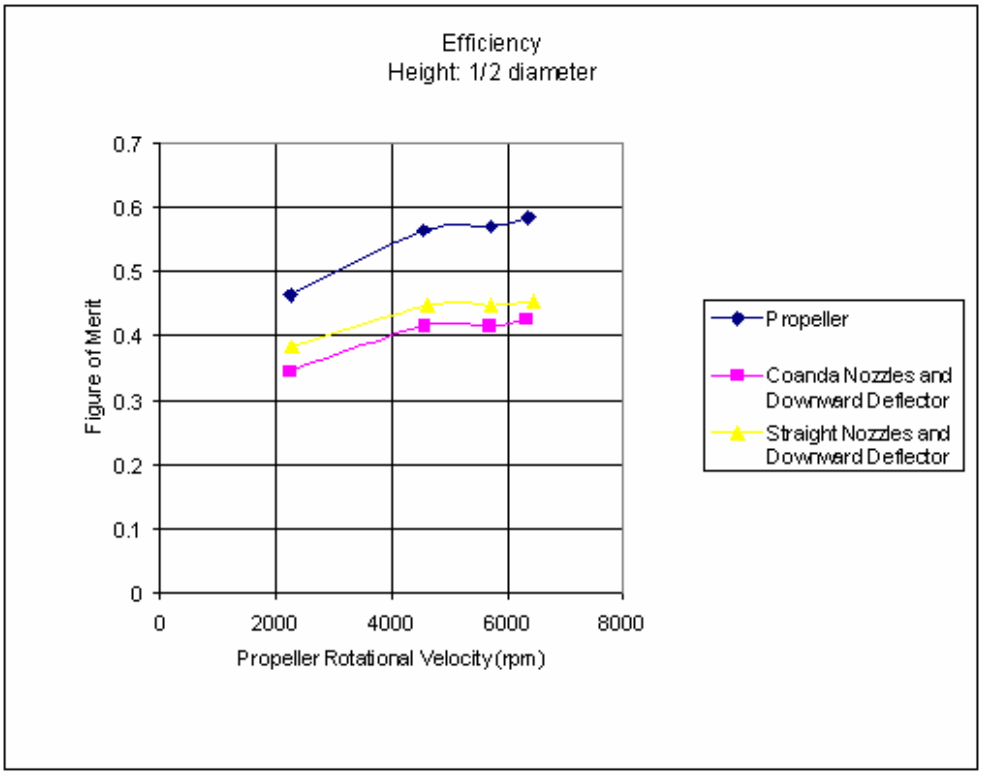

Figure 30: Efficiency vs. propeller rotational velocity at 1/2 diameter height

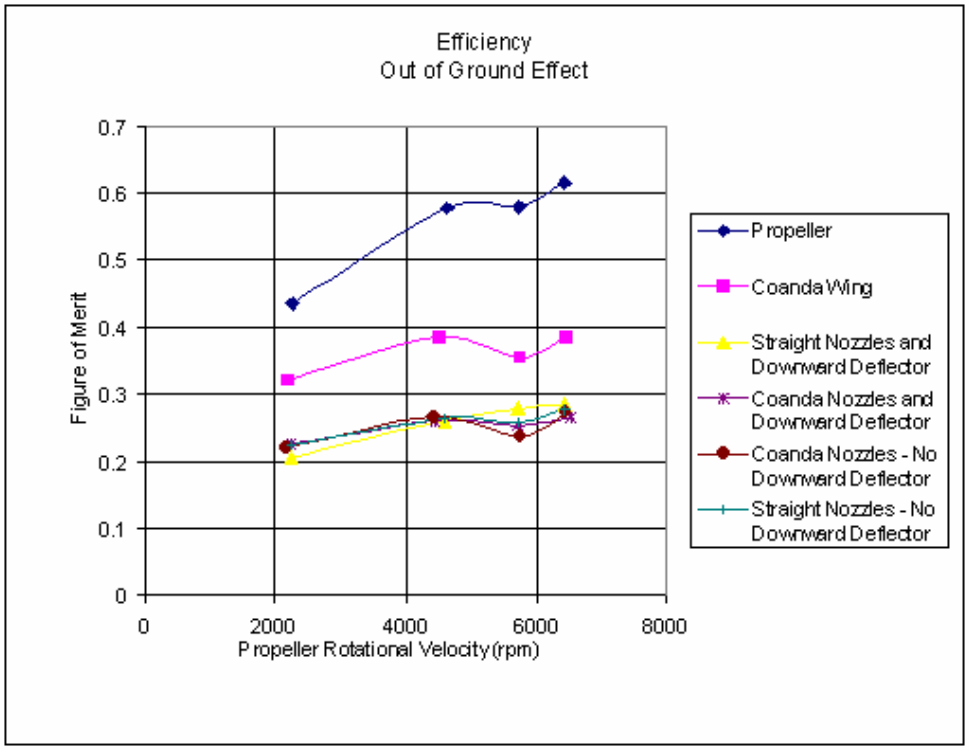

Figure 31: Efficiency vs. propeller rotational velocity out of ground effect

The efficiencies were calculated based on the figure of merit Equation [4], normally used in the analysis of helicopters. A maximum figure of merit value of one would be expected for an ideal case of a helicopter. Data from the 1/8 diameter height tests presented in Figure 28, however, shows a maximum figure of merit of near 1.04 for the straight nozzles configuration (and other values larger than one for both straight nozzles and Coanda nozzles configurations at the higher propeller rotational velocities). This may seem wrong, but it is important to take into consideration the fact that Equation [4] was derived studies performed on helicopters. The existence of nozzles and other components on the craft, as well as the stronger influence of the ground effect as the 1/8 diameter height causes the relationship between lift coefficient and torque coefficient to change, resulting in figure of merit values larger than one. The overall pattern between the different configurations, however, is unaffected by the value of the figure of merit. As expected, the efficiencies follow a similar trend as lift, with the straight nozzles configuration outperforming the Coanda nozzles configuration at all heights and propeller rotational velocities, and both performing better than the propeller only configuration when operating in ground effect. Both Coanda and straight nozzles configurations become less efficient than the propeller configuration at a point between 1/4 and 1/2 diameter.

When again comparing lift and efficiency produced by the configurations that include the downward flow deflector to the variants that do not (within the same Coanda or straight nozzles basic configuration), we can confirm a slightly better performance when the deflector is installed.

Section 3.4 - Constant Propeller Rotational Velocity, Varying Height

The lift produced at distances of 1/8, 1/4 and 1/2 diameter above the ground plane, was found to be inversely related to height. This was true for both Coanda and straight nozzles configurations (both with the downward flow deflector installed), while the propeller only configuration presented the opposite behavior. Better understanding of the overall behavior of the three configurations can be gained by plotting the values of lift coefficient (calculated with Equation [2]) at similar propeller angular velocities (6350 rpm range) and varying heights. Figure 32 below presents the lift coefficients at the 4 distinct heights.

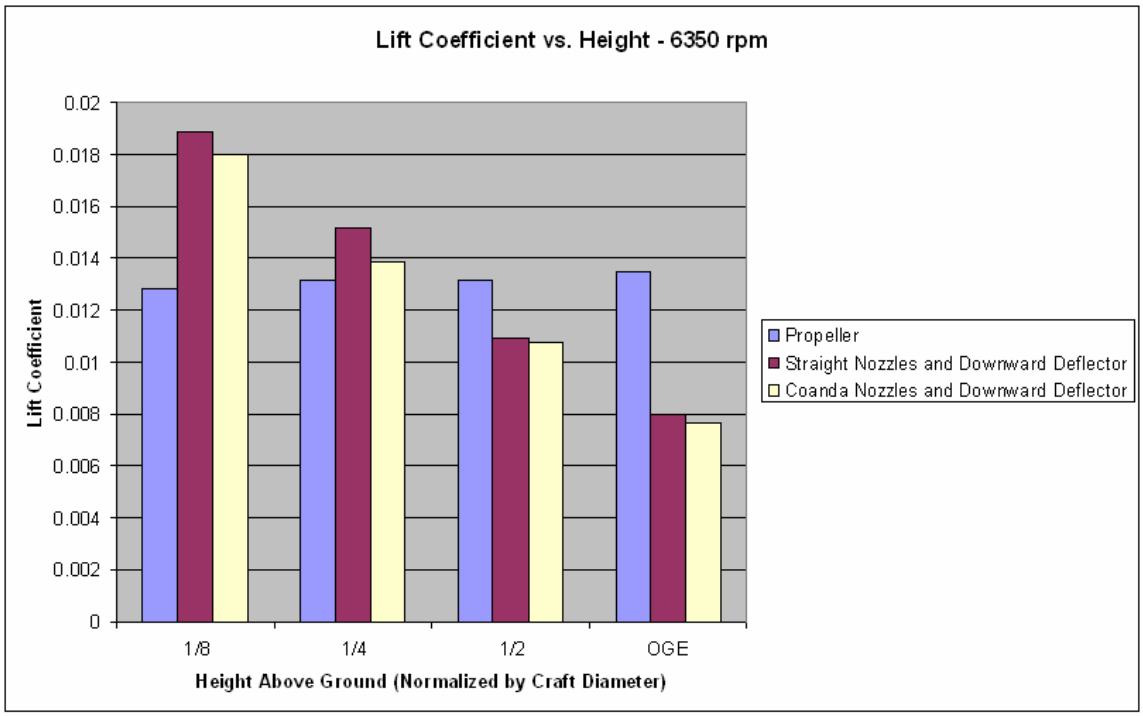

Figure 32: Lift coefficient vs. height - 6350 rpm range

The benefits of ground effect at the lower heights can be clearly seen in Figure 32, through the larger values of lift coefficient at the lower heights. The influence of ground effect in the lift coefficient, however, rapidly diminishes as craft-ground distance increases. The advantage of the straight nozzles configuration over the Coanda nozzles configuration also seems to decrease at higher altitudes.

A plot of the efficiencies in the form of figures of merit, Figure 33, based on the same data set at 6350 rpm, confirms the same observations made from the previous graph.

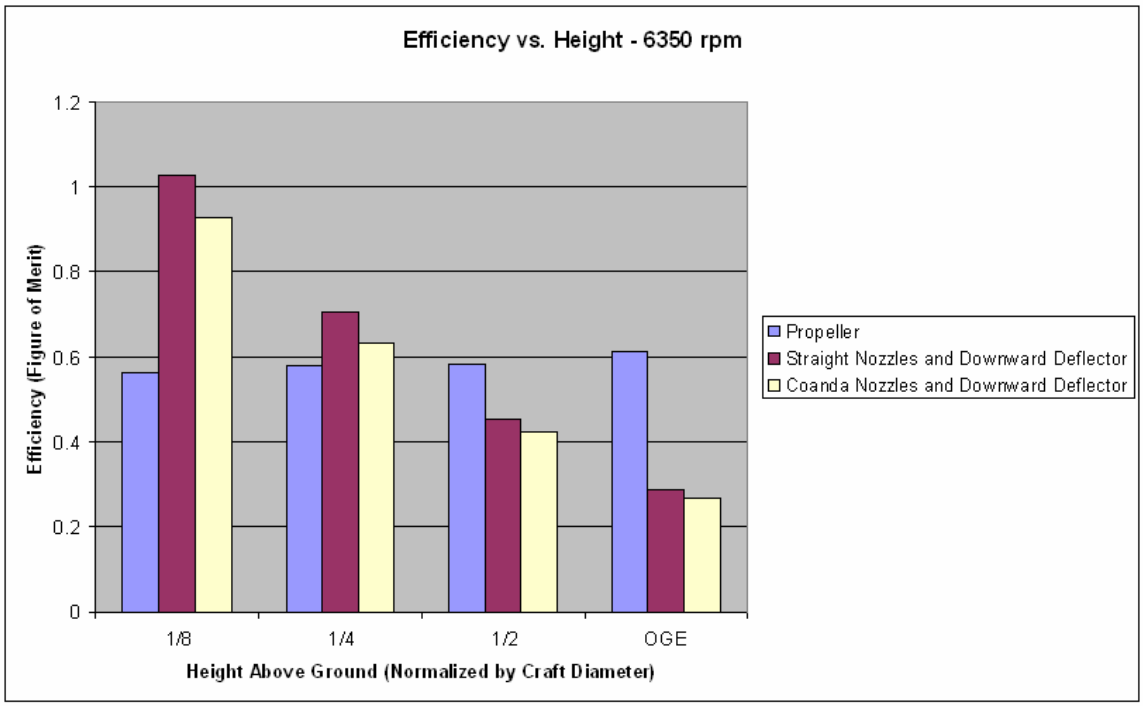

Figure 33: Efficiency vs. height at 6350 rpm

Section 3.5 – Propeller: Adverse Ground Effect

The plots of the projected data, Figures 32 and 33, indicate a trend not previously noticed. The "propeller configuration" showed a slightly increasing performance with

increasing heights, resulting in an overall improved efficiency of around 9% (Figure 33). The data for the propeller configuration was collected at the specified heights by simply removing the rest of the craft (Coanda Wing and nozzles section) from the setup; the propeller, was kept in its original position in relation to the ground plane. The change in the coefficient of lift is consistent with what Cerbe (11) reports regarding helicopters hovering at heights around 4 times the propeller radius. At these heights, the proximity to the ground produces an unfavorable effect, likely due to flow recirculation, while the benefits of an aircushion would only become significant at distances smaller than the critical hovering height of 1.7 blade radius. Recirculation is known to affect helicopters and result in a larger power requirement for certain hovering altitudes IGE than when hovering OGE.

Section 4 – Coanda nozzles vs. Straight Nozzles

To better understand the reasons leading to a better performance of the straight nozzles configuration compared to the Coanda nozzles configuration, more tests had to be made. In order to identify the exact cause of the difference in performance, the most probable source, or feature, was isolated. The inner nozzles (all nozzles with exception of the peripheral nozzles that form the peripheral air curtain) were removed and replaced by a flat surface (Figure 72 in Appendix D). The peripheral nozzles became the only outlet on the bottom of the craft. After these tests were performed, the peripheral nozzles were also covered (from inside the plenum), allowing no air to exit the plenum chamber from the bottom portion of the craft. The tests were performed at 1/8 diameter from the

ground plane and again OGE. The results from the lift measurements for all four variants of the craft are presented in Figures 40 and 41.

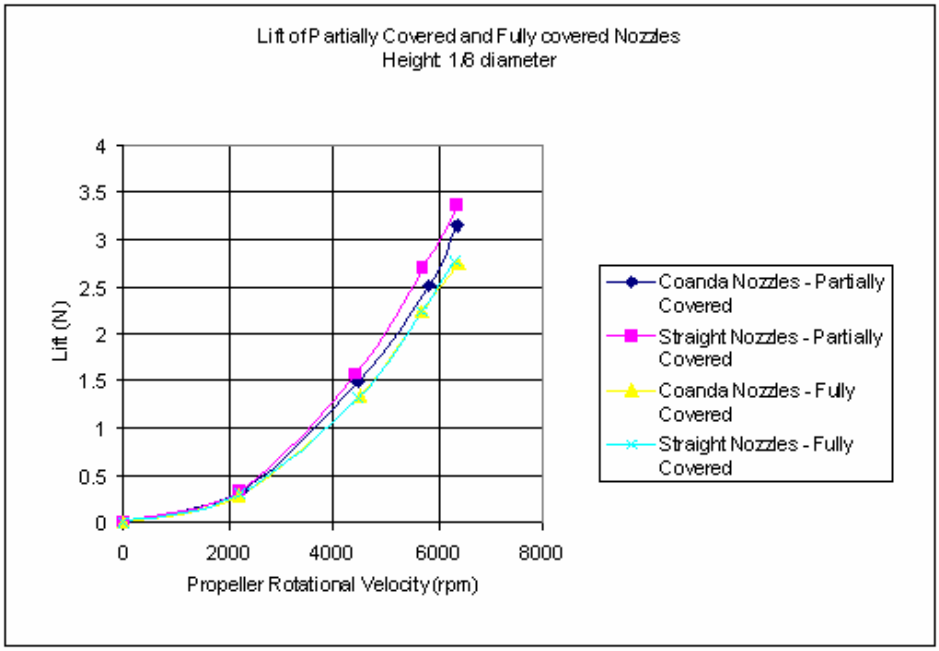

Figure 34: Lift vs. propeller rotational velocity. Covered and partially covered nozzles at 1/8 diameter height

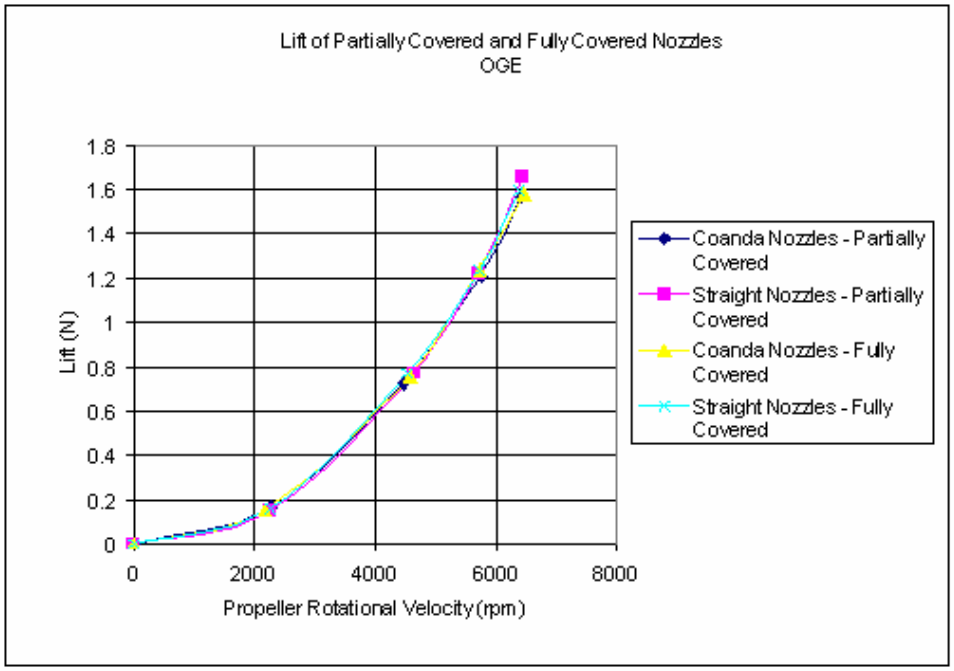

Figure 35: Lift vs. propeller rotational velocity. Covered and partially covered nozzles, out of ground effect

The plots of lift versus propeller rotational velocity for the partially covered nozzles configurations confirm what had been previously observed. The straight nozzles configuration produces more lift than the Coanda nozzles configuration. As expected, the results obtained with all nozzles fully covered indicate a reduction in lift compared to the partially covered nozzles configurations. These results also indicate what can be considered identical performances between the Coanda nozzles and the straight nozzles configuration when all nozzles are fully covered. A conclusion drawn from these groups of tests is that the peripheral nozzles are indeed important in the production of lift. The variations on these nozzles, having a Coanda surface or a straight surface immediately following the exit from the Plenum chamber, is also an important factor determining the amount of lift produced.

To study the performance of the inner nozzles, the data from the uncovered nozzles configurations as well as the propeller configuration were plotted in the same graph as above. This allows for an overall performance analysis by comparison of uncovered and covered inner nozzles. Figure 42 below shows a comparison of lift between the data sets.

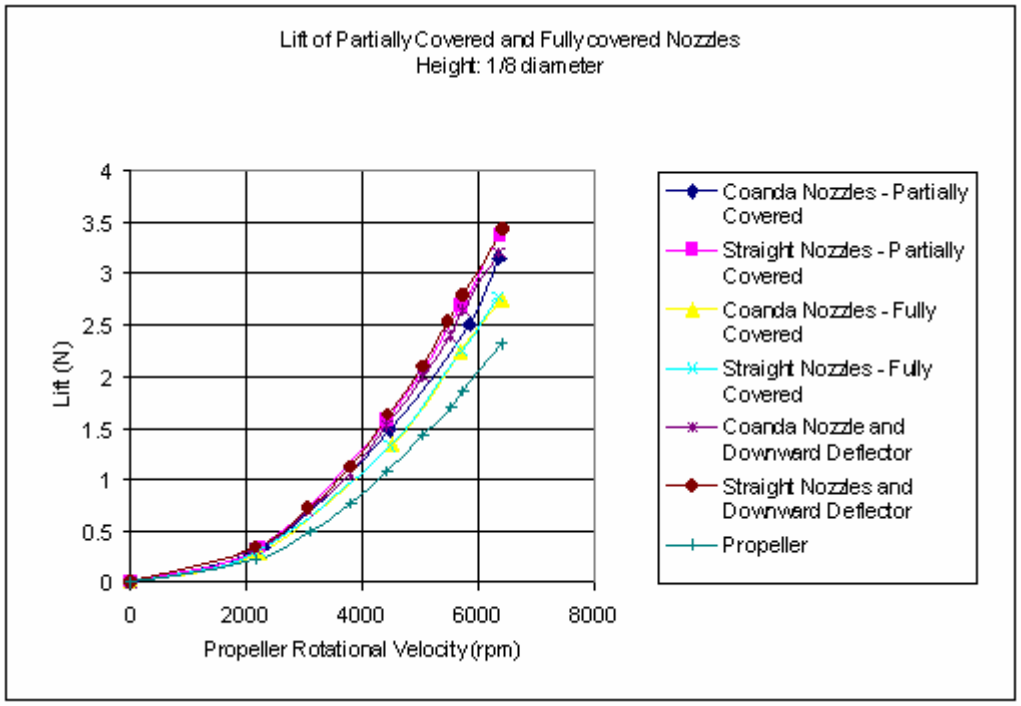

Figure 36: Lift vs. propeller rotational velocity. Covered and fully covered nozzles comparison with open nozzles configurations at 1/8 diameter height

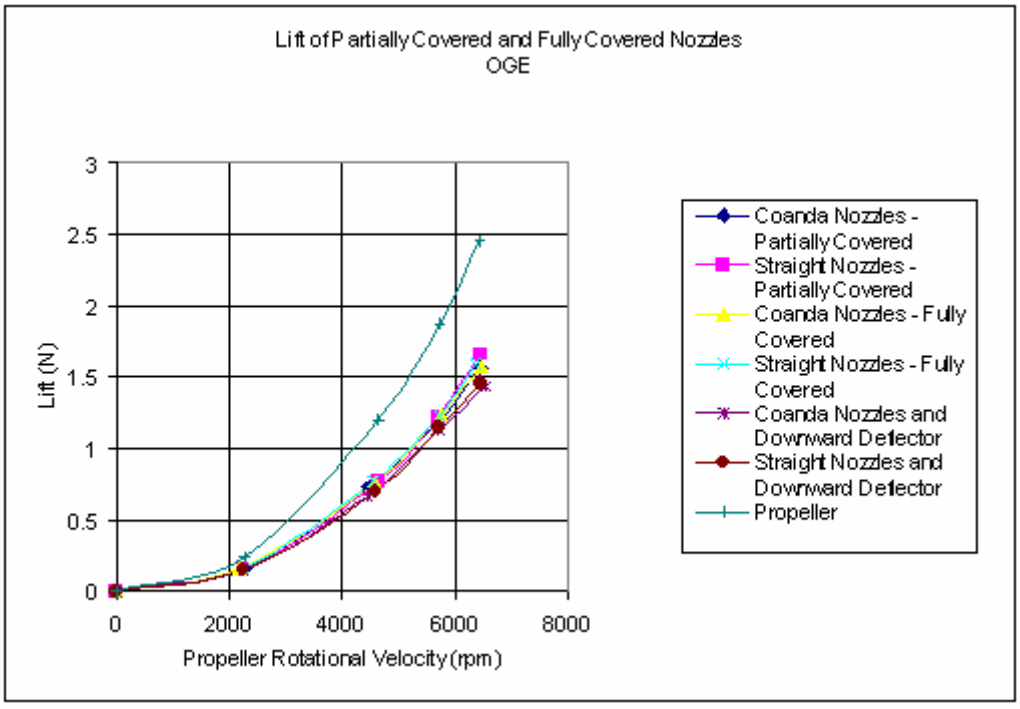

Figure 37: Lift vs. propeller rotational velocity. Covered and fully covered nozzles comparison with open nozzles configurations, out of ground effect

Curiously, the partially covered nozzles (inner nozzles covered) configurations seem to perform very similarly to their uncovered original configurations close to the ground plane (1/8 diameter height). This may point to an ineffectiveness of the central nozzles, at least during a static hovering situation as performed in this experiment. The plot of lift at heights OGE indicates that the fully covered and the partially covered nozzles configurations performed very similarly when not interacting with the ground plane. Very interestingly, the original uncovered nozzles configurations seem to under-perform in comparison to their covered nozzles variants. The lack of detailed information regarding the exact flow distribution around and inside the craft does not allow any definite conclusions regarding this fact. A likely explanation, however, might be found by analyzing the flow inside the plenum chamber and on the bottom surface of the craft, when operating OGE. The efficiencies for all seven configurations plotted for both heights (Figures 44 and 45) support the previous observations.

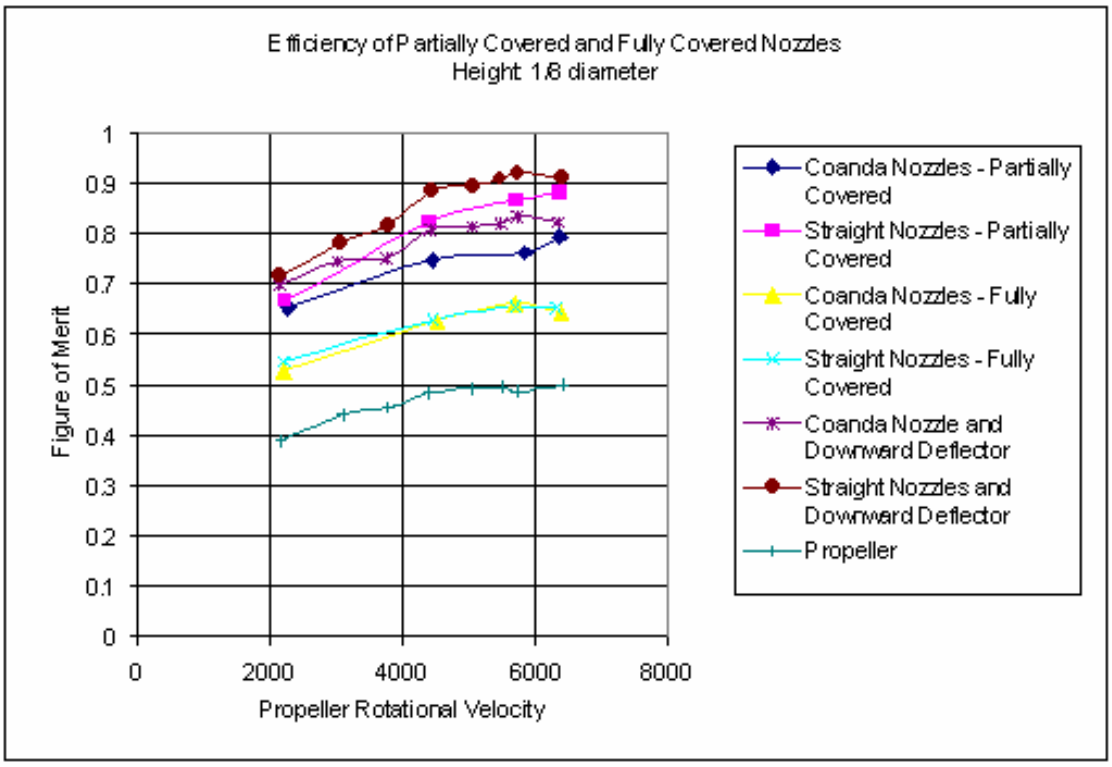

Figure 38: Efficiency vs. propeller rotational velocity. Covered and fully covered nozzles comparison with open nozzles configurations at 1/8 diameter height

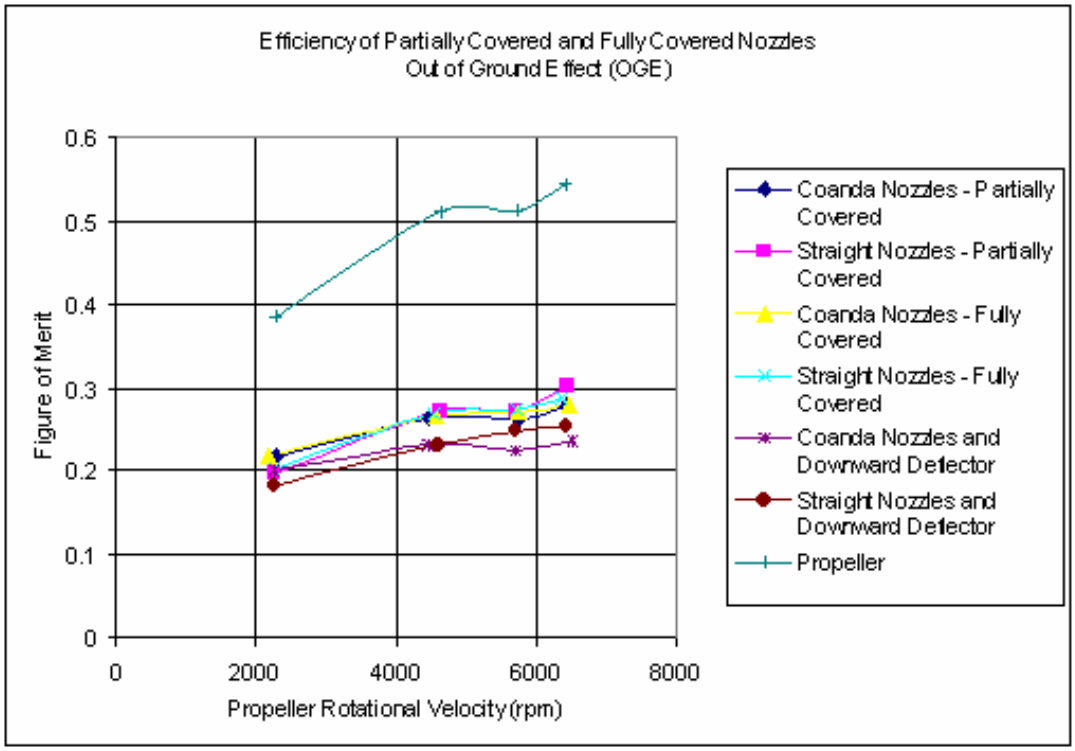

Figure 39 Covered and fully covered nozzles comparison with open nozzles configurations, out of ground effect

Section 5 – Flow and Pressure Distribution

Section 5.1- Pressure Distribution 1/8 Diameter Height

To better understand the mechanisms involved in the straight nozzles configuration more efficient performance over the Coanda nozzles configurations, velocity and pressure measurements were taken at distinct points around the craft. The two configurations were fully assembled (all nozzles and deflector present) and 5 pressure taps were installed on the lower portion and nozzles of the craft, and two more inside. The pressure measurements in other areas were taken using the static port of a Pitot-static probe. Measurements were taken at three heights, 1/8 diameter, 1/4 diameter and OGE at 6350 rpm. The pressure data collected at 1/8 diameter and OGE are presented in figures 46 and 47, on one half of the cross-sectional view of the craft. These numbers represent the difference between the local measured pressure and ambient pressure (gauge pressure) in Pa.

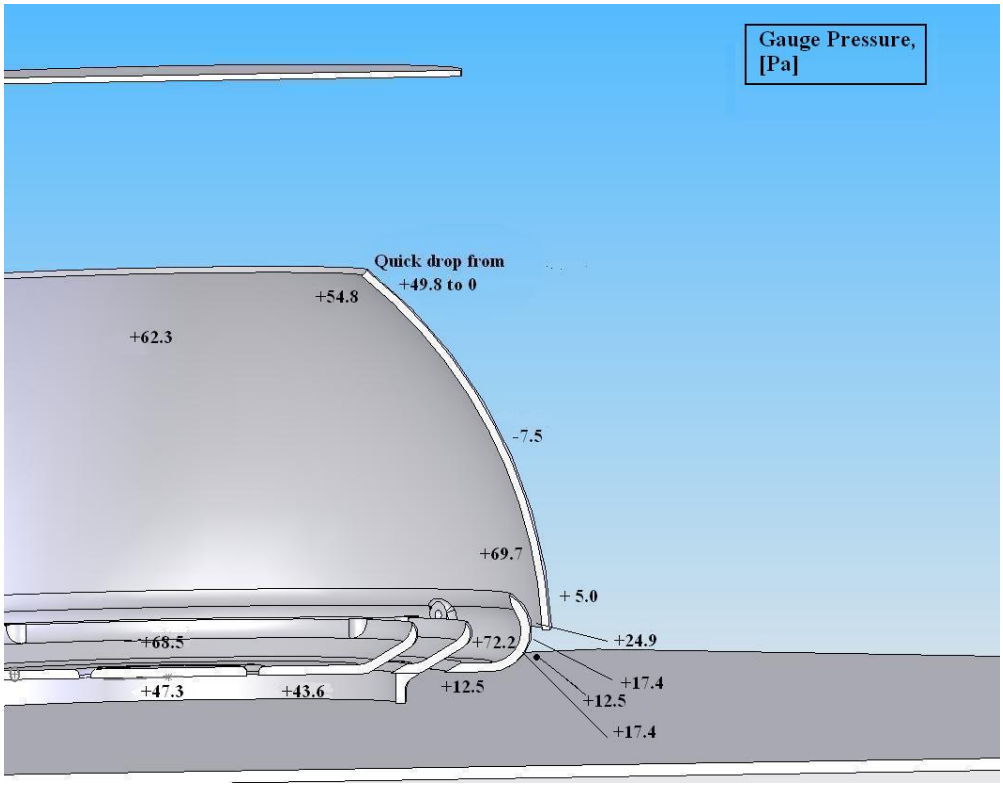

Figure 40: Coanda nozzles pressure distribution at 1/8 diameter height

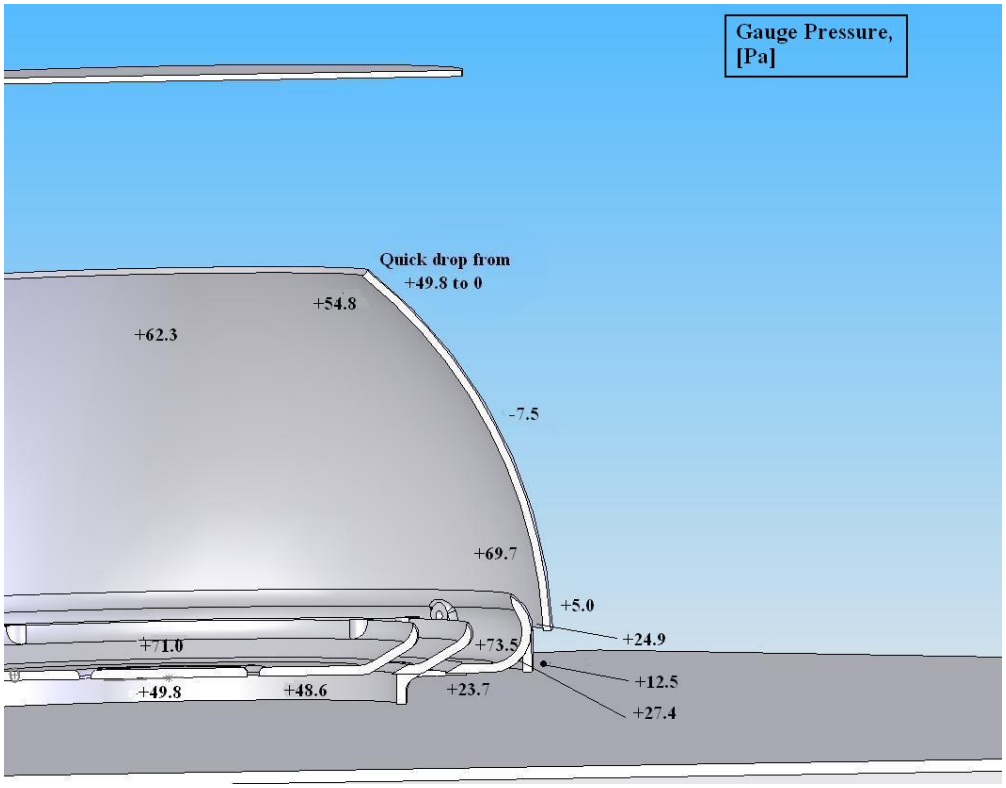

Figure 41: Straight nozzles pressure distribution at 1/8 diameter height

The pressure distributions are very similar on the inner and top portions of the craft for both configurations. However, the values found around the peripheral nozzles and the surrounding areas on the bottom surface show a difference between the two configurations. The pressure tap located at 45 degrees from the peripheral nozzles' exit was used to measure pressure in both cases. This pressure tap is located on the Coanda surface, but it remained open to collect pressure data even once the straight nozzles were installed (the straight nozzles were formed by adding a ring shaped device around the Coanda surface, canceling the effects of its curvature on the flow). Figures 48 and 49 below show a closer view of the peripheral nozzles and the pressures around them.

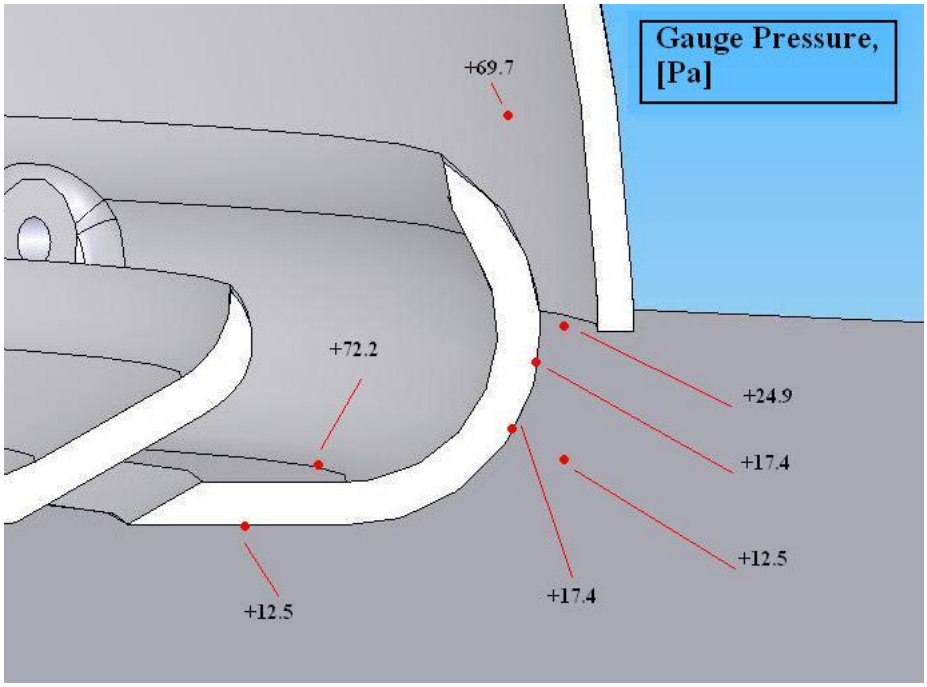

Figure 42: Close view of coanda nozzles pressure distribution at 1/8 diameter height

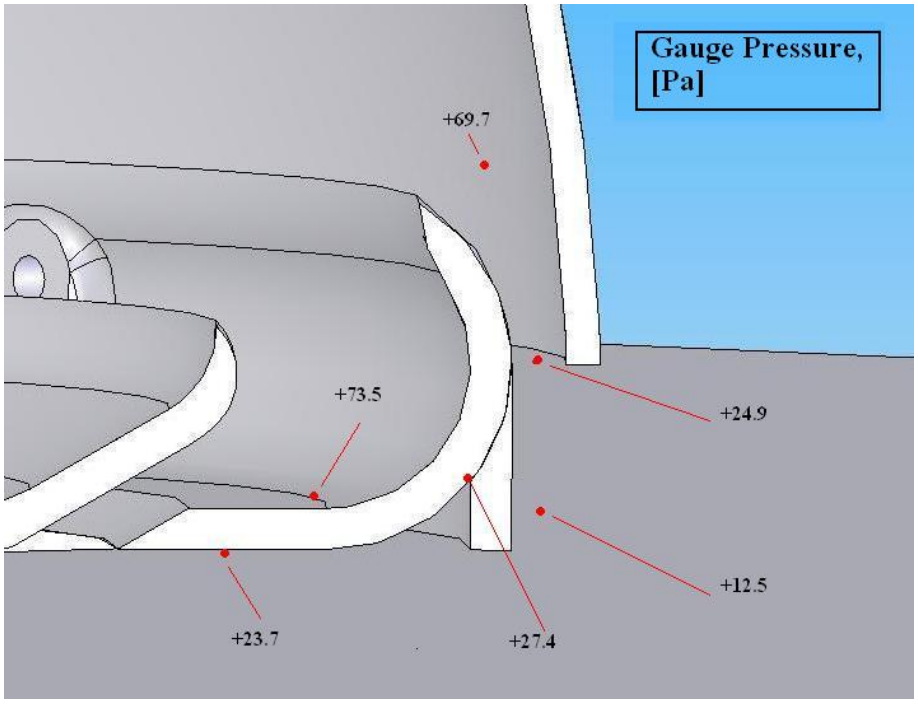

Figure 43: Close view of straight nozzles pressure distribution at 1/8 diameter height

The straight nozzles allow for a pressure build up on the peripheral region of the craft, especially in the area that would otherwise be occupied by the Coanda surface. This increase in pressure, of about 10 Pa, is the main cause of the difference in lift between the two configurations. The higher pressure in this region also leads to higher pressures on the surrounding areas under the craft. The mechanism behind this increase in local pressure could not be fully investigated with the time and resources available, but it may be caused by the simple increase in the surface area closer to the ground (by adding the straight nozzles, the effective total area of the lower surface increases). Given the large pressure increase in the region, however, it is also possible that the formation of vortices inside the "notch" formed by the added Straight Nozzle and the surface that acted as a Coanda surface, contribute to the pressure build up.

The difference in lift between the Coanda nozzles and the straight nozzles configuration can be found by integrating the pressures below the craft in both cases, and calculating the difference between the results. More time and resources would allow for a more detailed mapping of the pressure distribution under the craft, leading to a more accurate calculation of these forces. However, with the available data and a basic estimation of the pressure distribution under the vehicle, some crude but useful calculations can be made to justify the difference in lift between the two configurations.

The five pressure taps were located at the center of the craft, at 5 cm and at 10 cm from the center, and at 45 deg and 15 deg from the exit of the nozzle, on the Coanda surface (the pressure tap at 15 deg was not used in the straight nozzles configuration, it was physically blocked by the attachment ring that forms the straight nozzles). The pressure differences between the straight nozzles and the Coanda nozzles configurations are presented in Table 1:

Table 1: Difference in pressure between the two configurations at specific regions on the craft. Height: 1/8 diameter

Pressure Tap Location	ΔP=Ps - Pc- Pinternal [Pa]
Center	2.49
5 cm from Center	4.98
10 cm from Center	11.20
45 degrees (Coanda Surface)	9.96
Center, inside	2.49
Peripheral, inside	1.25

Figure 50 presents a rough estimate of the pressure distribution under the craft.

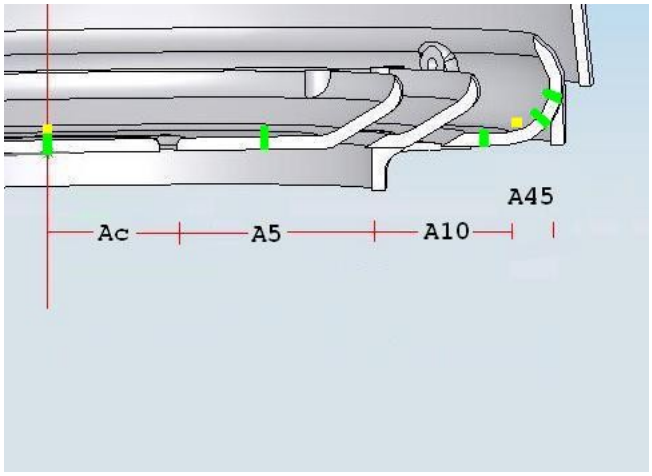

Figure 44: Estimate of pressure distribution regions under the craft

Where Ac, A5, A10 and A45 represent the areas affected by pressures equivalent to those found on the respective pressure taps. The green marks on the nozzles in Figure 44 indicate the locations of the pressure taps measuring pressures on the outer surface of the craft, and the yellow marks represent the internal pressure taps. The areas under each pressure tap were estimated and presented in Table 2:

Table 2: Estimated areas for each pressure region below the craft. Height: 1/8 diameter

Area under the influence of pressures measured at:	area [m^2]
Center	0.0070
5 cm from Center	0.0861
10 cm from Center	0.1813
45 degrees (Coanda Surface)	0.0744

The measurements taken by the two internal pressure taps can be used to calculate a pressure balance between the internal and the external pressures. The pressure measured with the tap located internally at the center can be subtracted from the pressures

at the Ac and A5 regions, and the pressure found at the internal peripheral pressure tap can be used to calculate the pressure balance under A10 and A45. The information presented above can be used to estimate the difference in lift between the two configurations through the Equation [5] below:

$$A_C.\Delta P_C + A_5.\Delta P_5 + A_{10}.\Delta P_{10} + A_{45}.\Delta P_{45} = Lift_{Straight} - Lift_{Coanda} \qquad [5]$$

The above equation yields a total difference in lift of 0.269 N. This figure is higher than the difference found when comparing measurements from the load cell at the same propeller rotational speed, which indicated a difference of about 0.220 N. The 0.05 N difference between these values, however, is very small and expected given the lack of detailed knowledge about the pressure distribution around the craft. More time and resources would likely close the gap between the results, but within the scope of this study, the results found using this method are adequate to justify the differences in lift between The Coanda nozzles and the straight nozzles configuration operating at 1/8 diameter height above the ground plane.

Section 5.2 - Pressure Distribution Out of Ground Effect (OGE)

When operating OGE, the pressure distribution under the craft differs significantly from what is found when in ground effect. Figures 51 and 52 show the values of pressure found at specific points once the ground plane was moved away from the craft.

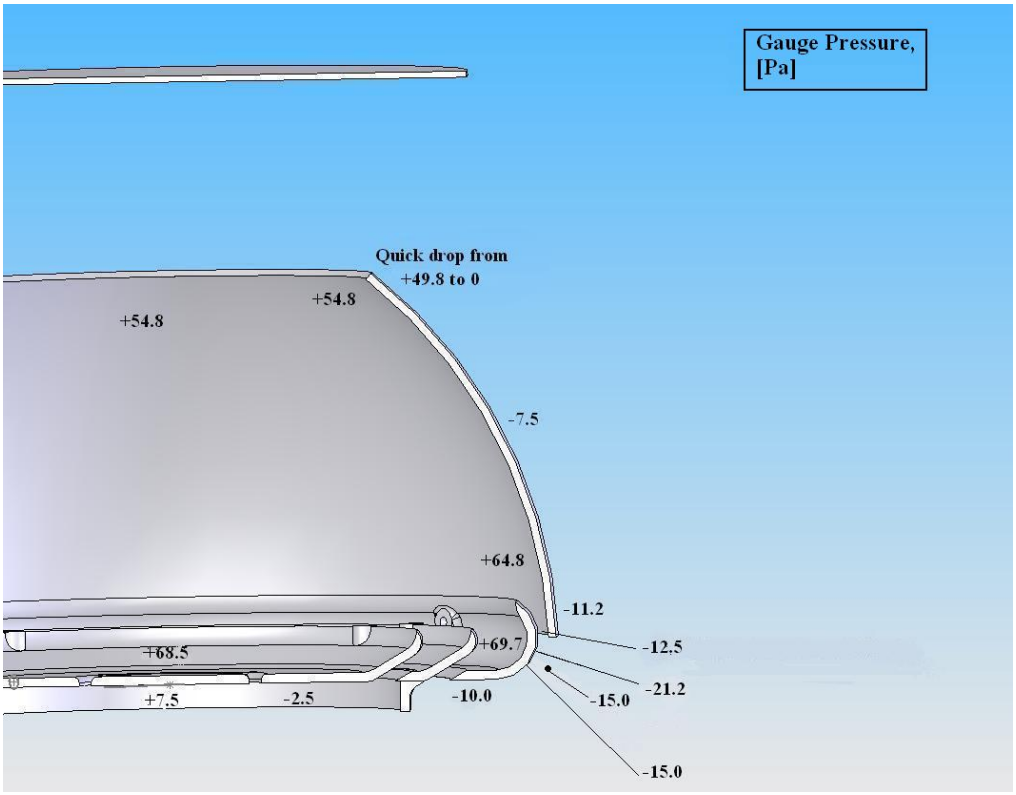

Figure 45: Coanda nozzles pressure distribution out of ground effect

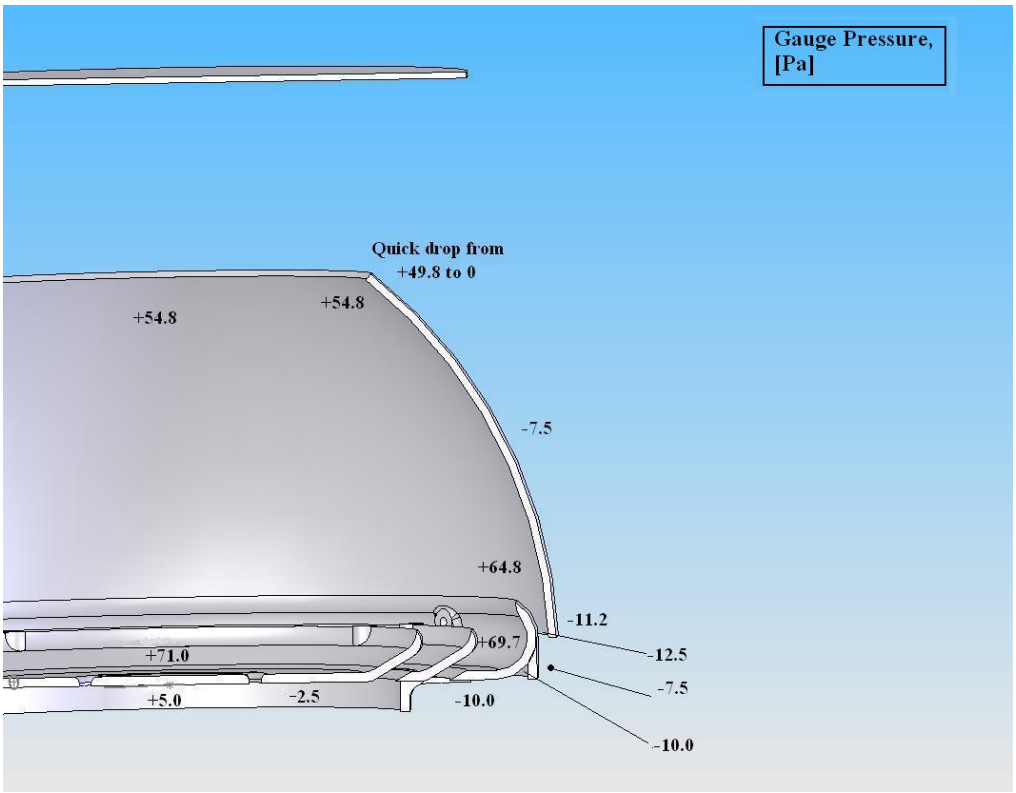

Figure 46: Straight nozzles pressure distribution out of ground effect

Contrary to what was found when operating in ground effect, the pressures on the lower surface of the craft are negative on the peripheral regions of the vehicle when the craft is OGE. These areas appear to be the main source of discrepancy in the pressure distributions between the Coanda nozzles and the straight nozzles configurations. The pressures at the inlet of the plenum and on the outer surfaces of the Coanda Wing appear to be similar for both configurations, but slight differences in pressure between them can be found in the internal and external pressures in the lower central region of the craft.

The flow exiting from the plenum chamber appears to lower the static pressure on the Coanda surface as it moves past it, indicating a flow attachment to the same. This is consistent to what theory predicts, resulting in a similar effect to that found on the upper surface of a conventional wing. A pressure integration analysis similar to the one performed in the previous case, however, results in a difference in force of –0.012 N between the Coanda nozzles and the straight nozzles configurations, not agreeing with the positive, although very small, difference measured with the load cell of approximately 0.024 N (a positive difference indicates a higher value of lift in favor of the straight nozzles configuration). The pressure differences used for these estimations are presented in Table 3 below:

Table 3: Difference in pressure between the two configurations at specific regions on the craft. Height: 1/8 diameter

Pressure Tap Location	ΔP=Ps – Pc –Pinternal [Pa]
Center	-2.49
5 cm from Center	0
10 cm from Center	0
45 degrees (Coanda Surface)	4.98
15 degrees (Coanda Surface	11.21
Center, inside	2.49
Peripheral, inside	0

This discrepancy between the measured lift and the estimated (by integration of pressures) lift can be justified by the limited knowledge about the flow and pressures around the lower portion of the craft (more pressure taps and more sensitive pressure detectors would be needed to provide a more accurate pressure mapping of this region). The differences in the central pressures (on both internal and external surfaces) between the two configurations indicate a dissimilar flow behavior around that region, most likely caused by the Coanda and the straight peripheral nozzles. This is supported by the large negative values of pressure on the Coanda surface (Figure 45), indicating a flow attachment and deflection towards the central axis of the craft, as predicted by Walter (6 and 7). This change in the flow under the vehicle adds variables to the pressure distribution that this experiment was not set up to investigate. Although the results found with the integration method did meet the results found with the load cells, the difference between the two is very minute.

The lower pressures around the Coanda Surface is an indication of flow attachment. As a result of that, an effect similar to those found during thrust vectoring experiments (12, 13, 15, and 16) may explain the small difference in thrust between the Coanda nozzles and the straight nozzles configurations. This difference in lift could be caused by a change in the thrust vector, going from the original direction of lift to a direction towards the central vertical axis of the craft. Although no data could be collected to confirm the above observations, they agree with theory and may be appropriate justifications for the very small difference in lift at heights out of ground effect.

Section 5.3 - Flow Attachment

To provide a visual confirmation of the flow attachment indicated by the pressure distribution on the Coanda surface (when OGE), tufts were placed around the Coanda surface and the Coanda effect can be observed in Figure 53.

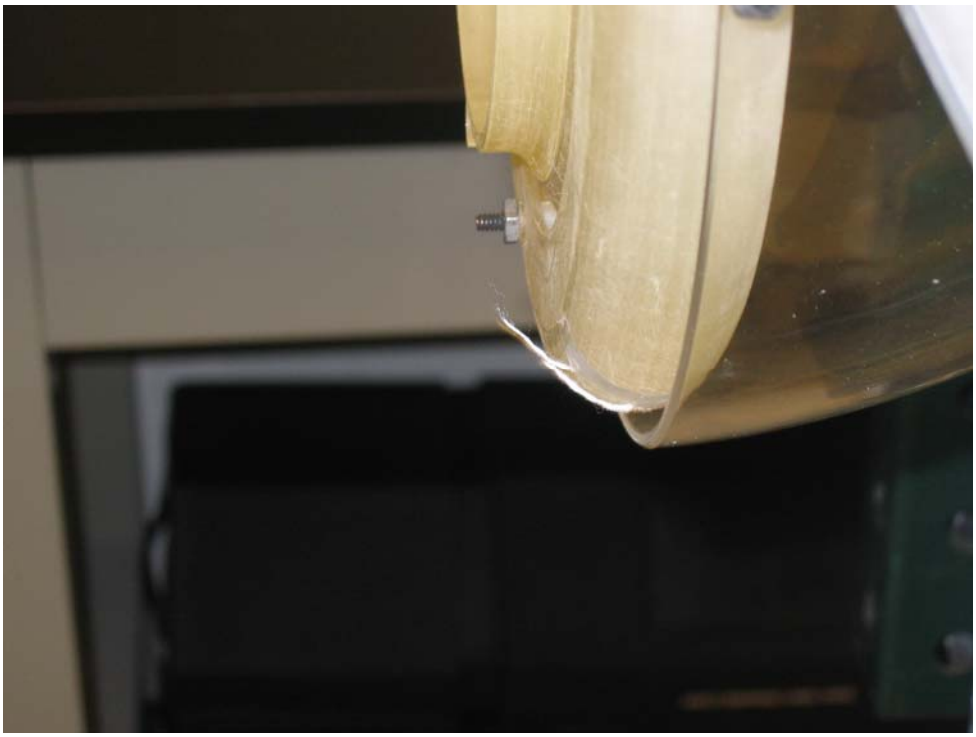

Figure 47: Tufts used to observe flow attachment to Coanda surface

When operating in ground effect (IGE) the flow does not remain attached to the Coanda surface. This is justified by the positive pressure gradient found along the bottom surface under these conditions (a behavior also described by Walter (6) in his patent). Increasingly higher pressures cause the flow to detach from the Coanda surface at points closer to the exit nozzle. The only flow visualization method used in this

experiment, the tufts, did not allow a detailed observation of the changes in detachment point along the Coanda Surface with changes in height. However, a limited amount of knowledge about this prototype was gained by slowly decreasing the height of the craft from an OGE position. One of the tufts seen in Figure 53 above was placed directly next to the exit gap, and seemed to detach from the Coanda surface at a height of approximately 3/4 diameter.

Section 5.4 - Flow Velocities

Flow velocities around portions of the craft were measured using a pitot probe. These measurements were taken while the craft was operating at 1/8 diameter away from the ground plane as well as OGE, with propeller velocities around 6350 rpm. The available measurement equipment did not provide useful data from points where the flow was too turbulent or hard-to-access regions such as the internal portions of the craft. The velocities measured at 1/8 diameter above the ground plane are presented in Figures 54 and 55.

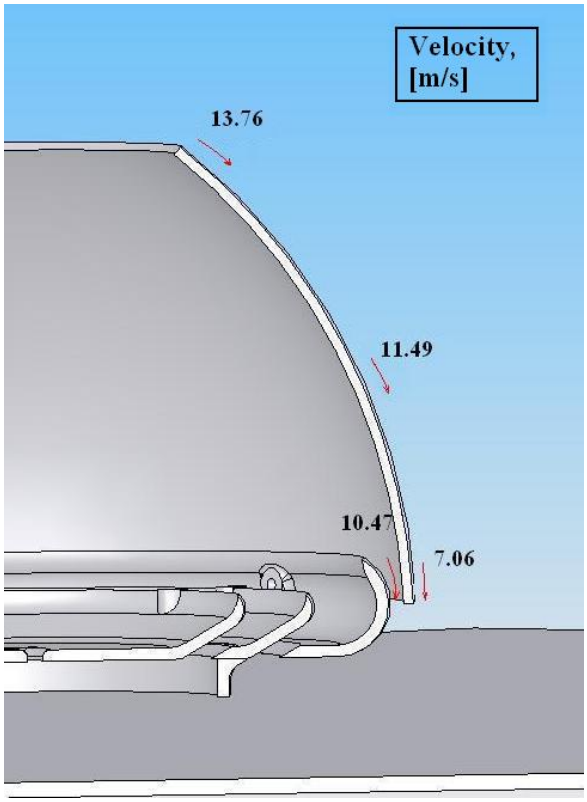

Figure 48: Coanda nozzles configuration velocity distribution at 1/8 diameter height

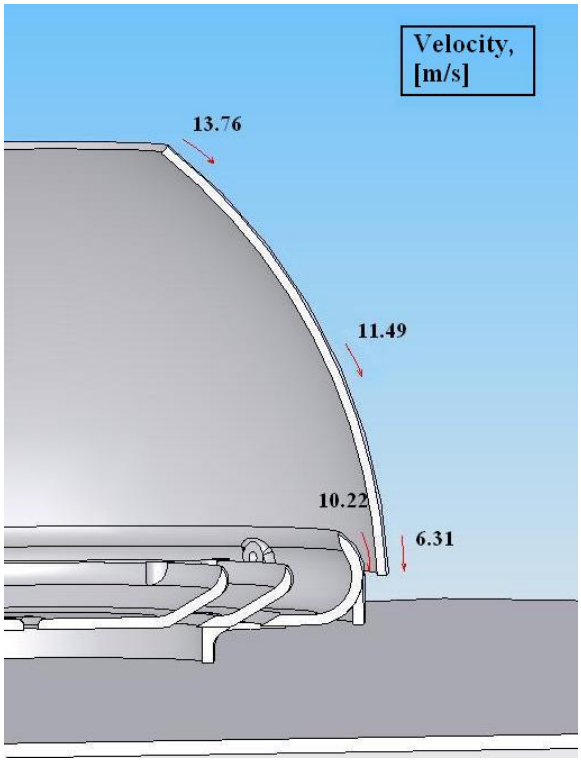

Figure 49: Straight nozzles configuration velocity distribution at 1/8 diameter height

The velocity distribution appears to be similar on the upper portions of both configurations. The higher values of pressure found under the straight nozzles configuration, however, cause the exit velocity from the peripheral nozzles to decrease in relation to the values found for the Coanda nozzles configuration. Figures 56 and 57 below show the velocity distributions found when operating both configurations OGE.

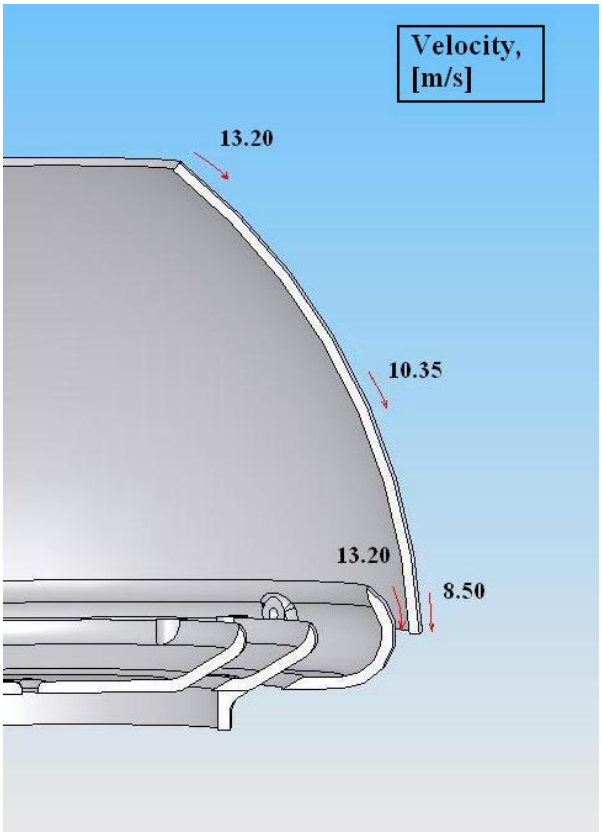

Figure 50: Coanda nozzles configuration velocity distribution, out of ground effect

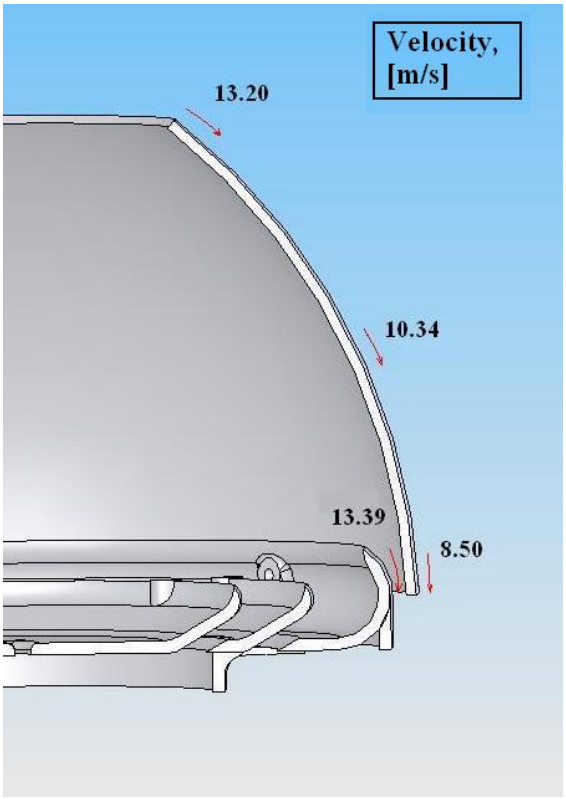

Figure 51: Straight nozzles configuration velocity distribution, out of ground effect

A comparison between the velocity data collected at IGE and OGE and the pressure distributions at the same positions, indicate a slight increase in flow velocities (about 5%) around the Coanda wing at lower heights (for both configurations). This is likely due to the higher pressures found inside the plenum when operating closer to the ground. The ground plane also affects the flow rates coming from the peripheral nozzles by increasing the local ambient pressure at the discharge point.

A basic estimate can be made about the air speeds in the flow originating from the propeller (downwash) by using the information provided by the propeller's manufacturer (APC Propellers) regarding the propeller pitch, as well as the known propeller rotational velocity. The propeller's pitch was specified by the manufacturer to be 10.2 cm per turn (it would advance 10.2 cm per turn in an "ideal" scenario – similar to a screw moving

through a solid). Using a rotational velocity of 6350 rpm , we can estimate an approximate airspeed of 10.6 m/s, a value consistent with the measured pressures in other portions of the vehicle.

Section 5.5 - Comparison to Kelleher's CFD Experiment

Kelleher found that his third model was capable of producing up to 5388.8 N, enough to support a craft of about 550 kg. He used a downwash velocity of 100 m/s and the radius of his propeller was equal to 0.3048 m. With the information collected in this experiment at 1/4 diameter height and 6400 rpm, the value of C_L was calculated to be 0.01385. This lift coefficient can be used to estimate the performance of a 4 ft diameter craft with equivalent characteristics. Using the diameter of the craft as a scaling parameter (going from the 0.255 m diameter craft tested in this experiment to a 4 ft diameter craft), the full size craft would have a propeller with a 0.486 m radius. If the propeller tip speed is set to a mach number of 0.3 (101 m/s, equivalent to a propeller rotational velocity of 2000 rpm) in order to avoid the effects of compressible flow, the full size craft is capable of producing roughly 122.5 N with a power requirement of 1728 w. The lift produced by the model in Kelleher's CFD analysis was a lot larger, but it its required power is estimated to be in the order of 175000 w (based on downwash velocities and propeller disk area).

The conditions set up for this experiment differ from those produced by Kelleher in his CFD analysis (4). However, a basic comparison can be made regarding air speeds and pressure distributions around the craft. Pressure and velocities were measured around the craft when operating at a height of 1/4 diameter (the same height used by

Kelleher (4)), and propeller velocities of 6350 rpm. The collected pressure data at 1/4 diameter height is presented in Figure 58. An illustration of the different pressure regions found by Kelleher in his analysis (4) is also presented in Figure 59 for comparison.

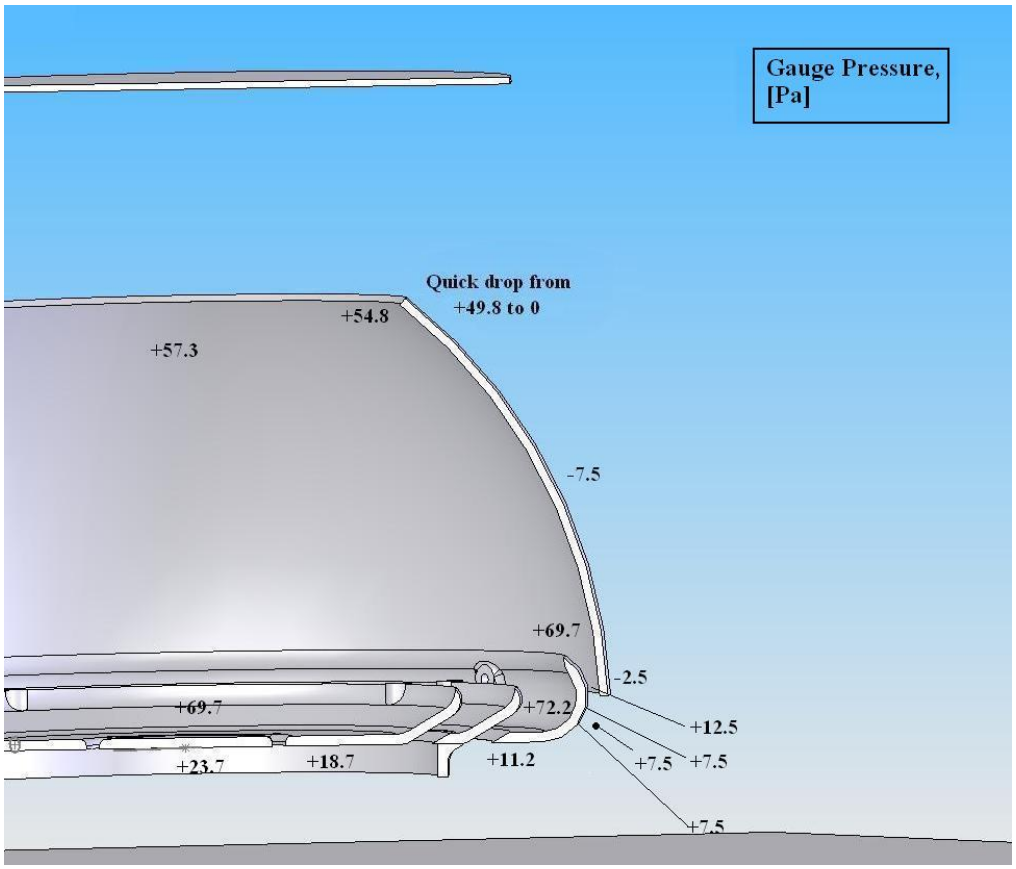

Figure 52: Measured pressures for Coanda nozzles configuration at 1/4 diameter height

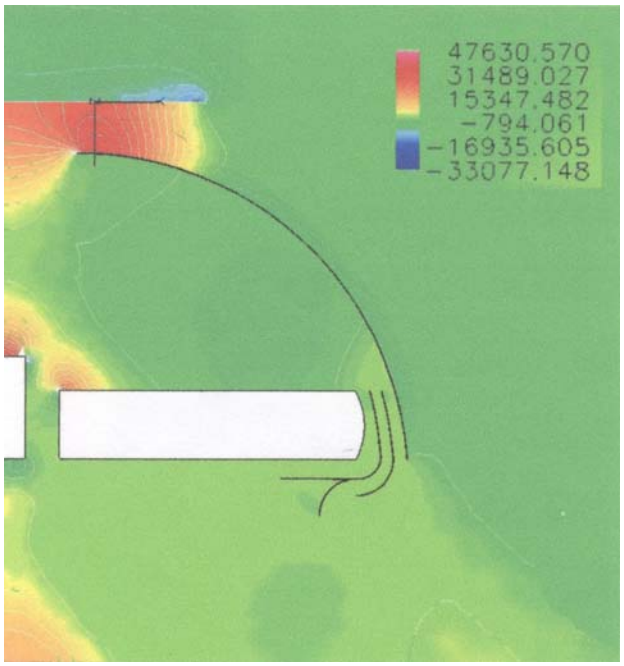

Figure 53: CFD pressure analysis of Kelleher's model (4)

Although the magnitudes of the pressures found around the model are not the same in this experiment and Kelleher's CFD study, the overall pressure distributions present many similarities. The main difference between the two studies can be found in pressure distributions inside the plenum chamber, surrounding the peripheral nozzles. This experiment indicated relatively higher pressures in that region than those found by Kelleher. This is likely caused by variations in the nozzles design (both follow basic specifications determined by Walter, but are not identical), and also the different shape and size of the Coanda wing. The nature of the flow internal to the craft, in the Plenum region, is also a factor and apparently determined by the downwash's speed and arrangement.

Deeper insight can be gained by comparing the velocity profiles between both designs. Figures 60 and 61 below present the data collected at 1/4 diameter using this

experiment's prototype, and the velocity profile found by Kelleher in his analysis at a similar height.

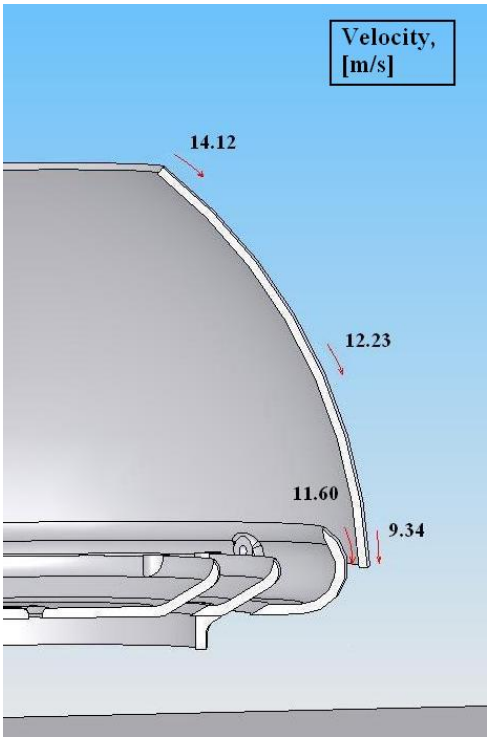

Figure 54: Coanda nozzles configuration velocity measurements at 1/4 diameter height

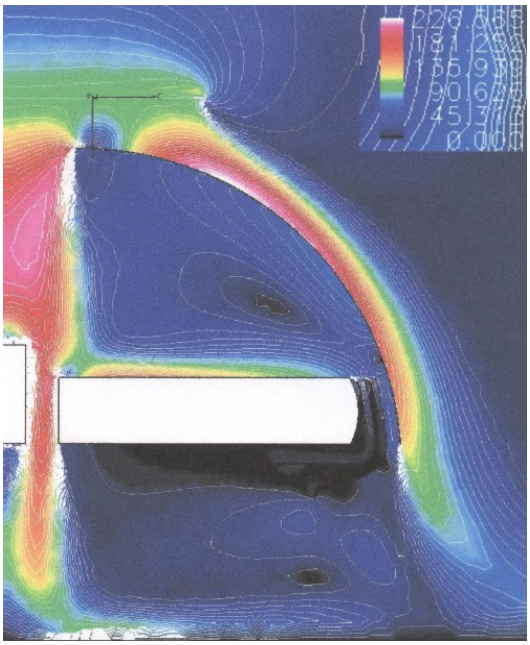

Figure 55: CFD velocity analysis of Kelleher's design at 1/4 diameter height

Similar to the pressure distributions, the velocity profiles from both designs seem to show similar trends on the outer surface of the craft, around the Coanda wing. Again, some discrepancy seems to exist on the internal region around the peripheral nozzles. The smaller relative size of the central nozzles in the prototype used in this experiment seems to contribute to a more even flow towards the peripheral nozzles, a contrast with the low velocities found in Kelleher's design around this region.

V. Conclusions & Recommendations

Section 1 – Conclusions

The results of the tests performed during this research project indicate that the use of ground effect to augment the lift produced by a propeller can be a feasible approach to decrease power requirements and increase payload capacity. The collected data provided further understanding into the mechanisms involved in the operation of a Ground Effect Platform. Evidence of increase in lift without the increase in power requirement was clearly seen throughout the tests performed on the craft at near-the-ground heights. This was true for all craft configurations (including the configurations in which the nozzles were fully covered) to varying degrees, when compared to the propeller only configuration.

The benefits from ground effect are inversely related by height; however, the lift-to-height as well as the efficiency-to-height relations do not follow a linear trend. At the lowest test height of 1/8 diameter of the craft, the models with Coanda nozzles and the straight nozzles produced 37% and 48% more lift than the Propeller only configuration, illustrating the clear benefits of a ground effect vehicle at these heights.

Results from this experiment show similarities in velocity and pressure distribution when compared to results found by Kelleher using Computational Fluid Dynamics. Although the test data are not quantitatively comparable to Kelleher's results, the trends observed in both experiments can be validated and strengths and weaknesses in the design of the craft can be identified. Lower values of pressure were found on the surface of the Coanda Wing in both experiments, and a moderate increase in pressure

under the crafts when hovering at heights of 1/4 diameter was also a common result between the two studies. Based on the latter, it can be predicted that Kelleher's results would agree with those in the present experiment if his tests had also been performed at different heights, both closer and farther from the ground plane. Some conclusions on the present study differ from those of Kelleher (4) in some aspects, mainly due to the larger amount of information collected at various configurations and heights. The peripheral nozzles proved to benefit the craft when hovering close to the ground (1/8 diameter data clearly shows this results), differing from Kelleher's conclusions (he found these nozzles to have little effect in the lift production (4), but his tests were performed at a height of 1/4 diameter, where the benefits from these nozzles will be smaller than observed at 1/8 diameter from the ground plane).

The placement of Coanda nozzles on the peripheral region of the craft did not prove to be the most efficient choice for the downwash velocities and overall craft design used during this study. This was true for in ground effect (IGE) as well as out of ground effect (OGE) tests, when compared to the performance of the straight nozzles configuration. When close to the ground (IGE), the cause of the straight nozzles better performance are the higher pressures around and below the peripheral region, compared to the pressures found in the equivalent area with the Coanda nozzle configuration. The pressure increase on the straight nozzles region appears to affect the entire bottom surface of the craft, causing pressures towards the center of the vehicle to also rise. When the difference in performance between the straight nozzles and Coanda nozzles configurations is likely caused by a loss in lift due to angular changes in the thrust direction (affecting mainly the thrust produced by the peripheral nozzles), an effect

similar what is created by thrust vectoring devices, but detrimental for the overall lift production in this application.

The use of a torque cell and a load cell mounted on an air bearing table proved to be an effective way of measuring and testing propeller driven devices. The figure of merit previously used by Noonan (18) proved to be useful not only when testing and comparing propeller's performance (as he did in his experiment), but also for when studying other factors that affect the overall production of lift. Although torque was essentially unaffected by changes in the craft's configuration during this experiment, any changes in this value would have been accounted for in the calculations performed during the evaluations of performance.

Section 2 – Recommendations

The static tests performed on this craft lead to positive results when operating close to the ground. However, control and stability tests have not yet been performed. Results from such research would be very important in determining not only the issues regarding control, but also the craft's ability to maintain the high pressure air cushion under its nozzles once horizontal speed begins to increase. Helicopters are known to rapidly lose the benefits of ground effect once they transition from hovering to horizontal motion at close to ground heights (11); an effective nozzle design may be required to prevent similar losses in this craft.

A more detailed mapping of ground effects at heights close to the ground could allow studies to be performed regarding the changes in lift caused by pitch and roll on the craft, as well as provide a means to evaluate the performance of the peripheral Coanda

nozzles (or other configurations) in these situations (an attempt was made to study the effects of pitch and roll during this experiment, but the lack of in depth knowledge about the lift-height relationship when IGE lead to inconclusive results).

There is a need to establish an appropriate Reynolds number to describe this craft. More tests with variations in downwash and propeller velocities, as well as variations in diameters and lengths of the different parts of the craft would help determining how each parameter affects the performance of the craft, and how a Reynolds number should be defined.

Further investigation into the mechanisms that allow a larger pressure build up under the straight nozzles (compared to the pressures in the same region found with the Coanda nozzles configuration) when operating at 1/8 diameter from the ground plane, might lead to a better understanding about the ground effect phenomenon acting on this craft.

The propeller velocities in this experiment were mainly limited by the available power supply, a factor that can be corrected before future research using this testing method. The increase in velocity ranges would not only provide more data but could eliminate the inherent (for this propeller and motor) problem of vibrations in the 5850 rpm range.

Appendix A: Construction and Testing of an Internal Flow Separator

Mason (12) performed experiments with varying gap height and radius of curvatures when studying the application of Coanda surfaces for thrust vectoring. Their research tested 2-d models with in which a primary exit nozzle is located between two secondary nozzles and two Coanda surfaces. The study finds relationships between the thickness to radius ratios (t/R) as well as the primary and secondary flows ratios that determine the deflection angle of the thrust vector. Mason also finds the existence of a dead zone, where low secondary mass flow rates (exiting from the peripheral gaps and discharged directly onto the Coanda surfaces) are unable to produce any effect on the primary flow. A saturation region is also found, where maximum deflection angle is achieved for all secondary to primary flow mass ratios, for values of thickness to radius above a certain minimum. Although different from Mason's experiment, the concept involving the Coanda nozzles on the peripheral region of Walter's Hybricraft follow similar principles. In the latter, the goal is to direct flow from the Coanda nozzles (mainly the flow originating from the gap) towards the bottom of the craft to create an air curtain used to maintain the desired air cushion. The air flow descending from the outer surface of the craft can be compared to the primary flow in Mason's experiment, and it would be of interest to make use of this added mass flow and momentum to augment the craft's air cushion. An initial assumption was made regarding the of the mass ratios for the flow originating from the propeller and being separated at the top of the craft, the outer portion of the stream being directed towards the outer surface of the craft and the inner portion being fed into the inner portion of the same, the plenum chamber. Based on the propeller diameter and the plenum chamber's inlet size, a rough estimation was made

about this flow distribution around the craft. Mass flow ratios were established following the findings of Mason (12), in an attempt to allow the operation of the craft's Coanda nozzles in the saturation region, giving it the best chances of operating properly.

Assuming that all the external flow would directly flow towards the lower portion of the craft, it was found that 30% of the flow should be directed towards the peripheral Coanda nozzles to ensure the desired effect, placing the craft in the saturation region (12).

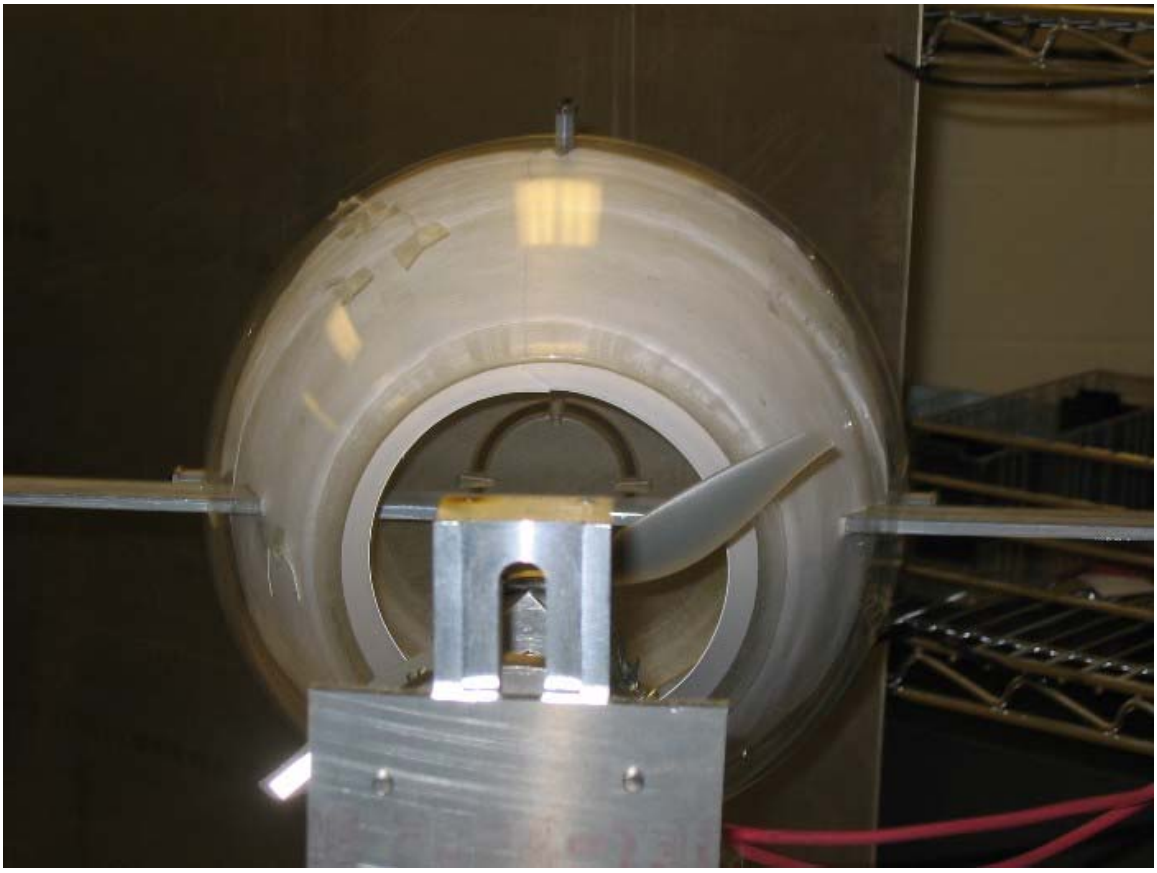

Figure 56: Flow separator inside the plenum chamber

The results from tests performed at 1/4 diameter are presented below in figures 63 and 64.

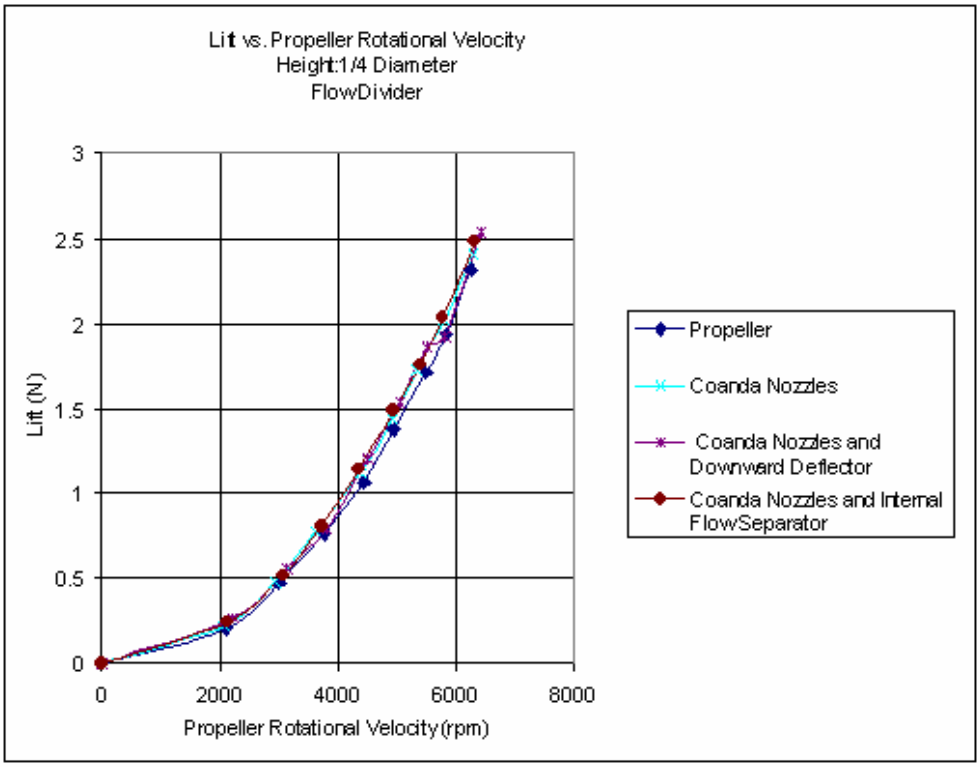

Figure 57: Lift vs. propeller rotational velocity for craft with flow separator at 1/4 diameter height

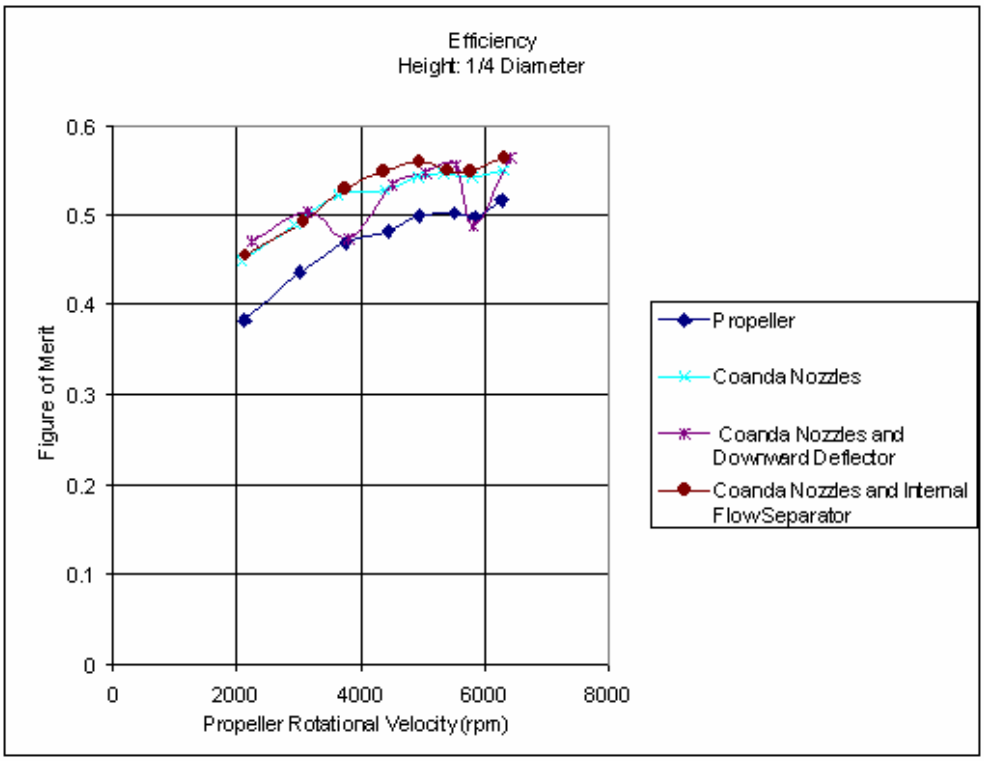

Figure 58: Efficiency vs. propeller rotational velocity for craft with flow separator at 1/4 diameter height

No significant differences were noticed between the data collected with the separator installed and without it, so this option was discarded from the other tests performed in the experiment. The results may not have differed from each other due to the natural shape of the plenum chamber (due to the dome used as the Coanda Wing), which seems to allow an equal or larger amount of internal flow towards the peripheral nozzles region without the need of a flow separator.

Appendix B: Full Data Set From the First Group of Tests

The following plots represent the data collected in the first group of tests. These plots show basic trends in performance for the different configurations at varying heights and propeller rotational velocities. The effect of vibrations can be noticed by the decrease in lift and efficiency for propeller speeds around 5850 rpm and to a smaller extent around the 3800 rpm range. The values at the remaining propeller rotational velocities were not affected. Plots of Torque vs propeller rotational velocity are presented in Figures 59 through 62. Figures 63 through 66 show values of lift versus propeller rotational velocity, and figures 67 throught 70 represent efficiency as calculated based on Equations [2], [3] and [4].

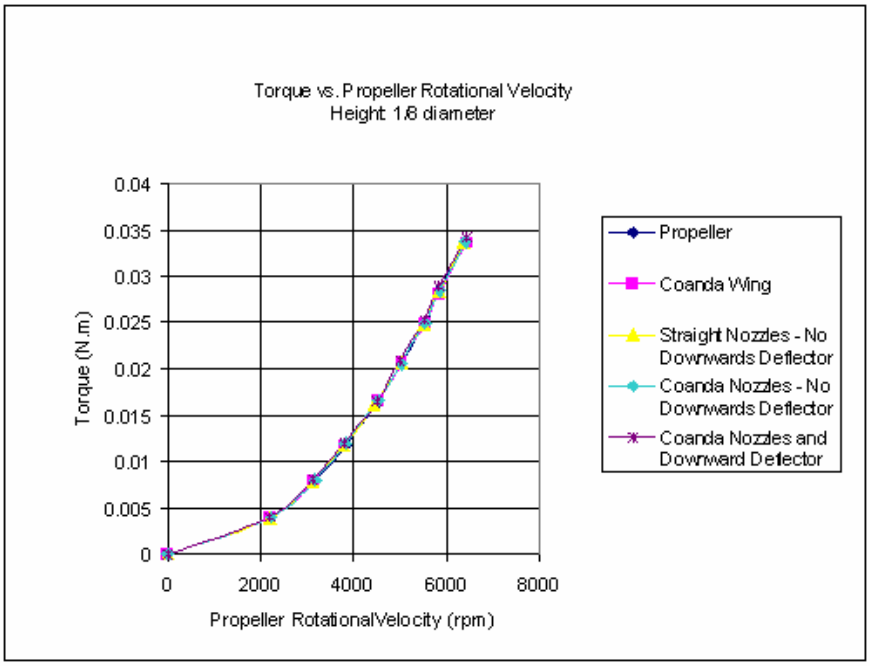

Figure 59:Torque vs. propeller rotational velocity. 1st group of tests, 1/8 diameter height

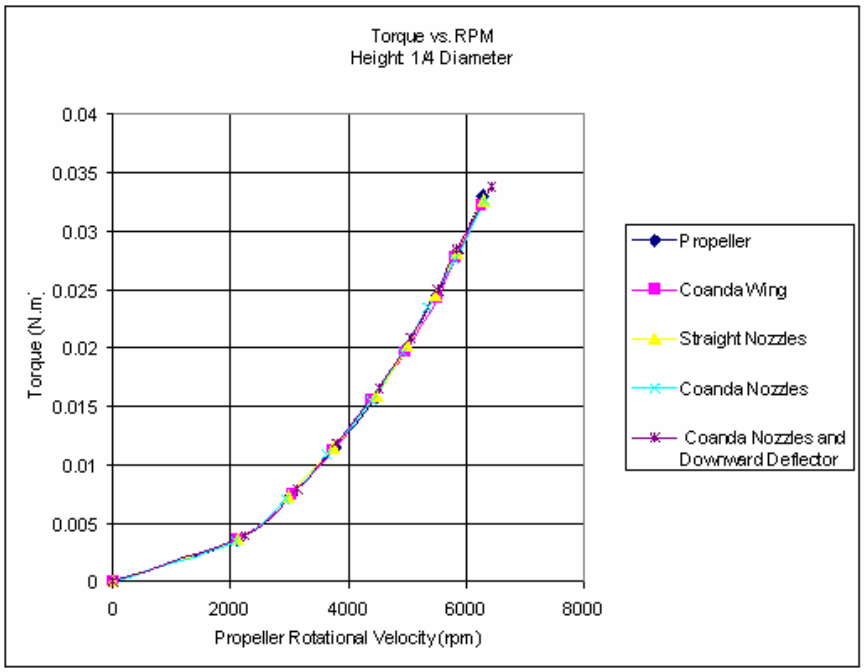

Figure 60:Torque vs. propeller rotational velocity. 1st group of tests, 1/4 diameter height

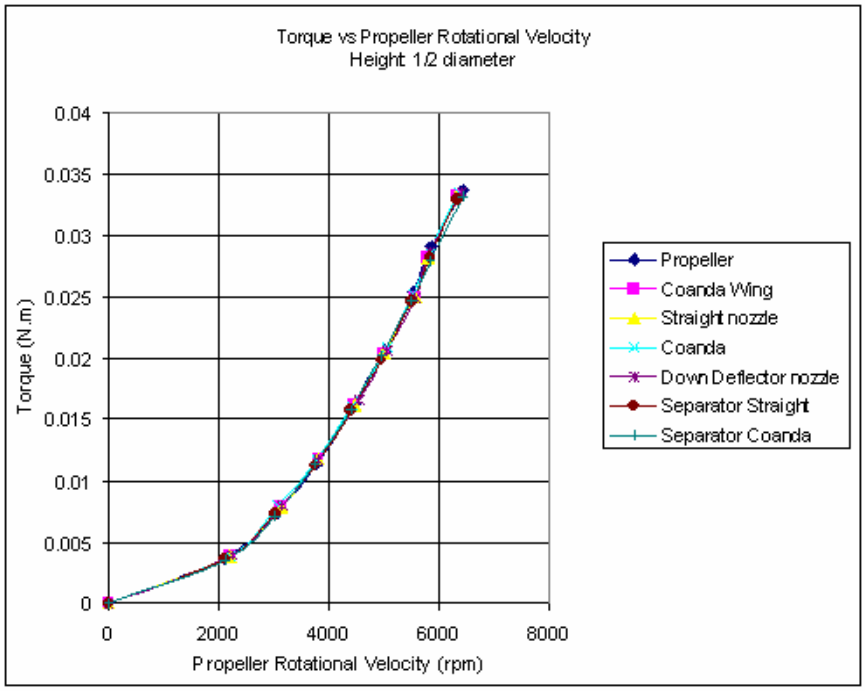

Figure 61: Torque vs. propeller rotational velocity. 1st group of tests, 1/2 diameter height

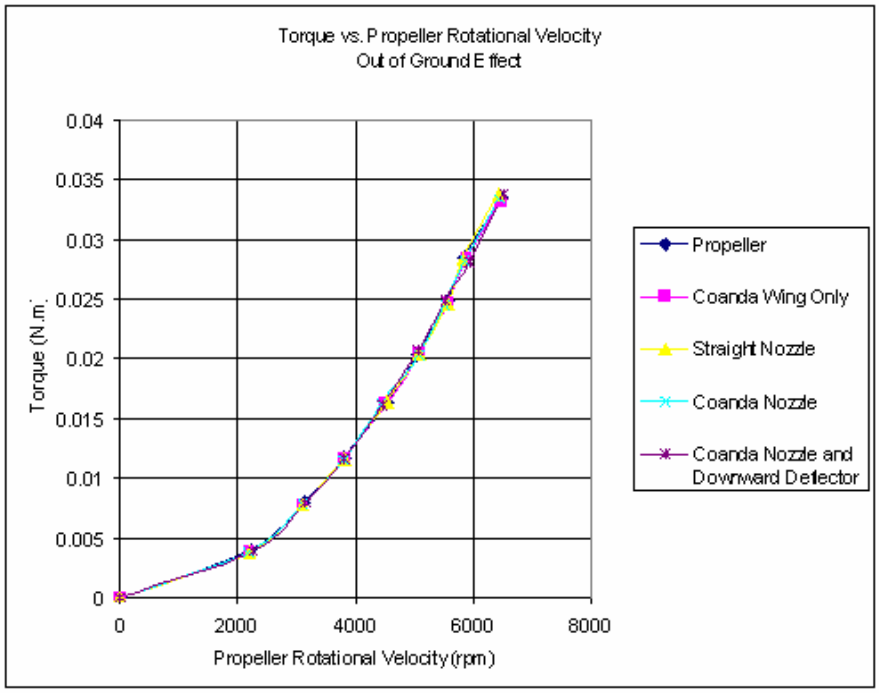

Figure 62:Torque vs. propeller rotational velocity. 1st group of tests, out of ground effect

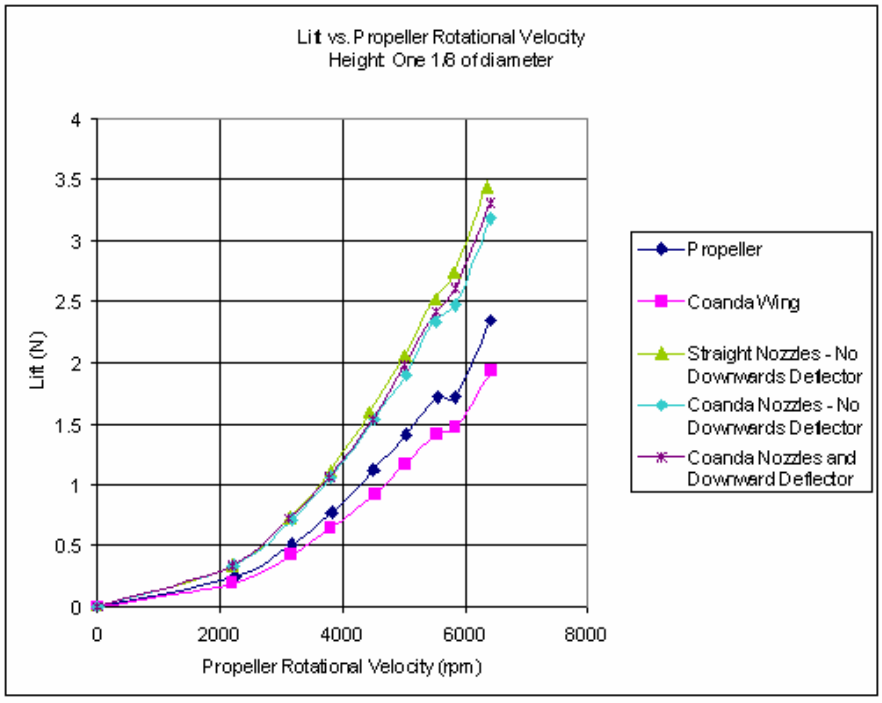

Figure 63: Lift vs. propeller rotational velocity. 1st group of tests, 1/8 diameter height

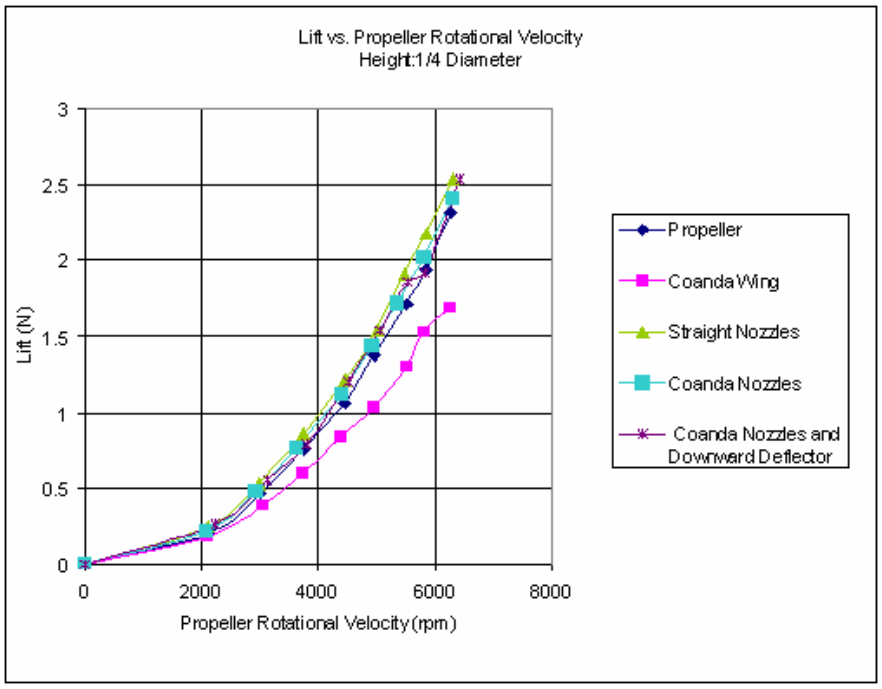

Figure 64:Lift vs. propeller rotational velocity. 1st group of tests, 1/4 diameter height

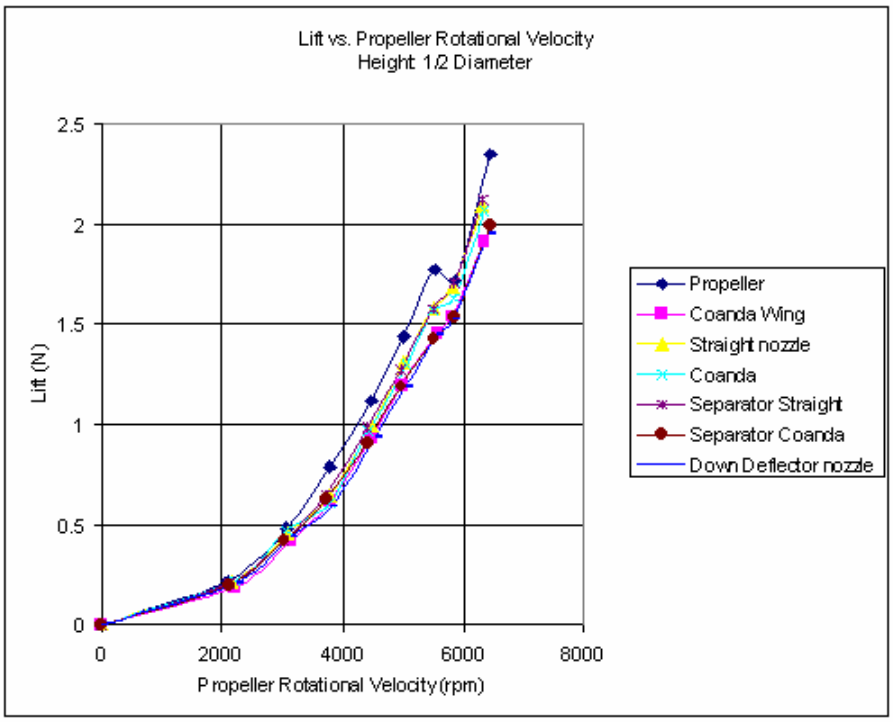

Figure 65:Lift vs. propeller rotational velocity. 1st group of tests, 1/2 diameter height

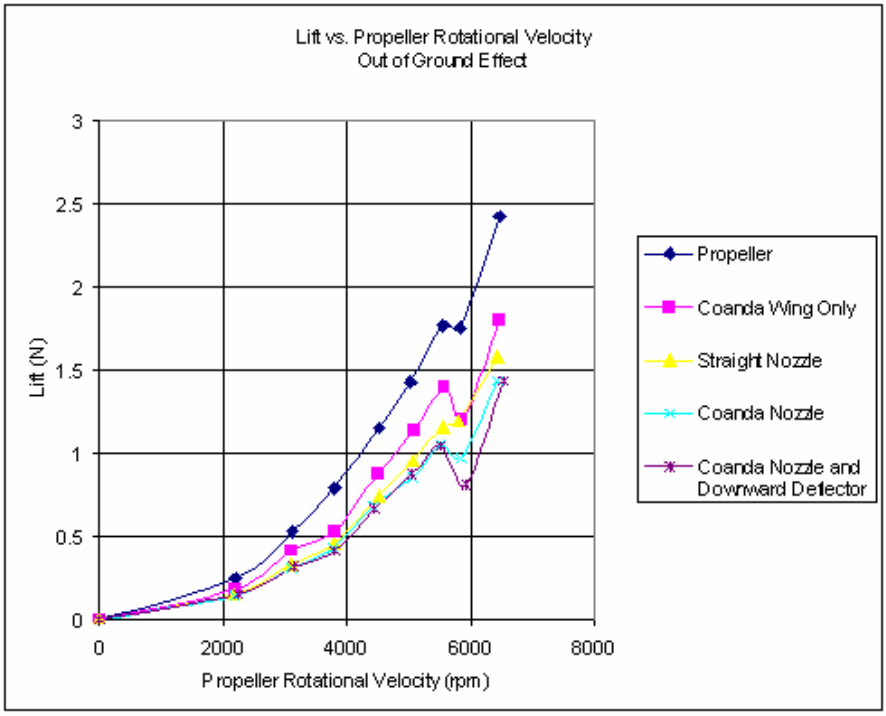

Figure 66:Lift vs. propeller rotational velocity. 1st group of tests, out of ground effect

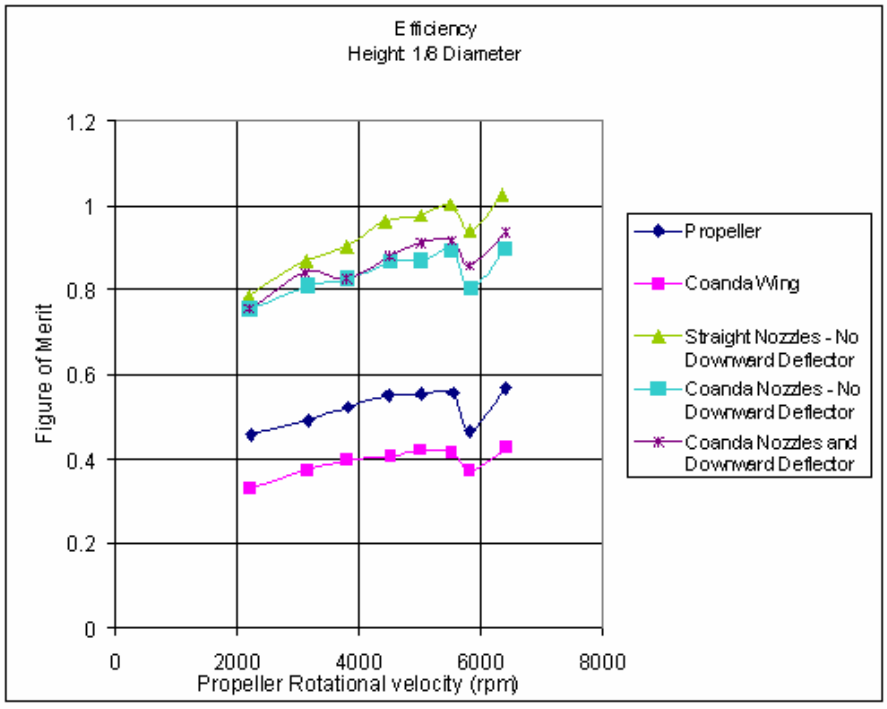

Figure 67:Efficiency vs. propeller rotational velocity. 1st group of tests, 1/8 diameter height

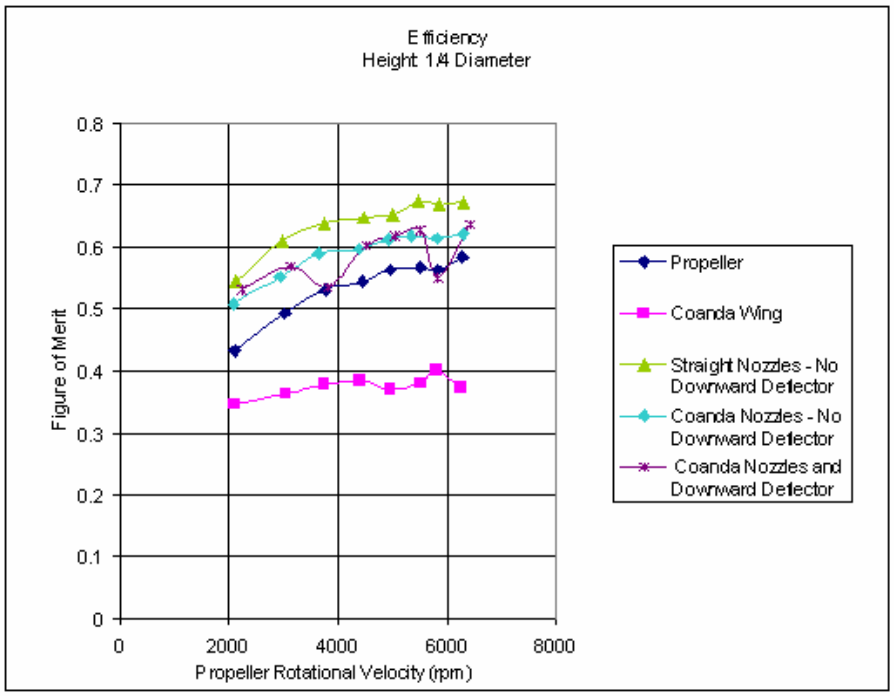

Figure 68:Efficiency vs. propeller rotational velocity. 1st group of tests, 1/4 diameter height

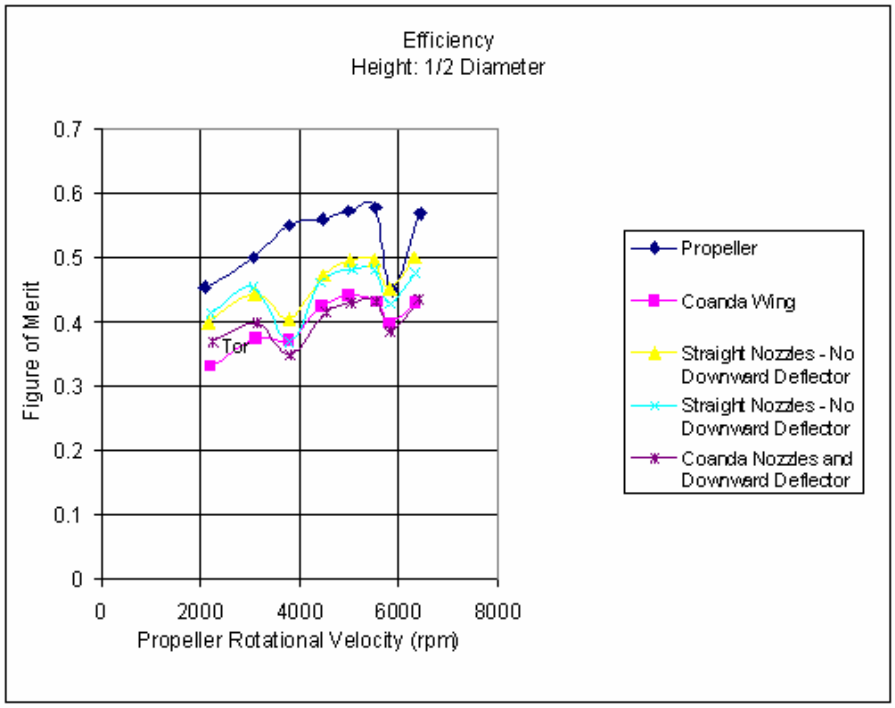

Figure 69:Efficiency vs. propeller rotational velocity. 1st group of tests, 1/2 diameter height

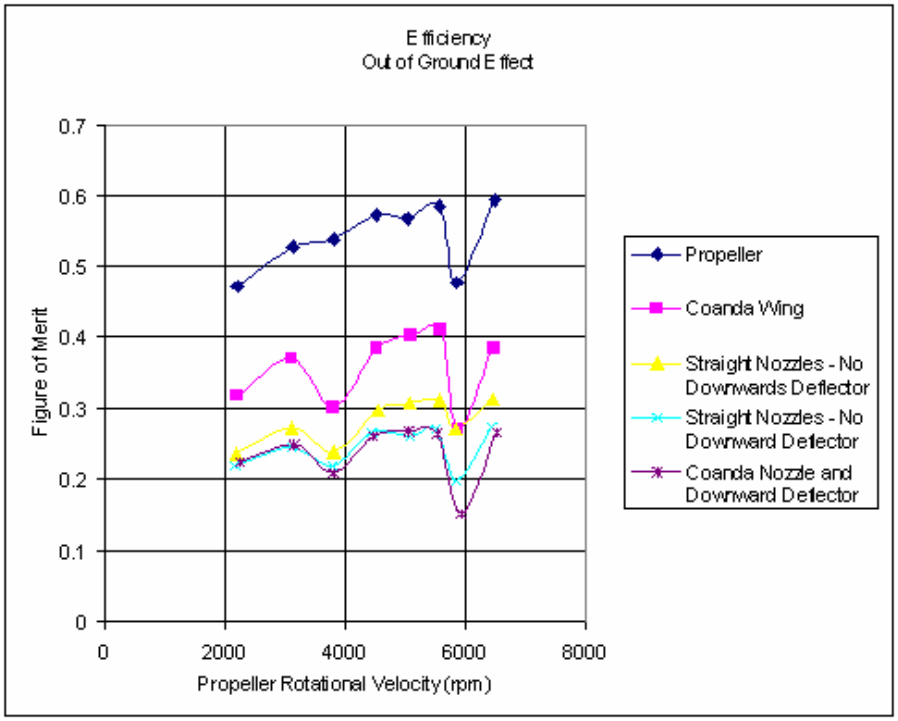

Figure 70: Efficiency vs. propeller rotational velocity. 1st group of tests, out of ground effect

Propeller

Despite the effects of vibration at the specific points in the data, the overall trend can be seen on the results from the first group of tests, plotted in the previous graphs. The propeller seems to present a constant value for lift and efficiency at all heights. It was positioned far enough from the ground, even at the lowest height tested (the test height was measured from the bottom of the craft, and the data for the propeller were collected by simply removing the rest of the craft without readjusting its position), as it can be seen in the plots of lift versus propeller rotational velocity and efficiency versus propeller rotational velocity. The propeller's measured torque also seems to be unaffected by any variation in height or craft configuration.

The efficiency plots make it clear that the propeller used for this experiment had a low efficiency, a figure of merit of about 0.5 at the different heights. This, however,

should not affect the overall results of the research. The same propeller was used for all test runs and the goal of this research was not to examine the performance of different propellers, but to study the overall behavior of different craft configurations at different heights and propeller speeds.

General Trends

In all four different hovering heights studied, the Coanda Wing alone under performed the lift provided by the propeller (labeled as "Coanda Wing" in the plots), even though it also experienced the influences of ground effect at low heights. These results can be explained by the simple existence of a body interfering with the downwash of the propeller. The drag force acting on the Coanda wings suppresses any benefits from the pressure reduction on its outer surface.

The most important observation from the first group of tests was the more efficient performance of all the configurations that included the Coanda Wing and the nozzles over the others (the Propeller configuration being the best basis for comparison) when operating at heights closer to the ground plane.

Two variations of the Coanda nozzles configuration were tested. One included a flow deflector in the lower portion of the craft that directed the air originating from the third set of nozzles (counting from the center outwards) towards the ground plane (the nozzles otherwise are directed at 30 degrees from the surface, towards a point directly below the center of the nozzles). This configuration was labeled "Coanda nozzles and Downward Deflector in the previous figures. A second variation did not include the flow deflector. This group of tests indicates a slightly more favorable result when the

deflector was present, especially at heights closer to the ground. This device was therefore incorporated in the following tests for both Coanda nozzles and straight nozzles configuration. It is worth noticing that the straight nozzles configuration tested in the first group of tests did not include the flow deflector.

Appendix C: Equipment List & Specifications

Table 4: Equipments list and specifications

Name	Description/Specifications
Agile 6038 System Power Supply	0-60V/0-10A, 200w
Instrument Division Visnay measurements Group 2310 Sinal Contitioning Amplifier	0-10 V output Non-linearity: 0.02% of rated capacity
Load Cell: Inerface (B46780 SM-25)	Capacity: 25 lbf Non-linearity % Rated output <0.03 Hysterisis % Rated output <0.02%
Torque Cell: Lebow Products Type: Reaction Torque Sensor Model: 2105-200 Serial # 1297	Capacity: 200 oz in Non-linearity: 0.02% of rated capacity
National Instrument BNC 2120	Computer Interface
Labview version 7.1	National Instruments
Computer: Pentium 4	2.80 GHz 496 MB Ram Windows XP
Pitot Static Probe: United Sensor	PBC-24-G-22-KL0036
Durablock Manometer	Scale: 0.01 in of H20
Pressure: Druck DPI 141	Resonant Sensor Barometer
Cole Parmer 08210	Pistol Grip Photo Tachometer
Motor: ElectriFly T-600R	7.2-9.6V Reverse Motor Performance with 8x4 propeller: RPM:10,500-10,800 Amps: 19-20 Watts: 140 Thrust: 17-19 oz
Propeller: APC 8x4 Propeller	Diameter: 8 in Pitch: 4 in

Appendix D: Additional Figures: Equipment and Configuration

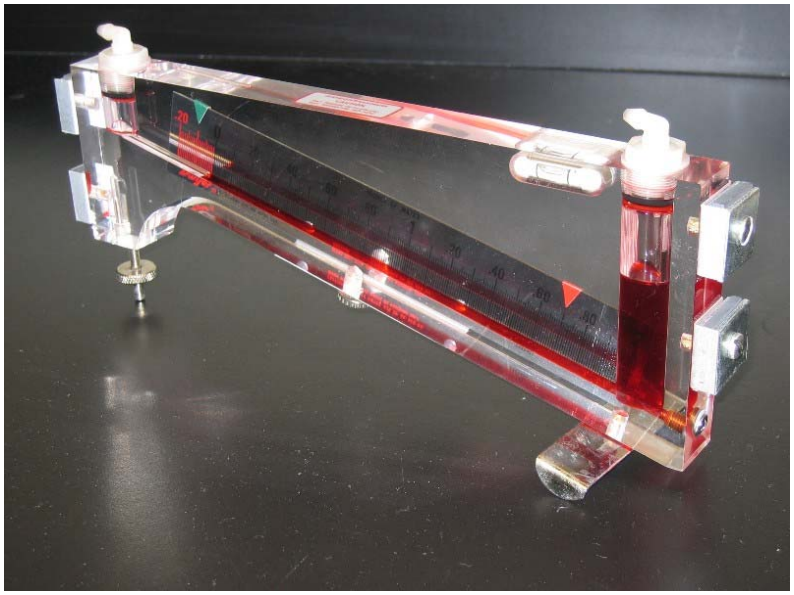

Figure 71: Water manometer used for pressure measurements

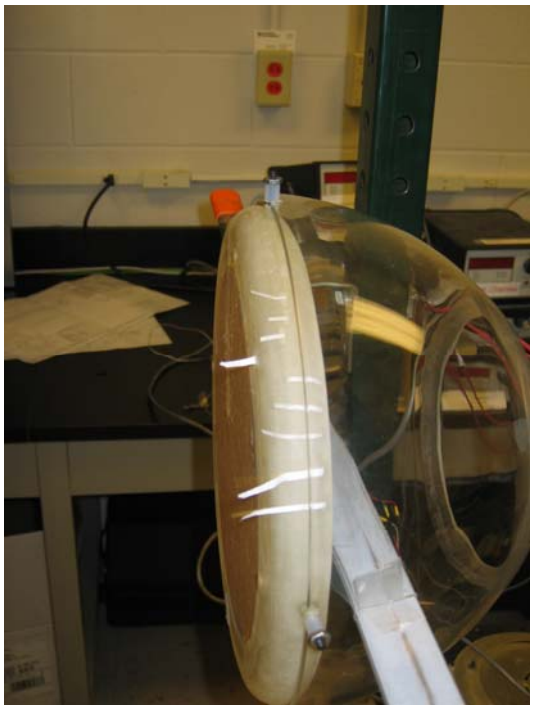

Figure 72: Partially covered Coanda nozzles configuration

Bibliography

1. References good Smithsonian, National Air and Space Museum Avro-Canada VZ-9AV Avrocar http://www.nasm.si.edu/research/aero/aircraft/avro.htm [cited 5 April 2005].

2. Bruce-Knap, Errol *VZ-9A AVROCAR.,* 1 August 2005 http://www.virtuallystrange.net/ufo/mufonontario/avro/avrocar.html

3. Walter, William C., "Home-grown Canadian Landspeeders," EXN.ca Discovery Channe1 November 2004 http://www.exn.ca/Templates/Story.cfm?ID=1999040752

4. Kelleher, Edward A., *A study of a Skirtless Hovercraft Design* MS thesis, AFIT/GAE/ENY/04-J05, Department of Aeronautics and Astronautics, Air Force Institute of Technology (AU), Wright-Patterson AFB, OH, June 2004.

5. "Landing Craft, Air Cushion (LCAC)," *FAS Miltary Analysis Network,* n.pag. 11 July 2005 http://www.fas.org/man/dod-101/sys/ship/lcac.htm

6. Walter, William, "Lift Augumented Ground Effect Platform," U.S. Patent Number 5,803,199. 8 Sep 1998

7. Walter, William, "Hybricraft Primer," VP Technology, Placerville, CA, December 7*,* 1998 (unpublished).

8. Jacobs, Warwick, *"*Sir Christopher Sydney Cockerell," *The Hovercraft Museum.* 15 July 2005 http://www.hovercraft-museum.org/cockerell.html

9. Jones, Brett, *Experimental Investigation into the Aerodynamic Ground Effect of a Tailless Chevron-Shaped UCAV* MS thesis, AFIT/GAE/ENY/05-J04, Department of Aeronautics and Astronautics, Air Force Institute of Technology (AU), Wright-Patterson AFB, OH, June 2005.

10. van Opstal, Edwin and others. *The WIG Page*, 2 Aug 2005 http://www.se-technology.com/wig/index.php

11. Cerbe, T., "Influence of ground effect on helicopter takeoff and landing performance," *Zeitschrift fuer Flugwissenschaften und weltraumforschung*, 14:155-167, (1990)

12. Mason, Mark S., Crowther, William J., "Fluidic Thrust Vectoring of Low Observable Aircraft," CEAS Aerospace Aerodynamic Research Conference, June 2002

13. Imber R., Rogers E., "Investigation of a Circular Planform Wing with Tangential Fluid Ejection," 34th Aerospace Sciences Meeting &Exhibit, Reno AIAA 96-0558, January 1996.

14. Crummer, C. A. "Aerodynamics at the Particle Level," 5 April 2005 http://physics.ucsc.edu/~ccrummer/aero1.pdf

15. von Glahn, U. H. "Use of the Coanda Effect for Jet Deflection and Vertical Lift with Multiple-Flat-Plate and Curved-Plate Deflection Surfaces." NACA Technical Note No, 4377. Washington: National Advisory Committee for Aeronautics, 1958.

16. Franke, M. E., Pelletier, M. E., and Trainor, J. W., "Circulation Control Wing Model Study," *Journal of Aircraft,* Vol. 32, No. 1, pp. 208-211, 1994.

17. Singleton, J. D., Yeager, W. T. "Important Scaling Parameters for Testin Model-Scale Helicopter Rotors." (AIAA-98-2881)

18. Noonan, K.W., "Wind Tunnel Evaluation of a Model Helicopter Main-Rotor Blad With Slotted Airfoils at the Tip," NASA/TP-2001-211260, December 2001.

19. Schlichting, Hermann, *Boundary-Layer Theory* (6th Edition). New York: McGraw-Hill Book Company, 1968.

20. Anderson, John D., *Fundamentals of Aerodynamics* (3rd Edition). New York: McGraw-Hill Book Company, 2001.

21. Barlow, Jewel B., Rae, W., Pope, A., *Low-Speed Wind Tunnel Testing* (3rd Edition). New York: John Wiley and Sons, 1999.

22. Panitz, T., Wasan, D. T., "Flow Attachment to Solid Surfaces: The Coanda Effect," *AIChE Journal,* 18:51 January, 1972.

23. Ameri, M., Dybbs, A. "Coanda Ejector – Why it works," *SPIE Vol 2052 Laser Anemometry Advances and Applications,* 2052:289-296, 1993.

24. Lopard, Vincent J. "The Effect of Resistors and Partial Enclosures on the Attachment Characteristics of a Coanda Surface," *National Technical Information Service.* Naval Academy, Annapolis, Maryland, 1 May 1975 (AD-A012 370).

25. Freund, J. B., Mungal, M. G. "Drag and Wake Modification of Axisymmetric Bluff Bodies Using Coanda Blowing," AIAA 10th Applied Aerodynamics Conference, June 1992.

26. Pozzi, A., Manzo, F., Luchini, P., "Compressible Flow in a Hovercraft Air Cushion," *AIAA Journal,* 31:528-533, March 1993.

27. Ducrée, J., Zengerle, R., "3.3. Fluid Dynamics," myFluidix.com, 23 Aug 2005. http://soulor.imtek.uni-freiburg.de/myfluidix/Materials/PDF/03_Physics_03.pdf

28. Kunz, D. L. Class notes, AERO 610, Rotorcraft Aeromechanics. Department of Aeronautics and Astronautics, Air Force Institute of Technology, Wright-Patterson AFB OH, Fall 2004.

29. Anderson, John D., *Aircraft Performance and Design.* New York: McGraw-Hill Book Company, 1999.

Vita

Roberto T. Igue was born in Raleigh, NC. He graduated from Rochester High School in Rochester, Illinois in 1996. He enlisted in the United States Navy and served as a Nuclear Electronics Technician until selected for the Naval Reserve Officer Training Corps program. He attended the Georgia Institute of Technology and earned a Bachelor of Science degree in Aerospace Engineering. He received a Commission into the United States Navy on July 1st of 2004. Ensign Igue was selected for the Immediate Graduate Education Program (IGEP) and entered the Air Force Institute of Technology in September of 2004. Upon graduation he will be assigned to NAS Pensacola to begin training as a Naval Aviator.

REPORT DOCUMENTATION PAGE

Form Approved
OMB No. 074-0188

1. REPORT DATE *(DD-MM-YYYY)*	**2. REPORT TYPE**	**3. DATES COVERED** *(From – To)*
13-09-2005	Master's Thesis	04 OCT 04 – 13 SEP 05

4. TITLE AND SUBTITLE
Experimental Investigation of a Lift Augmented Ground Effect Platform

5a. CONTRACT NUMBER

5b. GRANT NUMBER

5c. PROGRAM ELEMENT NUMBER

6. AUTHOR(S)

Igue, Roberto T., Ensign, USNR

5d. PROJECT NUMBER

5e. TASK NUMBER

5f. WORK UNIT NUMBER

7. PERFORMING ORGANIZATION NAMES(S) AND ADDRESS(S)

Air Force Institute of Technology
Graduate School of Engineering and Management (AFIT/EN)
2950 Hobson Way
WPAFB OH 45433-7765

8. PERFORMING ORGANIZATION REPORT NUMBER

AFIT/GAE/ENY/05-S04

9. SPONSORING/MONITORING AGENCY NAME(S) AND ADDRESS(ES)
N/A

10. SPONSOR/MONITOR'S ACRONYM(S)

11. SPONSOR/MONITOR'S REPORT NUMBER(S)

12. DISTRIBUTION/AVAILABILITY STATEMENT
APPROVED FOR PUBLIC RELEASE; DISTRIBUTION UNLIMITED.

13. SUPPLEMENTARY NOTES

14. ABSTRACT

This experimental study investigated the feasibility of applying the concept of a skirtless hovercraft into the production of an operational vehicle. A 0.255 m diameter prototype was designed, built and tested. An air bearing table was used as a testing platform, virtually eliminating the influence of friction and providing one degree of freedom for the experiments. Static tests were performed at various heights and craft configurations, providing a wide range of data for comparison. Lift, torque and efficiency were measured and calculated for each setting. Pressure and velocity information was also collected at specific points around the craft when operating at different heights above ground.

The results indicate a significant increase in total lift and efficiency when operating the model at close to the ground heights, in ground effect, compared to the lift produced by the propeller and motor alone. Even more significant changes were found when comparing the in ground effect results with the out of ground effect values of lift and efficiency. The study also investigated the use of Coanda nozzles on the peripheral region of the craft, and found them to be less efficient than straight nozzles with similar size and flow rates.

Comparisons between the experimental results and previous computational fluid dynamic analysis are also made and presented in this study.

15. SUBJECT TERMS
Ground effect, skirtless hovercraft, Coanda effect, Hybricraft

16. SECURITY CLASSIFICATION OF:			**17. LIMITATION OF ABSTRACT**	**18. NUMBER OF PAGES**	**19a. NAME OF RESPONSIBLE PERSON**
REPORT	**ABSTRACT**	**c. THIS PAGE**			MILTON E. FRANKE
U	**U**	**U**	**UU**	108	**19b. TELEPHONE NUMBER** *(Include area code)* (937) 255-6565, e-mail: MILTON.FRANKE@afit.edu

Standard Form 298 (Rev: 8-98)
Prescribed by ANSI Std. Z39-18